Republic of Iraq

Ministry of Higher Education

And scientific Research

University of Babylon

College of Science

Department of Chemistry

Synthesis, Characterization and Study of Some Applications of New Functional Luminol Derivatives

A thesis

Submitted to the Council of College of Science, University of Babylon in Partial Fulfillment of the Requirements for the Degree of Master of Science\ Chemistry

By

Teeba Saleh Kadhim Mohammed

B.Sc. in Chemistry/University of Babylon (2019)

Supervised by

Prof. Dr. Mohanad Mousa Kareem

Prof. Dr. Abbas Jassim Atiyah

2022 A.D **1444 A.H**

بِسْمِ اللَّهِ الرَّحْمَنِ الرَّحِيمِ

يَرْفَعِ اللَّهُ الَّذِينَ آمَنُوا مِنْكُمْ وَالَّذِينَ أُوتُوا الْعِلْمَ دَرَجَاتٍ وَاللَّهُ بِمَا تَعْمَلُونَ خَبِيرٌ

صدق الله العلي العظيم

سورة المجادلة

الآية 11

CERTIFICATION

We certify that this thesis was prepared under our supervision at the Department of Chemistry, College of Science, Babylon University, in partial requirements for the Degree of Master of Science in chemistry and this work has never been published anywhere.

Signature:

Name: **Dr. Mohanad Mousa Kareem**

Title: Professor

Address: Department of Chemistry-

College of Science-Babylon University

Date: / /

Signature:

Name: **Dr. Abbas Jasim Atiyah**

Title: Professor

Address: Department of Chemistry-College of

Science-Babylon University

Date: / /

In the view of the available recommendation, I forward this thesis for debate by the examining committee.

Signature:

Name: **Dr. Abbas Jasim Atiyah**

Title: Professor

Address: Head of Department of Chemistry-College of Science-Babylon

University

Date: / /

Dedication

To …...

The promised absent

Awaited justice

Al-Imam Al-Mahdi “aj”

Acknowledgments

Praise be to ***Allah****, Lord of the Worlds, and prayers and peace be upon the Seal of the Prophets and Messengers, who was sent as a mercy to the worlds, and upon his good and pure family.*

Thanks be to Allah first and foremost for all of his blessings, and thanks to him for his constant kindness and success. My thanks go to the Messenger of Allah and his pure family, especially the remnants of Allah the Awaited Justice and Resurrection (may God's blessings be upon them all).

Great thanks and great gratitude to ***Prof. Dr. Mohanad Mousa Kareem*** *and to* ***prof. Dr. Abbas Jasim Atiyah*** *for their continuous and continuous follow-up and their accurate observations during the study period.*

All thanks and gratitude to the Head of the Department of Chemistry for providing this opportunity and thanks to all the professors of the department for their efforts and providing a helping hand throughout the study period.

Prof. Dr. Saadon Abdullah and Asst. Prof. Dr. Fares Hammoud deserve my heartfelt gratitude for their guidance and assistance throughout the study term.

Sincere thanks are due to the Dr. Amar Abd al-Hussain, Assist. Ayad Ali Disher and Hamad Hameed Kazem for their help in this work, Thanks to every teacher who contributed to my education in my life.

Also, I thank all faculty members of the Department of Chemistry in the College of Science at the University of Babylon especially I thank Abeer and Tuqa for their worthless support of the work.

My father, my mother, my brothers and sister, my husband I thank you inexpressible thanks for your unlimited financial and moral support and for bearing all the burdens on me during the study period. Last but not least, thanks go to all those who contributed by word or deed to getting me through this stage.

TEEBA

Summary

The present study describes synthesis of some new Luminol derivatives. This work includes two lines:

First route: Involves reaction of Luminol compound with different carboxylic drugs such as (Naproxin, Mefenamic Acid, Ibuprofen, Diclofenac Acid, Ampicillin, Ciproflaxine, Cefotaxime, Ceftriaxone, Cephalxine). Synthesis processes were conducted by converting carboxylic group in the investigated drugs into acid chloride group by reacting with $SOCl_2$, .Then the synthesized chloride drug derivatives (T1-T9) were reacted with luminol in presences of DMSO and TEA to yield the final target molecules(TH1-TH9).

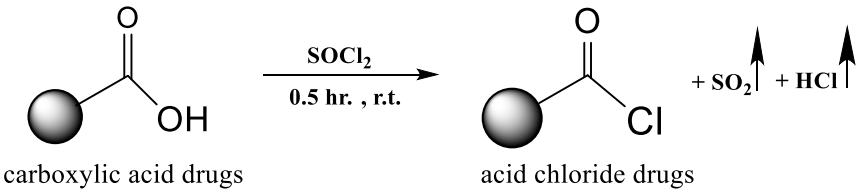

carboxylic acid drugs acid chloride drugs

Equation(1):General equation preparation of acid chloride drugs(T1-T9)

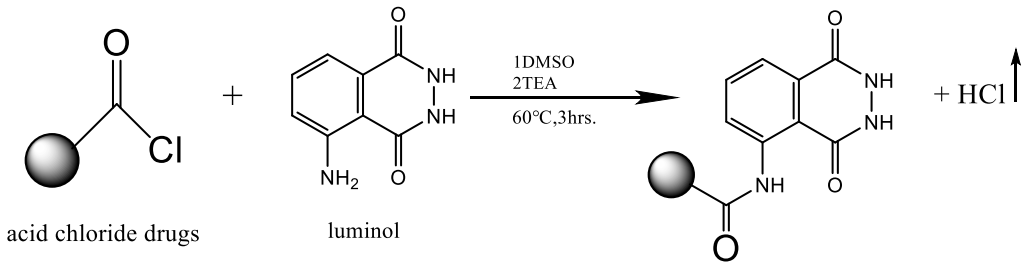

acid chloride drugs luminol

Equation (2):General equation for preparation compounds (TH1-TH9)

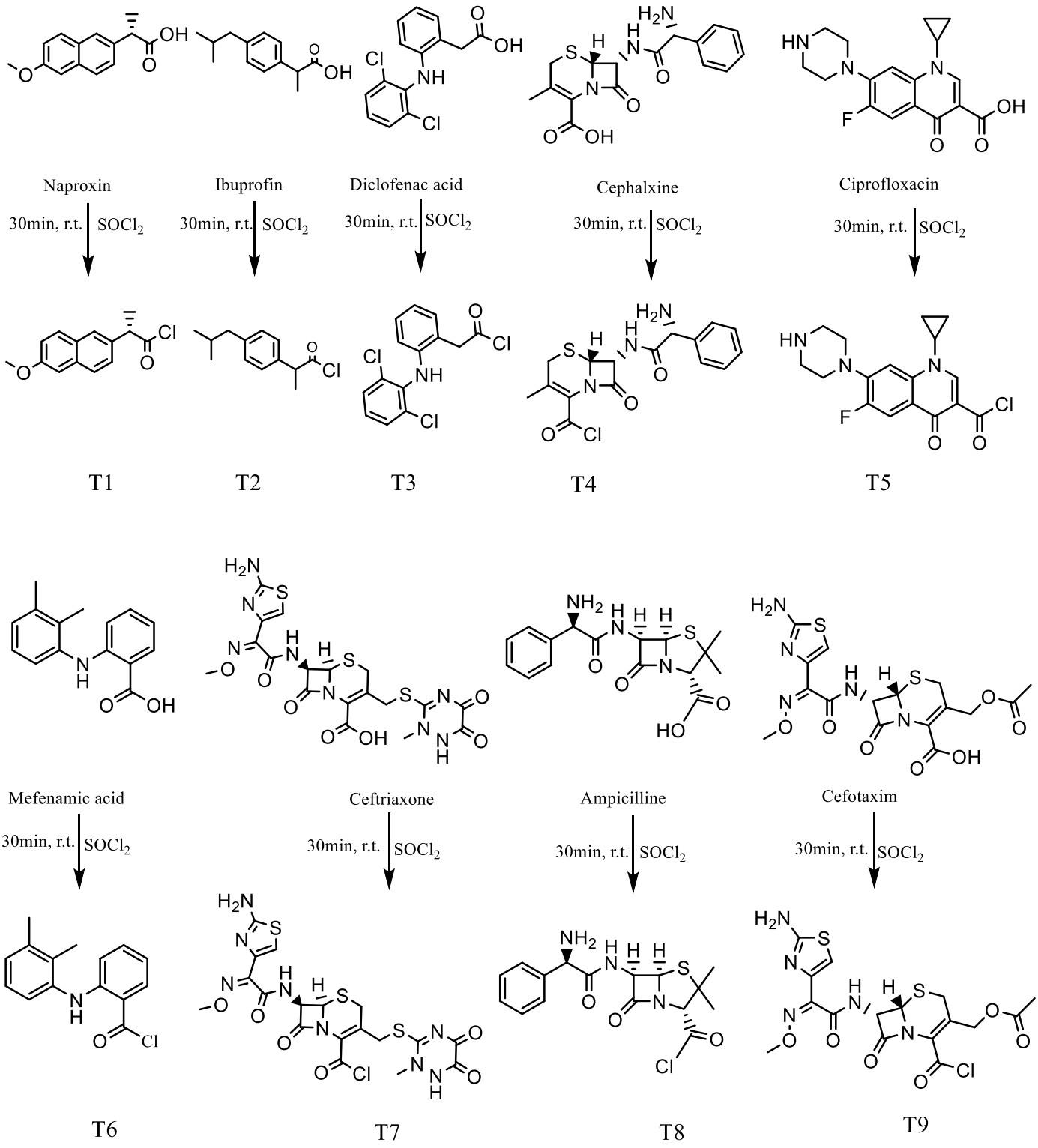

Scheme (1): Schematic description for the synthesis of the derivatives (T1-T9)

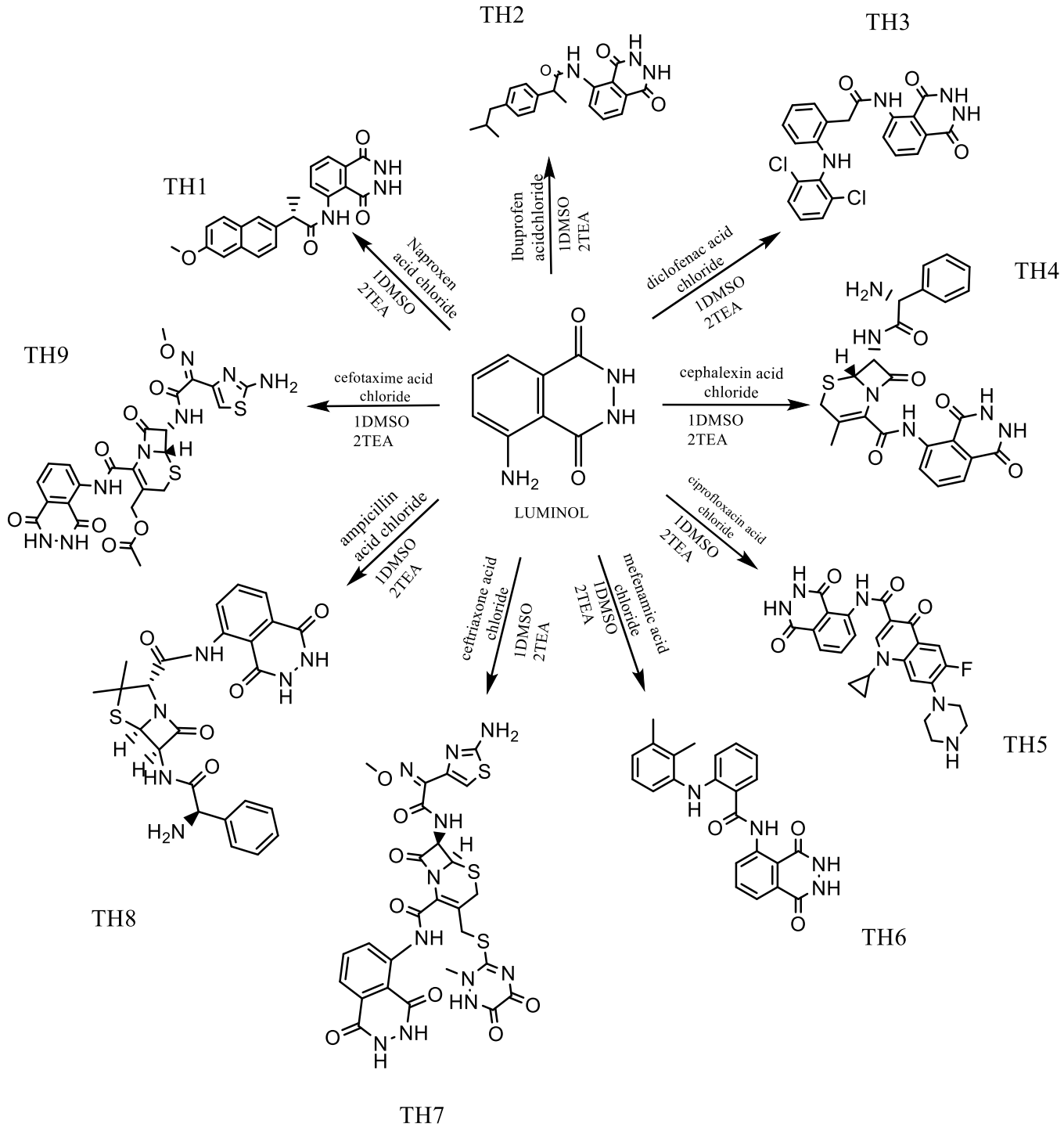

Scheme (2) :Schematic description for the synthesis of the derivatives (TH1-TH9).

Second route: This involves reaction of luminol with succinic anhydride by adding DMSO and then Converting the obtained mixtures into acid chloride by $SOCl_2$ after that added DMSO for mixture and added the amino drugs (Cephalexin, Mefenamic , Paracetamol ,Theophylline , Amoxicillin , Ampicillin) to reaction in presences of TEA to yield the final target molecules(TH10-TH15).

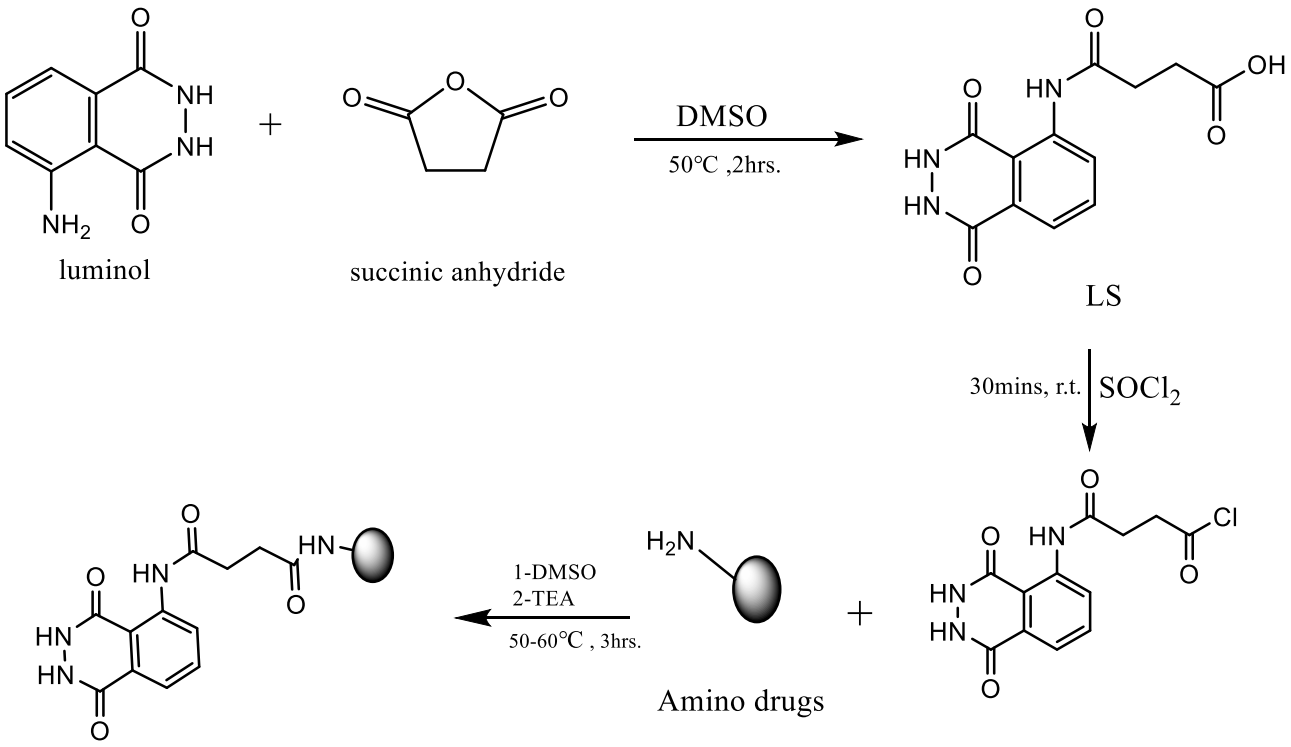

Scheme(3):Schematic description for the synthesis of the derivatives (TH10-TH15)

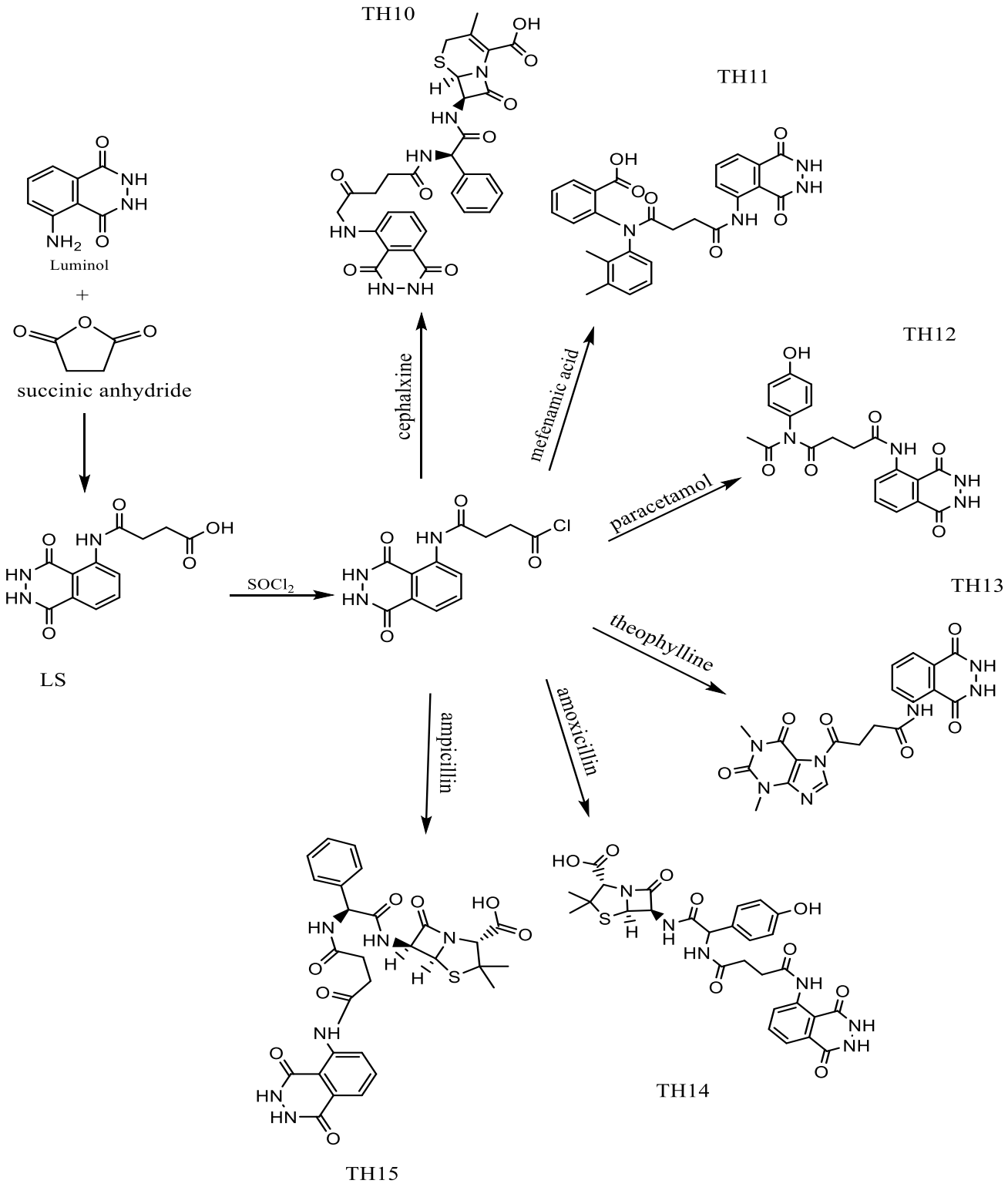

Scheme(4):Schematic description for the synthesis of the derivatives (TH10-TH15).

The synthesized compounds were characterized by using FTIR, ^{1}HNMR ,^{13}C-NMR and CHNS elemental analysis techniques. Besides that, their melting point and solubility were also investigated. All prepared derivatives were study as antibacterial reagents versus Staphylococcus aureus as (gram positive) and Escherichia coli (E. coli) as (gram negative) and most of the study compounds showed activity toward one or both classes of bacteria. Some of prepared derivatives were study as photolysis with UV illumination at different temperatures and also tested of photocatalytic degradation over cobalt oxide applied different reaction conditions and parameters.

List of Abbreviations

Symbol	Description
LM	Luminol
FTIR	Fourier Transform Infra-Red
TLC	Thin-layer chromatography
^{1}H-NMR	Proton Nuclear magnetic resonance
^{13}C-NMR	Carbon Nuclear magnetic resonance
δ	chemical shifts
ppm	Part per million
CHNS	elemental Analysis
g	gram
mmol	mill mole
hr.	hour
mL	Milliliter
DMSO	Dimethyl sulfoxide
TEA	Triethylamine
r.t.	Room temperature
Com. symbol.	Compounds symbol
M.F.	Molecular formula
M.Wt.	Molecular weight
m.p.	Melting point
℃	Celsius degree
R_f	Retardation factor
DCM	dichloromethane
min.	Minute
str.	Stretch
Al.	Aliphatic
Ar.	Aromatic
CL	Chemiluminescence
D.E.G	Di ethylene glycol
DPPH	2,2-diphenyl-1-picrylhydrazyl
NPs	Nanoparticles
DMF	Dimethylformamide
DMAP	4-Dimethylaminopyridine
THF	Tetrahydrofuran
AlBN	Azobisisobutyronitrile

Contents

CHAPTER ONE

INTRODUCTION

1.Introduction

1.1. Luminol:

Light emission occurrences have been described and connected to mythological and cultural events since the dawn of humanity. The first time luminol was produced in 1928 AD by to Albrecht's [1]. Luminol is a powerful chemiluminescent substance that emits blue light under oxidative conditions (the energy produced as a photon comes directly from a powerful exothermic reaction). Particularly for analytical applications, the method itself is highly beneficial and appealing. Additionally to heavy metal measurement (copper, for example, can be found in amounts as low as nm[2]. Chemiluminescence analysis accounts for in *vivo* analytical chemistry and biosensors with simple instrumentation, low detection limits, a wide calibration range, and quick analysis times[3]. As a result, chemiluminescence has been extensively used in sectors like life sciences, pharmaceuticals and the environment [4]. It is important to remember that luminol is most commonly utilized in crime scene investigations to distinguish items with cleansed bloodstains (residuals of haemic iron). Television programs like "Crime Scene Investigation," or "CSI," frequently use this technology.

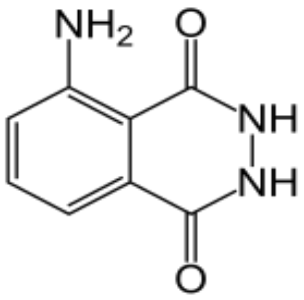

Figure 1. The molecular structure of the Luminol.

Luminol ($C_8H_7N_3O_2$) , is a chemical that exhibits chemiluminescence, with a blue glow. Luminol is a white-to-pale-yellow crystalline solid that is soluble in most polar organic solvents, but insoluble in water [5].

Forensic investigators use luminol to detect trace amounts of blood at crime scenes, as it reacts with the iron in hemoglobin. Biologists use it in cellular assays to detect copper, iron, cyanides, as well as specific proteins via western blotting [6]. When luminol is sprayed evenly across an area, trace amounts of an activating oxidant make the luminol emit a blue glow that can be seen in a darkened room. The glow only lasts about 30 seconds, but can be documented photographically. The glow is stronger in areas receiving more spray; the intensity of the glow does not indicate the amount of blood or other activator present.

1.2.Chemiluminescence

Chemiluminescence refers to the emission of light from a chemical reaction, which can occur in solid, liquid or gas systems[7]. The fundamentals of chemiluminescence have been comprehensively reviewed in a number of textbooks and articles in recent years [8–11]. Two main categories of chemiluminescent reaction have been described in the literature, direct and indirect. Direct chemiluminescence can be represented by:

$$A + B \rightarrow [I]^* \rightarrow \text{PRODUCTS} + \text{LIGHT}$$

where A and B are reactants and [I]* is an excited state intermediate. The luminol reaction is an example of this form of chemiluminescence. In certain cases where the excited state is an inefficient emitter, its energy may be passed on to another species (a sensitizer, F) for light emission to be observed. This is called “indirect chemiluminescence” and is exemplified by the peroxyoxalate (light stick) reaction:

$$A + B \rightarrow [I]^* + F \rightarrow [F]^* \rightarrow F + \text{LIGHT}$$

Once a molecule has been converted to a metastable intermediate in an excited state there are a number of routes by which it can return to the ground state. These routes can be displayed diagrammatically, as in Figure 2. by an “energy well” diagram, or more simply by the Jablonski diagram, first introduced in the 1930s. The light emission can either be fluorescence or chemiluminescence, if from a single state, or phosphorescence if from a triplet state. The light emitted from chemiluminescent reactions has differing degrees of intensity, lifetime and

wavelength with the latter parameter covering the spectrum from near ultraviolet, through the visible and into the near infrared.

For emission to be observed from a chemical reaction, three essential energetic requirements need to be met:

1. There should be an energetically favorable reaction pathway for the production of the excited state species. Of the total number of molecules participating in the reaction a significant number should reach the excited state.

2. The reaction is required to be exothermic, with the free energy change being in the range 170–300 kJ mol^{-1}.

3. There should be a favorable deactivation pathway for chemiluminescence emission, with other competitive non radiative processes such as intra- or intermolecular energy transfer, molecular dissociation, isomerization or physical quenching kept to a minimum.

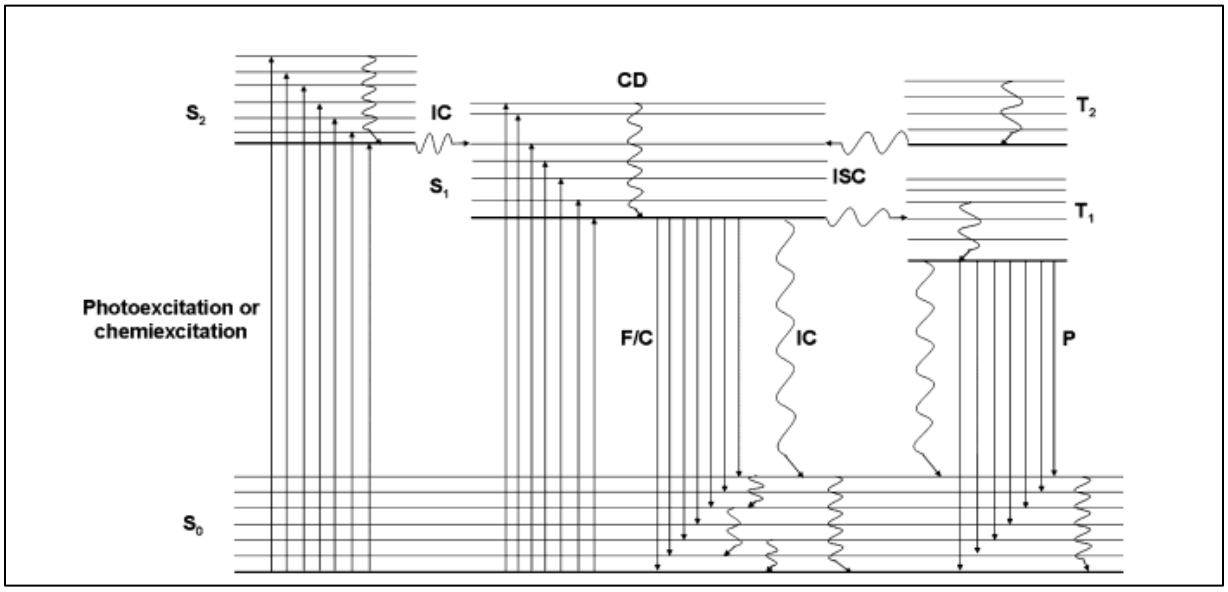

Figure 2. Jablonski energetic diagram showing energy levels and transitions in a molecular compound: C, chemiluminescence; F, fluorescence; P, phosphorescence; CD, collisional deactivation; IC, internal conversion; ISC, intersystem crossing; S_0, ground singlet state; S_1, S_2, excited singlet states; T_1, T_2, excited triplet states; →, radiative transition; , non-radiative transition.

Luminol chemiluminescence has been reviewed by Barnett and Francis [11]. The light-producing pathway for the oxidation of luminol is a complex multi-step process and is dependent on several factors including pH, temperature and ionic strength of the reaction medium and reactive species that can be present in solution and interact with luminol, metal catalyst or hydroxide ions [11]. White et al. [12–14] observed that the fluorescence spectrum of an intermediate molecule in the luminol oxidation process named 3-aminophthalate in an electronically excited state (3-APA*) perfectly matched the chemiluminescence spectrum of luminol, thus they concluded that this excited intermediate could be considered the light emitting species upon excitation to the ground state (3-APA). This was confirmed in 1965 by Gundermann [15]. In dipolar aprotic solvents such as dimethylsulfoxide (DMSO) containing O_2, or in moderate-strong alkaline protic solvents (pH ~ 8–11) such as water or lower alcohols and in presence of a strong-mild oxidant (in most cases H_2O_2) and a suitable catalyst such as a metal ion or some kind of oxidoreductase enzyme, the excited 3-aminophthalate di anion (3-APA*) returns to the ground state (3-APA) by releasing energy in the form of light (Figure 3). When the reaction occurs in protic media, the 3-aminophthalate di anion is produced in almost quantitative fashion [16-20].

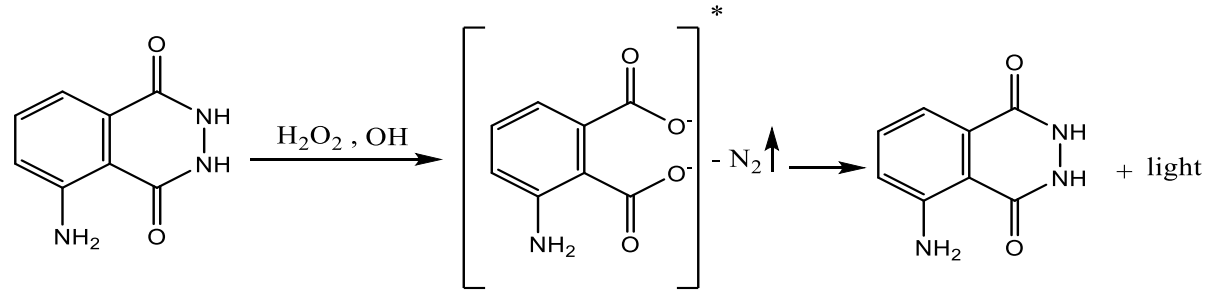

Luminol (3-APA)* (3-APA)

Figure 3. Luminol chemiluminescence reaction.

In aqueous solutions the light observed ranges between blue violet and blue-green Figure 4, although the spectral range of emission is often rather broad and the observed maximum is dependent on several parameters of the reaction [13–18], such as the presence of blood itself which strongly absorbs at 420 nm and may provide an inner-filter effect, thus shifting the observed maximum emission of luminol chemiluminescence to about 455 nm[21].

For the luminol reaction the exact role of the catalyst, which is required when the reaction is carried out in basic aqueous solution, and the reaction intermediates are not completely characterized. It is known that a wide range of other transition metal catalysts and metal-complexes catalyze the reaction and that the optimum conditions of pH for the reaction depends on the identity of the catalyst used and varies between pH (8 and 11) [22]. thus suggesting a multiplicity of potential catalysis mechanisms.

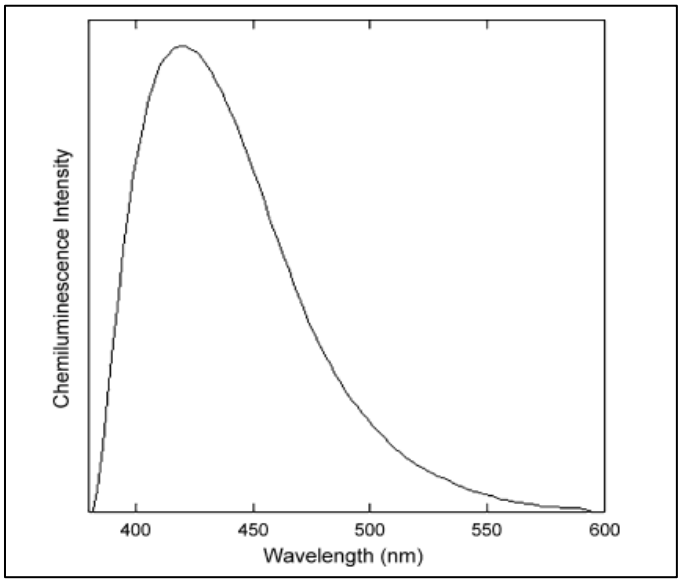

Figure 4. Typical chemiluminescence emission spectrum for the reaction of luminol with hydrogen peroxide in the presence of hematin.

1.3.Preparation of luminol

Albertin et al. [23] observed that light emission is associated with 3-nitrophthalic conversion to 3-aminophthalate. They explained the mechanism of the reaction from two steps to the formation of Luminol as shown in Figure 5 and Figure 6 .

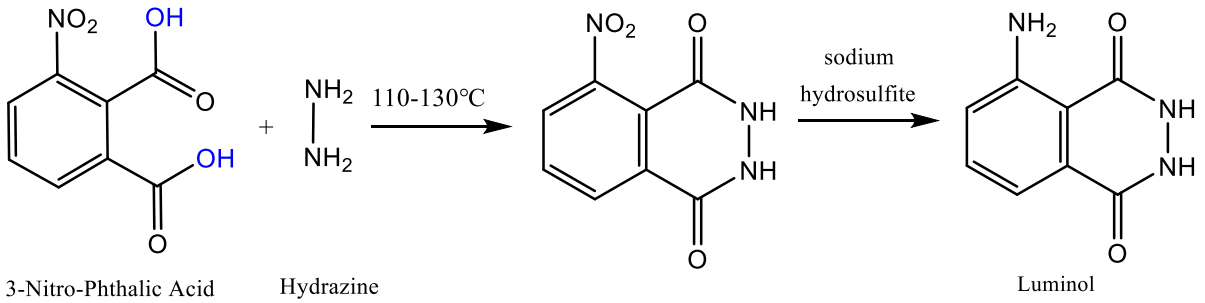

Figure 5. Synthesis of Luminol.

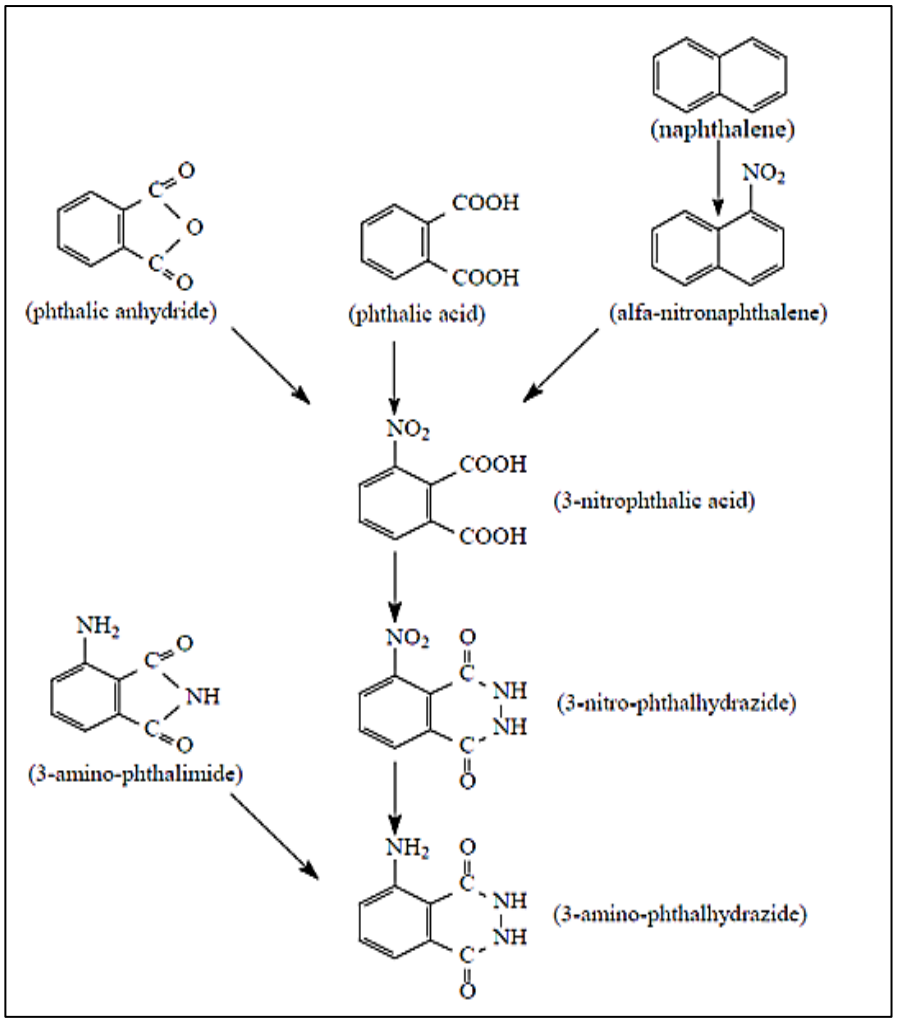

Figure 6. Synthesis of luminol compound.

The methods of preparation and purification of luminol and its derivatives are very expensive on the one hand, and on the other hand difficult because, of the use of very high purity reagents when preparing, because any impurities can affect the manufacture of the material, or may lead to chemical reactions side, in addition to the impact on the reactions generated by light where the luminol exists in the form of isomers and as shown in Figure 7[24].

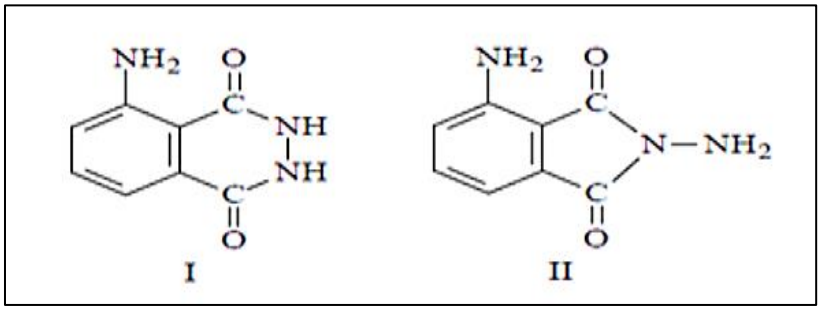

Figure 7. Structure of Luminol isomers.

1.4. Reactions of luminol

It has been observed that nanoparticles can enhance the chemical fusion strength of the citron-bound luminol-KIO_4 with the presence of a carbon dioxide root, giving more intense signals with nanoparticles for silver and a 22 nm diameter. Ultraviolet spectra and fusion strength spectra have been measured to determine the mechanism of enhancing the potential fusion force. In addition, 17 amino acids and 25 organic compounds with luminol-KIO_4 were studied through a flow injection of the citric acid which gave an effective method for detecting acid acids As shown in figure 8 [25,26].

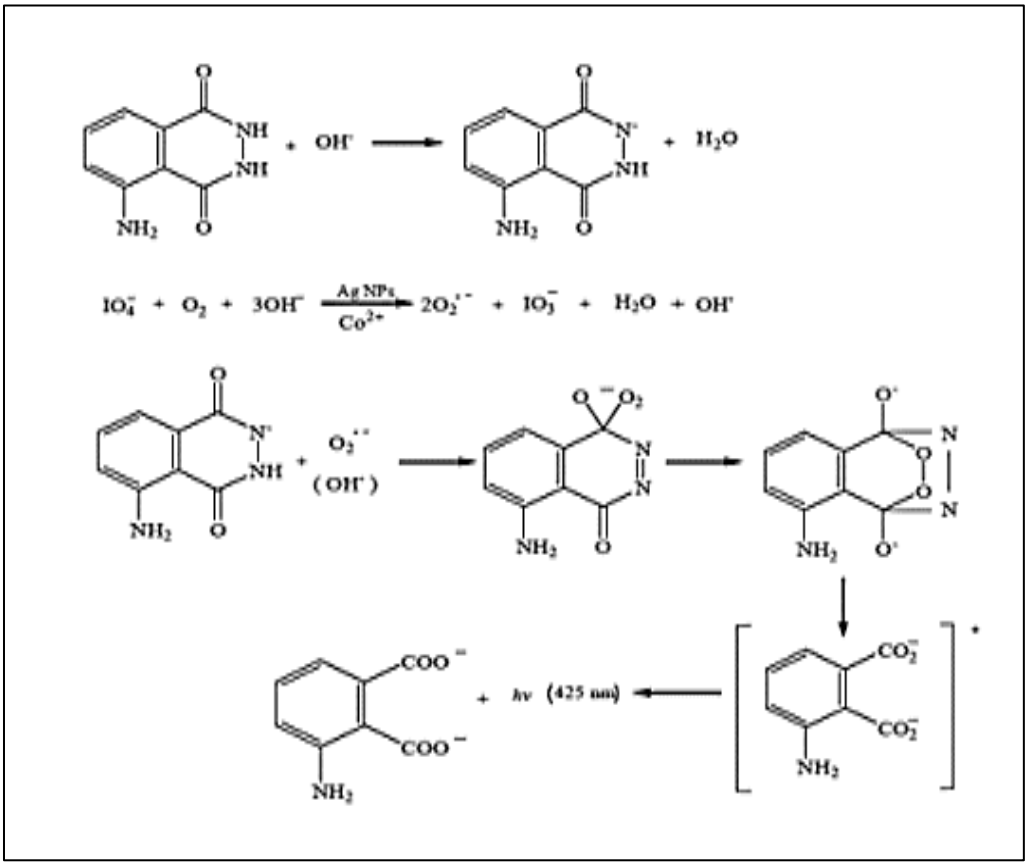

Figure 8. Proposed mechanism of Luminol with KIO_4

Beneficial effects of catalysis of dinuclear compounds (II) on the chemical reaction of the luminol (CL) were found. copper compounds (II), The luminol-H_2O_2 CL reaction of the biodegradable catalyst is the optimal level observed by the researcher, especially when the pH is high (at least 10). Since the work of biological media, it is necessary to reduce pH values. Therefore, the experiment found that the two-core copper nuclei (II) affect different pH values from 6.5 to 11.

Where the measurements were made and compared in the case of copper stimulation (II) once, and in the absence of copper compounds (II) again And comparing the values of PH meter . PH was found to have a radical effect on the promotion of CL values. Interestingly, an enhancement of the CL signal occurred in the presence of clear copper complexes (II). However, in the absence of the catalyst CL was observed neutral. After the reaction of Luminol with the H_2O_2 in solution mentioned in the absence of the Ultra weak CL catalyst, it is assumed that the nucleic acid (di nuclear) II may interact with the reactants or the medium of the

luminol reaction with H_2O_2 . It was expected that these complex mineral-free materials (L = N, N--dibenylethylenediamine, (L = N, N-dimethyl-N - Benzylethylenediamine and TAE) would have no catalytic effect. The Dynamic Copper Compounds (II), which have been found to have strong catalytic action, have a co-ordination of the copper with four residues. It is clear that the composition is sufficient to make the material active in a potential catalyst and other factors (side chains, ligament structure) also affect the movement and density of the CL chromium, the dynamic copper complexes (II) have a unique and powerful ability to promote Luminol Cl emission, Even in the absence of H_2O_2 in the primary media. This is useful in investigating new and effective molecules as an artificial peroxidase model to produce luminol efficiency [27] As shown Figure 9.

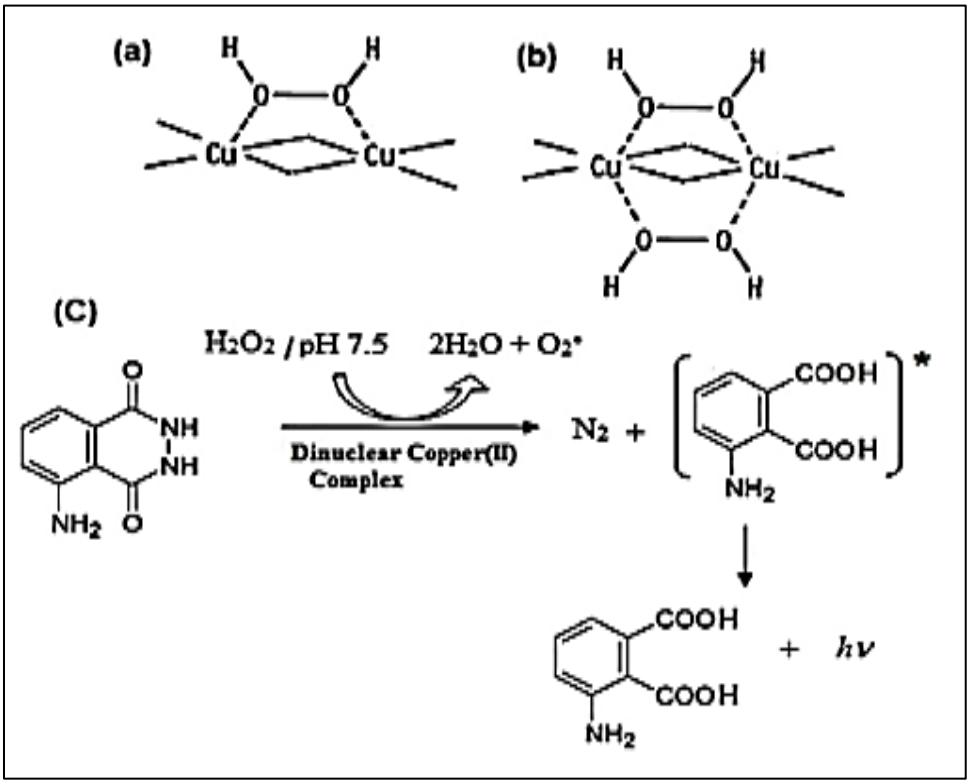

Figure 9. proposed mechanism of luminol-H_2O_2 CL system with di nuclear copper (II).

3-Aminophthalacidhydrazid alkaline hydrogen peroxide works on Luminol according to nitrogen oxidation N_2 is released free of Luminol .The reaction is stimulated by potassium hexacyanoferrat now for a long time, chemical weakness

can still be seen not the full mechanism of interaction well known [28], as illustrated in Figure 10.

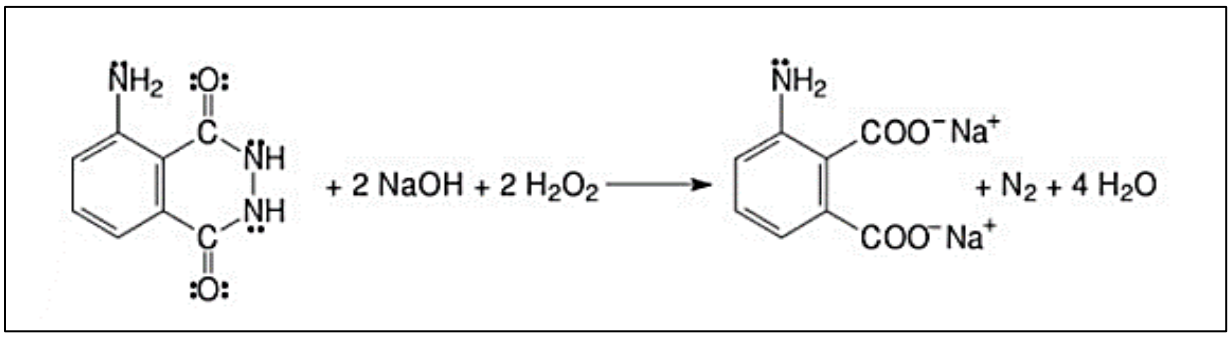

Figure 10. Mechanism of interaction luminol with peroxide and sodium hydroxide.

The researchers note that the use of luminol DPPH chemiluminescence (CL) system, better than the use of luminol solution stored in the dark for one weak, which needs to rebalance because of the free radicals formed and play an important role in the generation of a new luminol CL system. This study provided a new perspective on the process of chemiluminscence.

The technique was developed using FL-CL methods and was considered an easy and rapid method of using inhibitors on the luminol system and could be applied in several areas. The accuracy, restoration and stability of the verified method were acceptable for estimating scutellarin in both mice injected with drugs and plasma. Figure 11 illustrates the formation of diazaquinone as intermediate products using two methods of reacting once with oxygen and hydroxide, and again with hydroxide only [29].

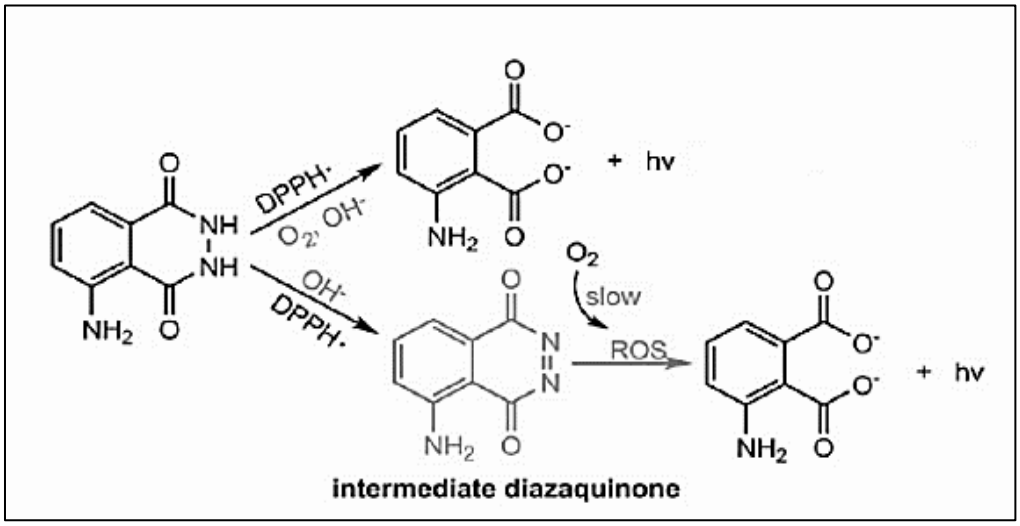

Figure 11. Luminol reaction with DPPH.

1.5. Luminol derivatives

Abeer and et al. [30] reported synthesis eight new Azodyes , derived of Luminol **L1** = 5- [(phthalyl hydrazide) azo]-6-amino indzole, **L2=** 2- [(phthaly hydrazide) azo] phenylephrine, **L3** = 3-[(phthalyihydrazide)azo]-2-Hydroxy indole Figure 12.

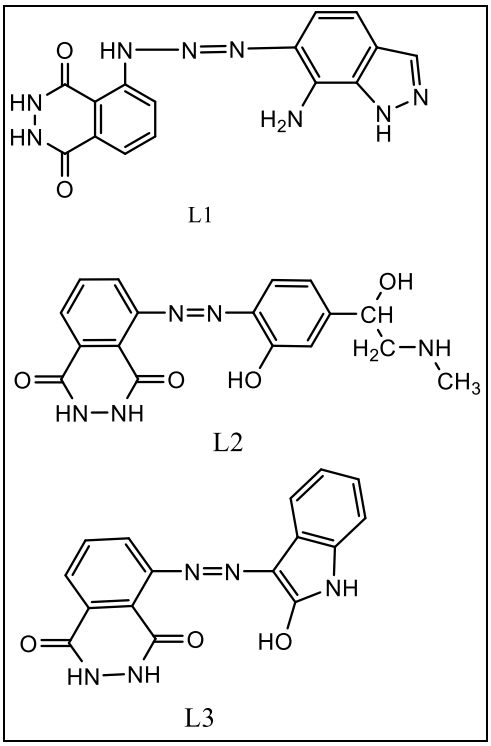

Figure 12. Luminol derivatives.

Anna pantelia et al. [31] reported the synthesis and chemiluminescence properties of eight novel phosphonium-functionalized amino-acylated luminol and isoluminol derivatives, designed as mitochondriotropic chemiluminescence reactive oxygen species trackers. Three different phosphonium cationic moieties were employed (phenyl, p-tolyl, and cyclohexyl), as well as two alkanoyl chains (hexanoyl and undecanoyl) as bridges/linkers. Synthesis is accomplished via the acylation of the corresponding phthalimides, as phthalhydrazide precursors, followed by hydrazinolysis. As depicted in Figure 13:

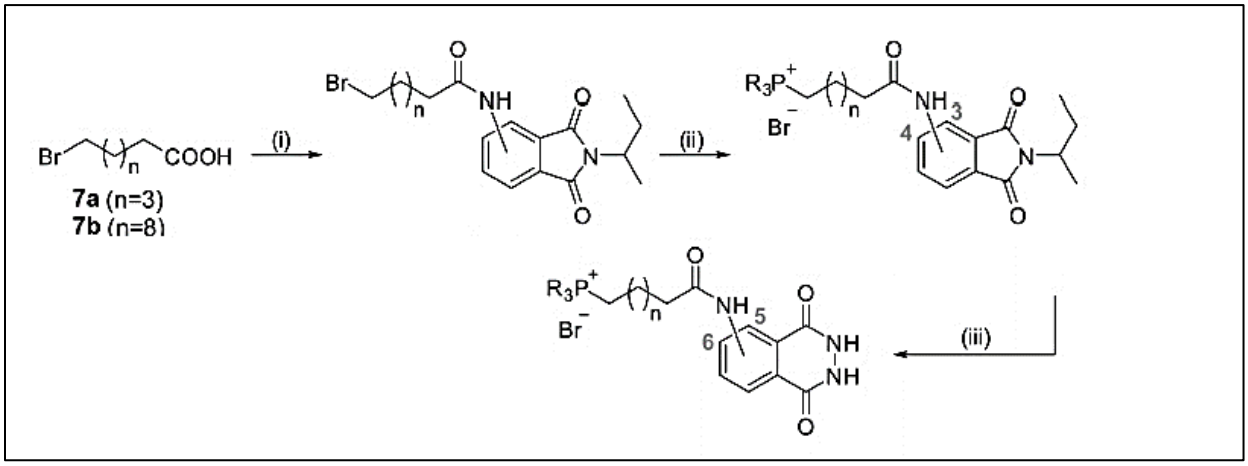

Figure 13. Synthesis of phosphonium bearing phthalhydrazides.

Luminol derivatives' chemical compositions (LC11, TF46) were prepared by : Jiao et al.[32].

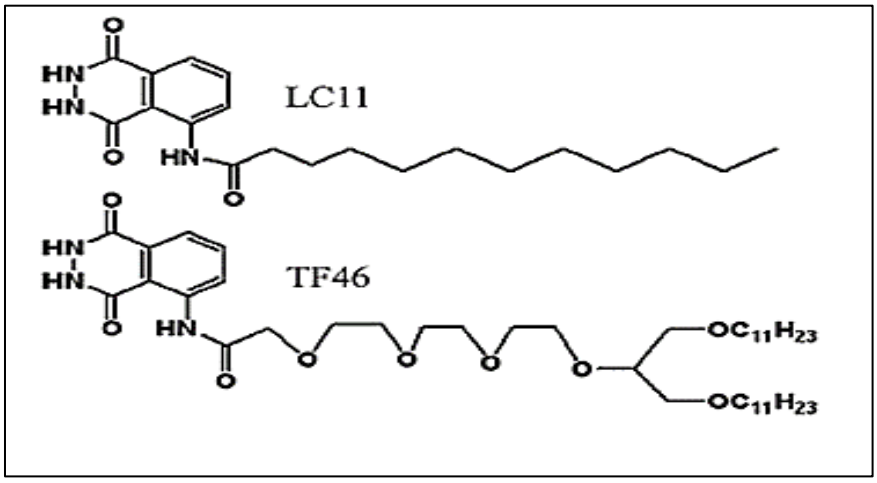

Figure 14 : Luminol derivatives (LC11, TF46).

Jiao et al. [33,34] produced some functional luminol derivatives with cholesteryl or aromatic substituted groups where designed and synthesized from the reaction of the corresponding aromatic acyl chloride precursors with luminol.

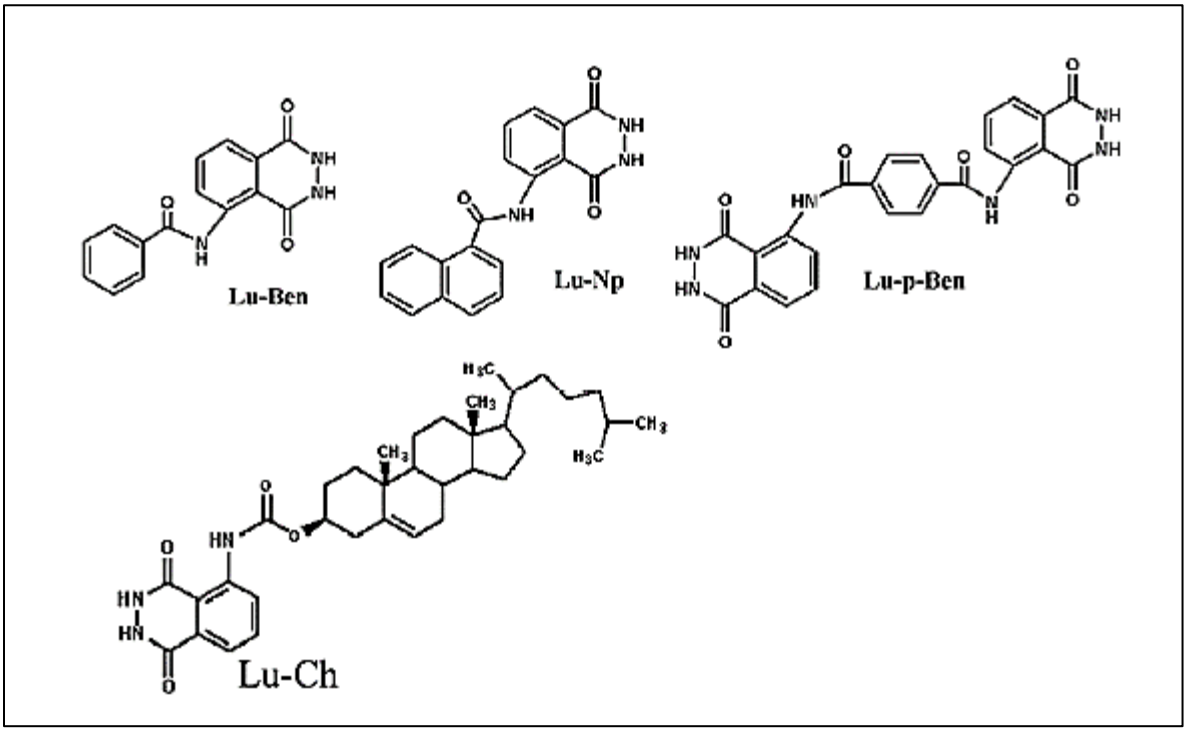

Figure 15 :Chemical structures and abbreviations luminol derivatives.

A symmetrical azo-based Luminol derivative in Figure 16 was synthesized using catalytic dehydrogenative coupling reaction procedure. This symmetrical molecule shows blue fluorescence in polar aprotic solvents (λmax = 450 nm) [35].

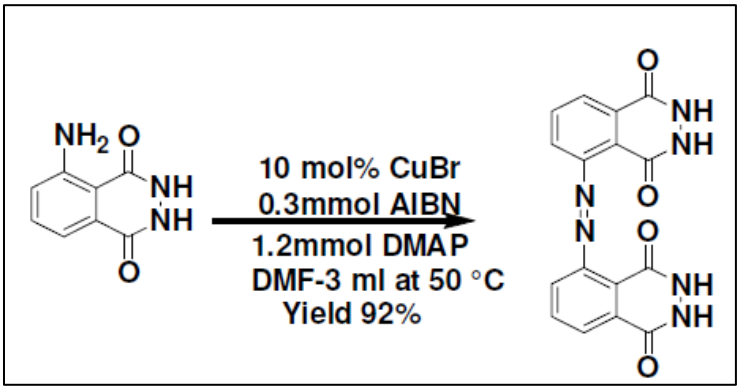

Figure 16 :Synthesis of Luminol azo derivative.

A new luminol imide derivatives with different alkyl substituent chains were designed and synthesized by Jiao and co-authors [36].

Their gelation behaviours in 26 solvents were tested as novel low molecular mass organic gelators Figure 17.

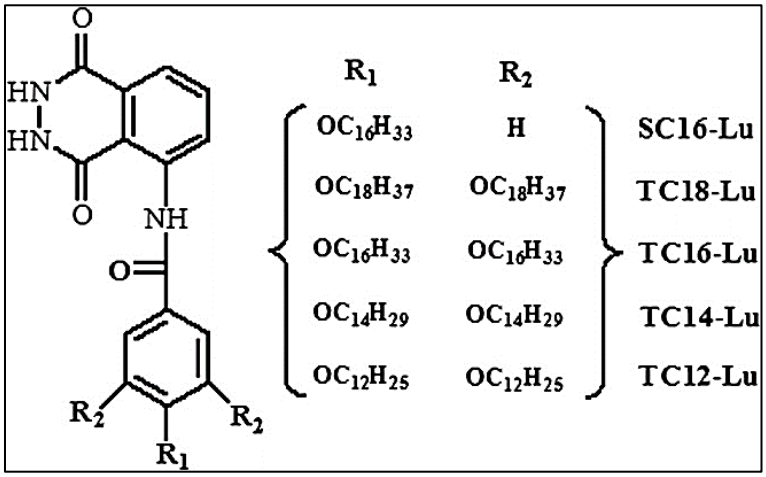

Figure 17: Molecular structures and abbreviations of these luminol imide derivatives.

A diaminophthalic hydrazide has been synthesized in seven steps from chloronitrophthalimide. The compound proved to be only about one third as efficient in light production as luminol [37]Figure 18.

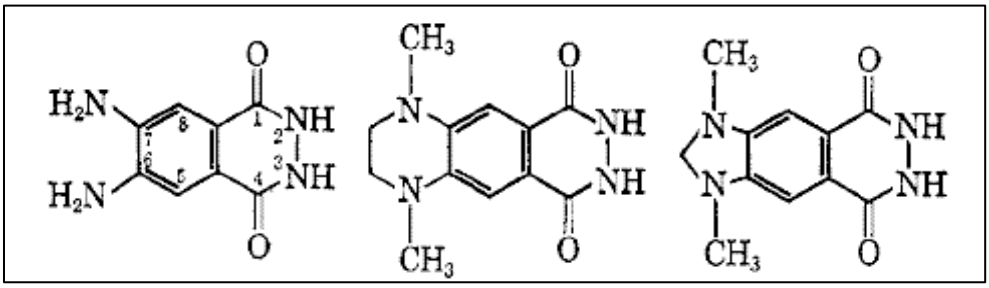

Figure18: Diaminophthalic hydrazide created in seven steps

Tyrosine-specific chemical modification was achieved using in situ hemin-activated luminol derivatives. Tyrosine residues in peptide and protein were modified effectively with N-methylated luminol derivatives under oxidative conditions in the presence of hemin and H_2O_2[38] Figure 19.

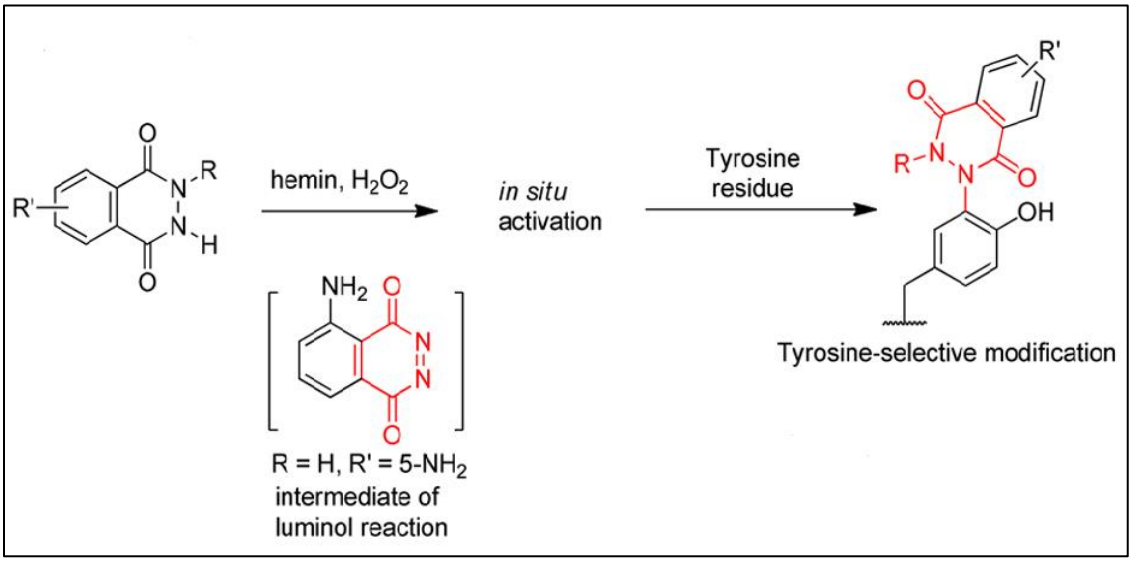

Figure 19: In situ activation of luminol derivatives .

Shibata et al. [39], synthesized a series of luminol derivatives having a hydrazide group by an easy derivatization method. Each reaction was simple and each purification was not laborious, and the reaction yields were satisfactory. The luminol hydrazide containing a dimethylene linker, could be useful for the labelling of macromolecules in the sensitive bioassay such as chemiluminescence immunoassay (Figure 20).

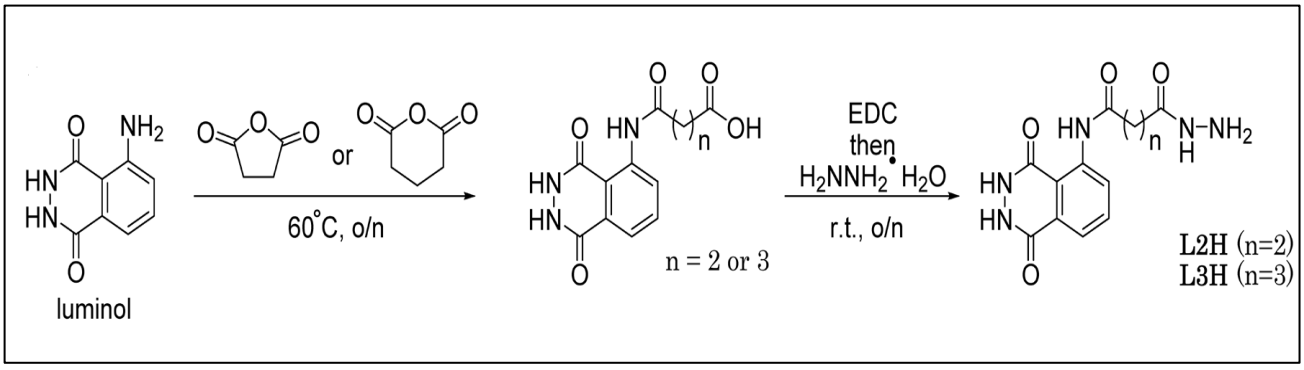

Figure 20 : Synthetic Route to Luminol Derivatives Having a Hydrazide Group.

Recently, Ewies et al [40] reacted of Luminol with various phosphorus and thiating reagents indicated the creation of distinct compounds depending on the type of the reagents (Figure 21). The less steric carbonyl group of Luminol is the favored

attack site. The antibacterial activity of the produced compounds were tested. Most of the novel chemicals' antibacterial action was highly selective against fungus.

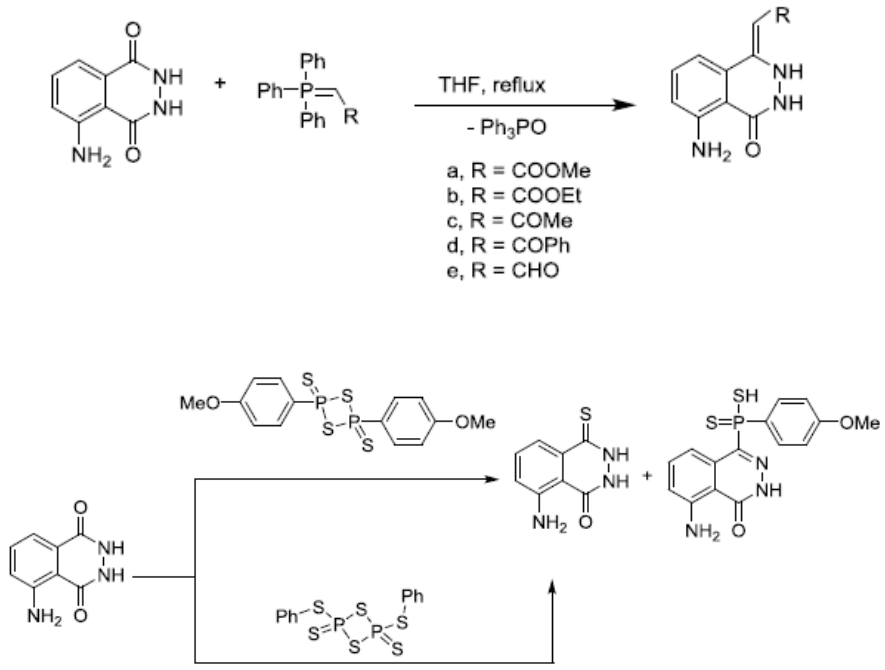

Figure 21: Reaction of Luminol with various phosphorus.

Fahad et al. [41, 42], reported that using acetylacetone to create the two new azo dyes luminol. To create complexes of metals (II) with a general stoichiometry, CuL_2 and NiL_2, these new dyes were combined in a 1:2 molar ratio with Copper and Nickel ions (Figure 22). Both gram positive and gram-negative bacteria were tested and both the ligand and their complexes were confirmed to exhibit antibacterial action.

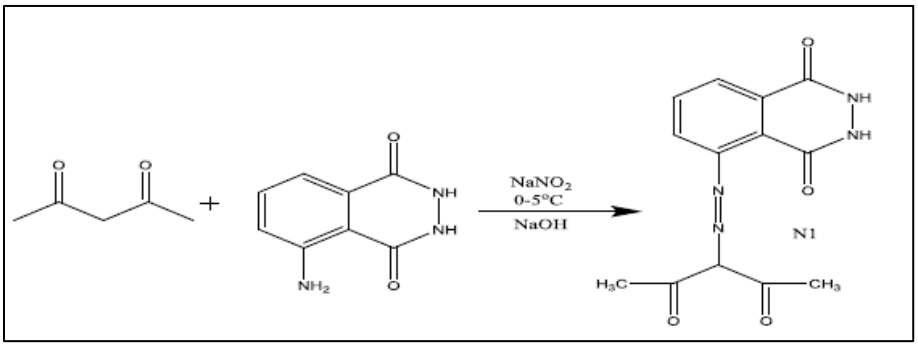

Figure 22: Creation the two new azo dyes luminol.

1.6.Applications of luminol

Over the last 30 years luminol has become one of the widest used chemiluminescent reagents for application to molecular biology and analytical chemistry. It has been used as the basis for a multitude of sensitive and selective detection methods including high performance liquid chromatography (HPLC), immunoassay, DNA probes, DNA typing and as substrate in western blot detection. More recently, also historical and archaeological studies using luminol have been successfully carried out disclosing an interesting new application field for luminol-based assays[43].

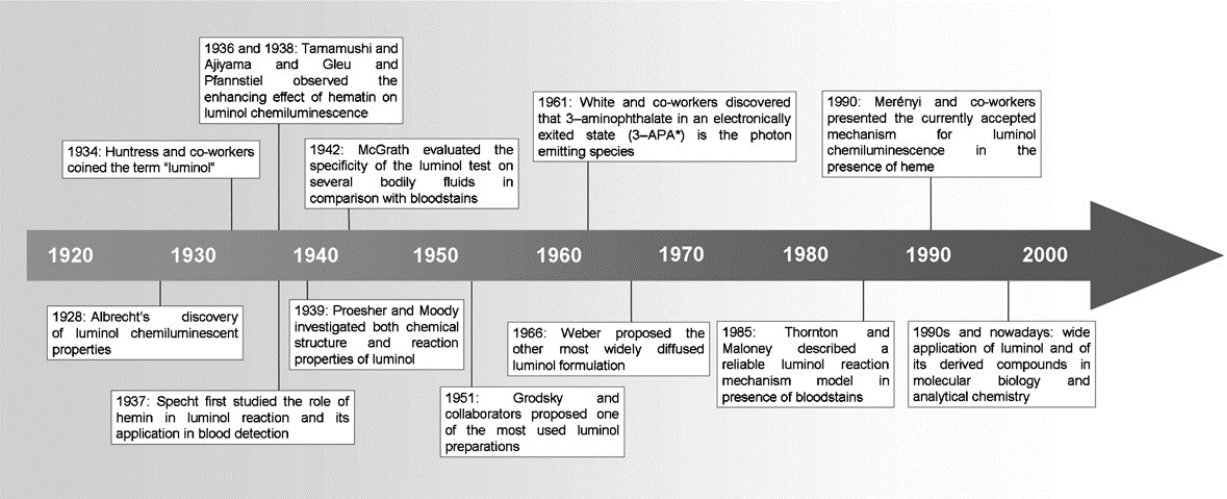

Figure 23. Luminol timeline from its discovery to the most recent developments.

Luminol is commonly used in forensics as a diagnostic tool for the detection of bloodstains. Most crime scene investigation, known as criminalistics, is based on the fact that nothing vanishes without a trace and minute particles of blood will adhere to most surfaces for years. The basic idea of luminol is to reveal these traces with a light-producing chemical reaction between several chemicals and hemoglobin , an oxygen-carrying protein in the blood. The presence of unnoticed, minute, or hidden blood stains diluted to a level of 1×10^{6} (1 μL of blood in 1 L of solution) can be detected using luminol [44, 45], disclosing the distribution of bloodstains and allowing easy evaluation of their patterns. Investigators are then able to reconstruct the source of the events of a crime by

visualizing and analyzing these patterns [46,47]. Another technique based on CL, optically pumped CL, was used in clinical laboratories for diagnostic purposes. In this technique, luminol was oxidized by pulsed laser light in an excited state with or without the participation of oxygen [48]. A relatively simple CL assay was also developed for antioxidants (e.g., vitamins C and E and proteins)[49]. based on the abolition of light emission from the enhanced CL reaction between HRP–luminol and 4-iodophenol caused by an antioxidant. The CL emission resumed after consumption of the antioxidant and duration of delay was proportional to the antioxidant [50].

CL reactions are also useful as detection reactions for components of mixtures separated by HPLC [51], flow injection and capillary electrophoresis [52, 53]. These techniques are useful in the detection of polymerase chain amplified hepatitis C DNA [54] separated by capillary electrophoresis and post-column detection (peroxyoxalate reaction) of phosphatidyl-choline and phosphatidyl ethanolamine hydroperoxides in red blood cells [55]. A method for simultaneous monitoring and identification of antioxidants in Fructus sp. Has been used by coupling high-performance liquid chromatography-diode array detector-electrospray ionization-ion trap-time of flight-mass spectrometry with post-column derivatization and luminol-potassium ferricyanide CL.

HPLC fingerprint, structural identification, and radical scavenging profile were rapidly obtained by online assay using ultraviolet absorption ,Mass spectrometry, and luminol-potassium ferricyanide CL. This method is precise, rapid, sensitive, and effective for quality analysis of medical samples and foods [56]. Nucleic acid and protein microarrays are important tools in genomic and proteomic investigations, respectively.

Although fluorescence is the dominant detection technique, CL imaging with charged, coupled detection device cameras could be used to detect molecules bound to arrays [57–61]. This technology is used for the detection of allergen-specific ige [57], cytokines [62], and differential gene expression profiling [63]. Another emerging application of imaging coupled with CL is in microscopy [64] and monitoring assays in high-density micro well plates for drug assays [65]. Another successful research application for CL is detecting the expressed products of reporter genes developed as alternatives to the traditional chloramphenicol

acetyl transferase gene[66]. Chemiluminescent dioxetane, luminol derivative-type substrates are also available to detect and quantitate expression products of genes for placental alkaline phosphatase, β-galactosidase, and β-glucuronidase [67]. These assays are sensitive and have a linear range over several orders of magnitude.

The nanomaterial-based ECL detection system has become an important subject in biosensor applications. Chai et al. [68] reported a novel strategy for the ECL detection of specific DNA sequences by combining luminol-functionalized gold nanoparticle (luminol-AuNPs) labeling and amplification of AuNPs with the biotin–streptavidin(SA)system. With the help of a novel approach, networked gold nanoparticles were prepared, along with nonionic fluoro surfactant assistance.

A strong oxidizing agent is attached to the surface of the networked gold nanoparticles that causes emission of CL from luminol without the addition of H_2O_2.These networked gold nanoparticles have been used for ultrasensitive detection of aminthiols in human plasma and urine samples [69]. A very sensitive and simple LCL method using DNA-stabilized gold nanoparticle has been used for the detection of Hg^{2+} ions in aqueous solutions [70]. Non-enzymatic determination of sugars like glucose, fructose, and other hydrolysable sugars was possible by analyzing CL emission from a luminol-tetrachloroaurate system on amicrofluidic chip [71].

1.7. General introduction to photochemistry

Photochemistry is a branch of physical chemistry that deals with the interaction of light with the matters in the UV-Vis region of the solar spectrum, normally (400 - 800 nm). When absorbing light with a sufficient energy, that is comparable to the band gap (Eg) energy of the absorbing species. This process leads to produce excited state of the absorbing species as a result of transfer electron from ground state(E_o) into the excited state (E*) of the absorbing species as follows [72–73]:

$$A + h\nu \longrightarrow A^*$$

Whereas, A is the absorbing species, h is a Blank constant, ν is the frequency of the incident light, and A* is the excited state of absorbing species.Upon absorbing

light, each of physical and chemical properties of the excited state (A*) will be different from its corresponding ground state(A). In this manner, it can be concluded that, photoreaction is a reaction that is activated by the energy of the absorbed light(E=hν).

Total energy of photons of light (E) can be calculated as follows:

$E = h\nu$,

Whereas, h is a Blank constant (6.62×10^{-34} J.sec) and ν, is the frequency of light that is calculated by the relation of $\nu = C/\lambda$, C is a speed of light $=3\times10^{8}$ m/sec, and λ is the wavelength of the absorbed light.

Generally, in recent years photochemistry play a significant role in many applications including chemical, biological, environmental and industrial applications [74]. Too recent applications of photochemistry include developed applications that are related to more complicated issues such as classical fuel problems and these are seen in applications such as clean fuel production, solar cell and other photosensitive system [75-78].

1.7.1. Photophysical and photochemical processes

When a substance particles absorb light, this results in occurrence of some processes such as transfer energy, reflection, scattering and absorbing of light. According to Law of photochemistry, only absorbing species can undergo photochemical change. In this observation, only absorbing photons of light would contribute in this process, while other part of the incident light would dissipate out of the system as a thermal or photo energy. In this case, photochemical reactions depend mainly on the energy and the intensity of the absorbing light, while normal thermal reactions depend mainly on activation energy for the formed activated complex, and on the reaction temperature. Activation of photoreaction can be presented as follows [79,80]:

$$A + h\nu \longrightarrow A^{*}$$ (Ea herein is derived from hν)

Generally, absorbing species can lose its photo-excitation energy in different ways , these involve chemical and physical routes. These routes can be summarized in the following Figure 24.

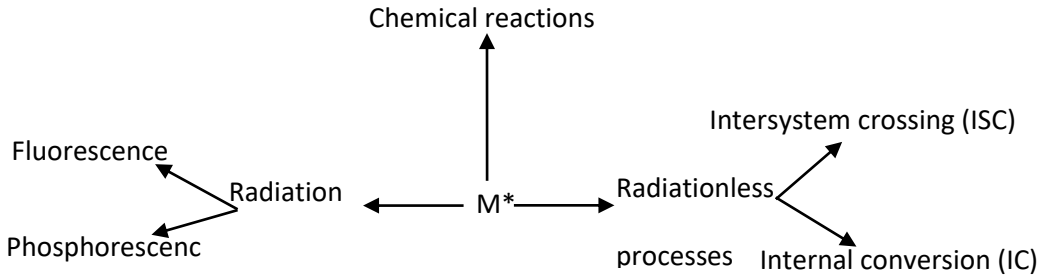

Figure 24: Fates of lose energy from photoexcited molecule(M*)

1.7.2. Photolysis processes

Photolysis reactions are a type of photochemical reactions that are initiated by absorption of radiation with a proper energy that is comparable to the Eg of the absorbing species. For example, decomposition of ozone into oxygen is performed by absorption UV light at the upper atmosphere. Synthesis of chloromethane from CH_4 and Cl_2, which is initiated by absorption of radiation according to the following reaction and the overall reaction is as follows

$$CH_4(g) + Cl_2(g) + h\upsilon \rightarrow CH_3Cl(g) + HCl(g),$$

Photolysis (also called photo dissociation and photodecomposition), is a chemical reaction in which the bonds in organic or inorganic molecules(absorbing species) are broken down to yield new formed species. The photolysis reaction is not limited to the effects of visible light but any photon with sufficient energy can cause the chemical transformation of the inorganic bonds of a chemical.

Since the energy of a photon is inversely proportional to the wavelength, electromagnetic waves with the energy of visible light or higher such as visible and ultraviolet light can initiate photolysis reactions.

Photolysis also can be defined as the decomposition of absorbing species by absorption of solar spectrum or artificial light of a chemical mixture composed of direct and indirect photolysis. The organic compounds absorb UV rays in the direct photolysis process, while photosensitizers such as oxygen and hydroxyl or peroxide radicals do the disintegration of light in indirect photolysis. If the organic

compounds are light sensitive, the main method of elimination will be optical dispersion. The photolysis method is common in surface water, which plays an important role in surface water or wastewater management as an additional step of elimination [81]. The strength and frequency of light are based on photochemical decomposition. Several studies investigated tetracycline optical disintegration (a category of antibiotics that are very light sensitive) and found that their efficiency of removal was about 80%, and the efficiency of removal of for total organic carbon was about 14%, reflecting the development of intermediate compounds. Wastewater treated was more toxic than the wastewater input. In the case of antibiotics, the proportions of direct and indirect photolysis for different compounds in the water system are different [82].

1.7.3. Photoctalytic reactions

The photocatalysis process is a type of photochemical reactions that requires presence of a solid photocatalyst suspended in reaction mixture with irradiation with light. Excellent properties of photoctalytic nanoparticles have been applied in a wide range of applications such as treatment of pollutants in wastewaters, soil and air. These materials are also used in producing of energy as in fuel cells and solar cells. Some nanomaterials such as oxides [83–85], Due to their improved and tunable optical properties, semiconductors [86, 87], metals [88, 89], and graphene [90, 91] have demonstrated a significant impact on photocatalysis processes [92, 93]. due to their enhanced and controllable optical properties, which makes them excellent photocatalysts.

In general, photocatalysis can be defined as a series of chemical reactions that are initiated by absorption of electromagnetic radiation by the reacting species. This will cause excitation of atoms or molecules of the irradiated materials that results in radicals that affect as scavenger [83]. Photocatalysis process can be divided into two main stages: reduction and oxidation [94]. When a material is irradiated with photons with energy equal to or higher than its bandgap (Eg), electrons in the valence band (VB) would transfer to the conduction band (CB) leaving positive holes(h^+) in the valence band. The generated electrons and holes lead to the formation of reactive oxygen spices such as $O^{\cdot\,2-}$ and $OH^{\cdot}$ The kind of produced reactive species depends on the type of materials that are adsorbed on the surface of the photocatalyst and irradiated photons.

The formation of reactive species is an important role photocatalysis processes as it can cause various effects such as degradation of dyes and other organic molecules [92] and antibacterial activity [95].

1.7.4. Homogeneous and Heterogeneous catalytic processes

In homogeneous photocatalysis, catalyst and reactants have same phases (single-phase) under visible and UV irradiation with production $OH^{\cdot}$ radicals that play an important role in damage of organic pollutants commonly in water such as textile dyes and other organic molecules. The first applications concerned the use UV/ ozone and UV/Hydrogen peroxide.

The usages of UV light in the photodecomposition of organic contaminants can be classified into two main areas

1- Photooxidation, which deals with the employment of UV light plus an oxidant to generate hydroxyl radicals, that attack the organic pollutants.

2- Direct photo degradation depends on direct excitation of the organic contaminant by UV light.

For homogeneous photocatalysis system, all the reacting species are present in the same physical state, this type of photoreactions is carried out by mixing reacting species with irradiation using a light with energy that is comparable to the Eg of absorbing species. This type of reactions is very important from environmental and industrial view. For example, the use of UV light and UV/H_2O_2 was applied in purification of water from some toxic organic materials, removing of organic pollutants from air, water, and soil , also many industrial applications are conducted using this phenomenon [96]. For heterogeneous photocatalytic reactions, the used photocatalyst is normally found in different phase from other reaction mixture (solid), and the other components of reaction mixture are present in liquid phase. Irradiation of reaction mixture is performed using either normal sunlight (solar radiation), or using artificial radiation from different sources such as mercury vapor lamp, xenon lamp and tungsten lamp [97,98]. For this system, illumination of reaction mixture with light leads to absorb photons of light by particles of the used solid photocatalyst. This process leads to produce valence band hole(h+) at the valence band hole of the particle (VB), with conduction band

electron (e-) at the conduction band (CB). These redox species would contribute in oxidation/reduction reaction for the pre-adsorbed species at the surface of the photocatalyst particles, normally these adsorbed species will be oxygen, reacting species molecules and water molecules [98].These events are presented in Figure 25.

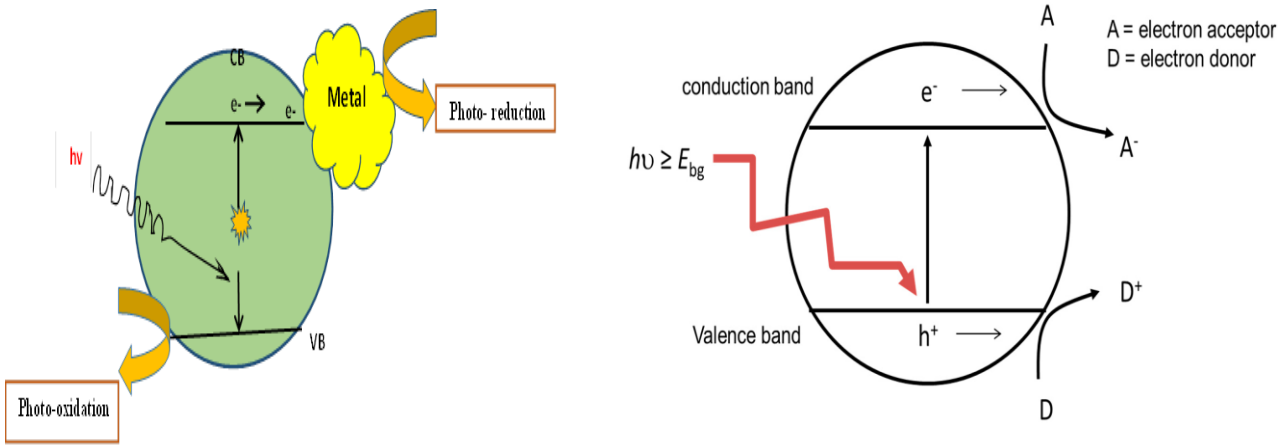

Figure 25: Events upon photo excitation of particle of a desired photocatalyst

The result of these redox reactions is the formation of some reactive species such as $O^{\cdot}$, O^{2-} , OH^{-} , $OH^{\cdot}$ and H_2O_2 [99,100]. Now, these reactive species would contribute in reaction with reacting species that are adsorbed at the surface of the used photocatalyst. The result of the later step is the destruction or fragmentation and/or other type of chemical reactions.

1-7-5. Semiconducting photocatalysts

1.7.5.1. Semiconductors

Semiconductors are crystalline or amorphous solid materials, which have different values of electrical conductivity. The intermediate values for its bandgap (Eg) is varied between a metal (Eg< 2) and an insulator (Eg > 4), its band gap can be altered by introducing some impurities or by surface modification , or size in quantum dot or by illumination with light [101].

According to band theory, at zero Kelvin (0 K), a perfect crystal of semiconductor materials (SC) consists of group of very close and filled electronic states, fill with electrons and this is valence band (VB) of the SC and no electrons in the conductive band, the region between valence band and conductive band is called band gap [102]. Semiconductors are particularly useful as photo catalysts such as ZnO, CdS, TiO_2, CoO, NiO, and Cr_2O_3) because these semiconductors can absorb photon with a proper energy with high efficiency. As a result of this absorption, both of conduction band electrons and valence band holes are generated. After that, these produced redox species would contribute in redox reactions at the surface of the used photocatalyst [103–108]. In recent years, more interest was directed towards developing catalytic properties of photocatalysts, especially the concern of its photo response in the visible region of the solar spectrum to avoid all aspects that are dealing with use artificial light.

An important deal with the photocatalysts includes inorganic molecular, and hybrid organic/inorganic materials incorporation of these materials within photocatalyst. This modification of the photocatalyst can lead to reach specific requirements that can enhance the efficiency of the used photocatalyst such as achieving a red shift in absorption towards visible region of solar spectrum, photo induced charge separation, and a faster photocatalytic reaction. Generally, semiconducting materials are used widely in wide range of applications and this is due to their low cost, high photocatalytic activity, chemical and photochemical stability , nontoxicity, high thermal and photo stability [109,110].

1.7.5.2. Cobalt oxide as a photocatalyst

The degradation of the synthetic dyes and other organic species can be achieved in the presence of photocatalysts such as zinc oxide, cobalt oxide (Co_3O_4), nickel oxide (Ni_3O_4) and TiO_2 and other photocatalysts. These photocatalysts can be used effectively in treatment of pollution of water, air and soil with the polluted dyes [111]. Different methods can be applied in pollution treatment and among these methods, photocatalytic degradation methods seems to be an interesting alternative method that can be used effectively in the removal of these dyes from textile effluents. According to this method, semiconductors photocatalysts play an important role in dyes removal from their waste waters.

These photocatalysts have large surface area, chemically inert, low cost, thermally and photos table stable, easy to synthesis and they are easy to be recycled for mulyusages [112,113].

Generally, cobalt oxide (Co_3O_4) has important catalytic properties which enable it to be used for many environmental applications.

Recently, Co_3O_4-NPs have gained considerable attention due to their unique and important applications. These NPs have applications in gas sensors, lithium ion batteries, solar selective absorbers, capacitors, field emission materials, energy storage systems, eletrochromic thin films, magneto resistive devices and catalysis [114]. In recent years, graphene and Co_3O_4 composites have been reported in which cobalt oxide helps in increasing the dimensional stability of substrate [115]. cobalt oxide (Co_3O_4) NPs have been used widely as a photocatalyst due to its excellent catalytic properties including its moderate band gap energy, high thermal stability, nontoxicity, low cost of synthesis and its eco-friendly properties. applications [116]. Co_3O_4 is an antiferromagnetic p-type semiconductor with a Eg 2.19 eV [117,118]. Generally, cobalt oxide consider as a multifunctional material and can be used in wide range of applications such as biomedical applications (antibacterial, antiviral, antifungal, therapeutic agents, anticancer, and drug delivery), gas sensors, solar selective absorbers, anode materials in lithium-ion batteries, energy storage, pigments and dyes, field emission materials, capacitors, heterogeneous catalysis, magneto-resistive devices, and electronic thin films .The oxides of cobalt are abundant in nature, as only the Co_3O_4 and CoO are stable , with Co_3O_4 possessing the highest stability [119,120].

The aims of study:

- Synthesis of new functional derivatives based on luminol and different carboxyl drugs and different amino drugs and characterization by FT-IR, ^{1}H NMR ,^{13}C-NMR and CHNS .
- Study of different physical properties and the solubility for the synthesized compounds in different solvents .
- Study anti–bacterial activity for drugs and prepared compounds.
- Study photolysis and photocatalytic degradation of some of these synthesized compounds.

CHAPTER TWO

Experimental part

2. Experimental part

2.1. Chemicals

The chemicals used are of the highest purity available. The chemicals, supplier, and purity were recorded in Table 1 .

Table 1: Supplier and Purity for used chemicals

Chemicals	Supplier	Purity%
Acetone	Fluka	99.9
Chloroform	Fluka	99.9
Dichloromethane	Fluka	99.7
Diethyl ether	Fluka	99.9
Dimethylsulfoxide	Fluka	99.5
Ethanol absolute	CDH	99.9
Ethyl acetate	CDH	99.9
n-Hexane	Fluka	99.7
Petroleum ether	Fluka	99.9
Triethylamine	Fluka	99.9
Methanol	Fluka	99.9
Thionyl chloride	Fluka	99.9
3-nitrophthalic acid	Sigma-Aldrich	99.8
hydrazine	Fluka	99.9
diethylene glycol	CDH	99.7

Sodium dithionite	Fluka	99.9
Ceftriaxone	Samarra comp.	99.8
Ibuprofen	Samarra comp.	99.9
Naproxen	Samarra Comp.	99.9
Mefenamic acid	Samarra Comp.	99.9
Sodium hydroxide	Fluka	99.9
ampicillin	Samarra Comp.	99.9
Diclofenac acid	Samarra Comp.	99.9
Ciprofloxacin	Samarra Comp.	99.9
Cephalexin	Samarra Comp.	99.9
Cefotaxime	Samarra Comp.	99.9
theophylline	Samarra Comp.	99.9
Paracetamol	Samarra Comp.	99.9
Theophylline	Samarra Comp.	99.9
Amoxicillin	Samarra Comp.	99.9
Succinic anhydride	Sigma-Aldrich	99.8

2.2. Instruments:

2.2.1. Fourier Transformation Infrared spectrophotometer FTIR

FT-IR spectra for the synthesized compounds were recorded on a Bruker, in the Chemistry Department, College of Science, University of Babylon ,Iraq.

2.2.2. Melting point apparatus

SMP30-Melting point apparatus, melting points for prepared derivatives were determined ; Chemistry Department, College of Science, Babylon University, Iraq.

2.2.3. Nuclear magnetic resonance spectrophotometer

^{1}HNMR and ^{13}C-NMR were recorded on an Innova , model Innova 5-oxford 500 Magnet NMR spectrophotometer, operating at (500MHz) for ^{1}HNMR and (125 MHz) for ^{13}CNMR. The chemical-shifts (δ) were measured in ppm in the University of Tehran's Central lab, Iran .with TMS as a standard (δ=0.0ppm).

2.2.4. Elemental Analysis (CHNS)

Euro EA3000Elemental Analyzes in the central laboratory of the University of Tehran, the analysis of the microelements carbon, hydrogen, nitrogen, and sulfur was carried out ,Iran.

2-2-5.Thin layer chromatography (TLC)

Aluminum plates covered in a 0.25mm layer of silica-gel underwent TLC.

2.2.6. UV-Visible spectrophotometer

UV-absorptivity's were recorded with double beam PG CECILCE7200 Spectrophotometer, using quartz cells with a light path of (1cm) in two pre-prepared puffer solutions (pH= 2 and 8), at University of Babylon, College of Science.

2.2.7. Optical irradiation system

Irradiation for some prepared derivatives were determined on optical irradiation system ; Chemistry Department, College of Science, Babylon University

2.2.8. Field emission scanning electron microscopy

FE-SEM, Zeiss , Germany Tehran University, IRAN.

2.2.9. X- Ray Diffract meter

Philips pw 1730 , Tehran University, IRAN.

2.2.10. Centrifuge

Laboratory R8C,REMI-Germany,Babylon University/Chemistry Department

2.3. Preparations:

2.3.1. Synthesis of luminol

A 20x150-mm test tube was heated using a bunsen burner, after mixing 1g of 3-nitrophthalic acid and 2 mL of an 8% aqueous solution of hydrazine until the solid is dissolved. Exact 3 mL of diethylene glycol (D-E. G) was transferred to the tube and clamp vertically on a bunsen burner.The solution has been forcefully boiled to remove any remaining water (110-130) °C. The temperature was allowed to rapidly climb until it reaches 215 °C for 3-4 minutes. The temperature of this reaction was determined using a thermometer.The heat was turned off, then the time was recorded, and a temperature was maintained of (215-220) °C for 2 minutes using occasional mild heating. The tube of reaction was removed from the burner, then was cooled to about 100 °C (crystals of the product frequently form). The 15 mL of hot water was added, chilled under running water, and collected the light yellow granular nitro compound. A 3 M NaOH solution was added immediately to the uncleaned test tube, which the nitro compound produced inside it, and stirred using a glasses rod, then added 3g of sodium hydrosulfide hydrate ($Na_2S_2O_4$. H_2O) that leads to form a deep brown-red solution. Wash the edges of the tube with a little water. The solution was heated to the boiling point, stirred, and kept the mixture hot for 5 min, during which time some of the reduction products may separate. 2 mL of acetic acid was added to the solution. Then below, the tap cools and mixes. Gather the resultant yellow luminol was precipitated, filtered more than once, and washed with ethanol.

2.3.2. Synthesis of acid chloride (T1-T9)

In a fume hood ,in a beaker 100 mL, an excess of thionyl chloride was added to (1.0 mmol) of carboxylic drugs ((0.34 g.) ampicillin, (0.24 g.) Mefenamic acid, Diclofenac acid (0.29 g.), Ibuprofen (0.21 g.) , Naproxen (0.23 g.) , Cephalexin (0.35 g.) , Ceftriaxone (0.55 g.) , Ciprofloxacin (0.33 g.) , Cefotaxime (0.46 g.)) respectively and left at room temperature for 30 min with stirring, after that the mixture was separated by diethyl ether and then the precipitates were filtered. The reaction of this preparation as shown in the following equation 1[121] .

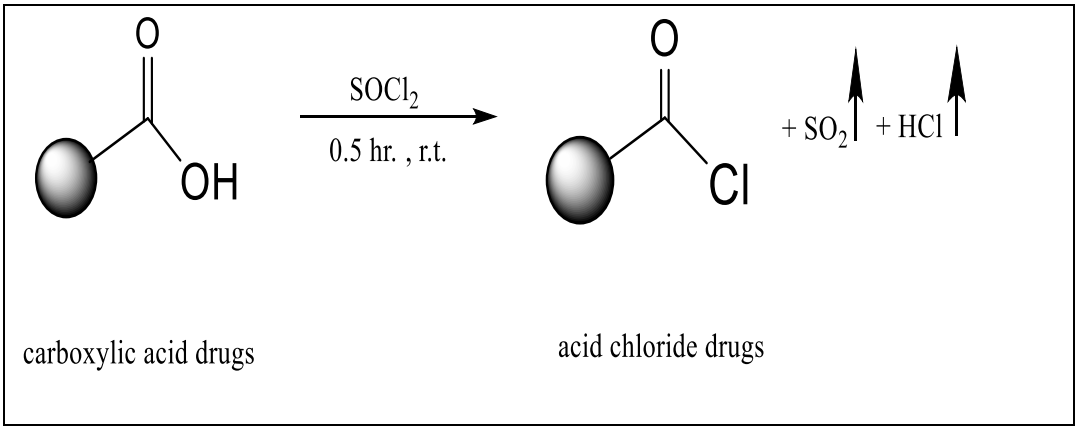

Equation 1 : synthesis of acid chloride drugs (T1-T9)

2.3.3. Synthesis of derivatives (TH1-TH9)

Synthesis of LM derivatives TH1-TH9 were synthesized as follows : (0.2g.,1mmol) of luminol was dissolved in 10 ml of DMSO and then added to the beaker containing (1mmol) of acid chloride : ampicillin (0.37 g.), Mefenamic acid (0.26 g.), Diclofenac acid (0.31g.), Ibuprofen (0.22 g.), Naproxen (0.25 g.), Cephalexin (0.36 g.), Ceftriaxone (0.57 g.) , Ciprofloxacin (0.34 g.), Cefotaxime (0.47 g.) dissolved in (10 ml) of DMSO. The mixture was heated at 60 ℃ for 3 hr. , After that,(0.087 g., 3.0 mmol) of triethylamine was added to the mixture and the obtained mixture was kept under these conditions for 30 min. Then, the mixture was cooled by ice bath until the precipitate was appeared, filtered and dried.The product as shown in equation 2 [122].

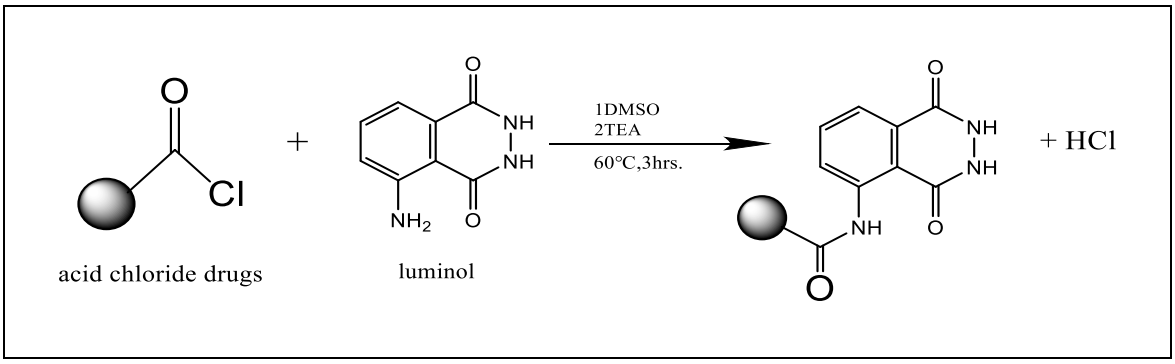

Equation 2: General equation for synthesis (TH1-TH9).

2.3.4. Chemical structure and physical data for prepared compounds (TH1-TH9).

Compound TH1:

The Molecular formula of TH1 ($C_{22}H_{19}N_3O_4$) and molecule weight was 389.41, Dark brawn solid , the percentage of obtained was 89% and melting point was observed between 210-213 ℃ . the solvent of system in TLC was (9:1)(acetone /hexane) and the R_f was 0.76 .

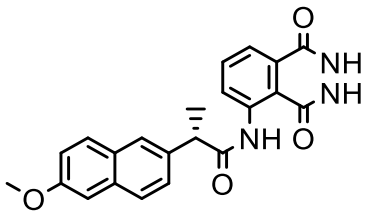

Compound TH2:

The Molecular formula of TH2 ($C_{21}H_{23}N_3O_3$) and molecule weight was 365.43 , Light Green , the percentage of obtained was 87% and melting point was observed between283-286 ℃ . the solvent of system in TLC was (7:3) (acetone /hexane) and the R_f was 0.78 .

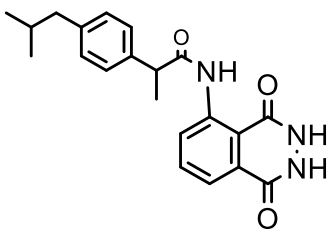

Compound TH3:

The Molecular formula of TH3 ($C_{22}H_{16}Cl_2N_4O_3$) and molecule weight was 455.30 , orange solid, the percentage of obtained was 92% and melting point was observed between 264-266 ℃ . the solvent of system in TLC was (8:2) (acetone /hexane) and the R_f was 0.71 .

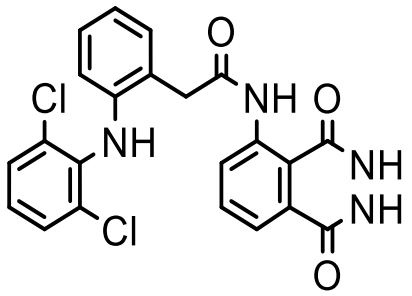

Compound TH4:

The Molecular formula of TH4 ($C_{24}H_{22}N_6O_5S$) and molecule weight was 506.54, orange solid , the percentage of obtained was 85% and melting point was observed between105-107 ℃ . the solvent of system in TLC was (9:1) (acetone /hexane) and the R_f was 0.68 .

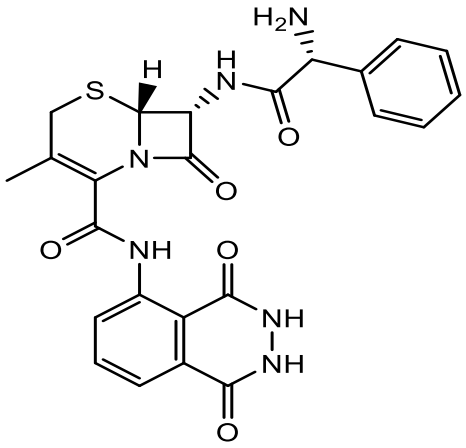

Compound TH5:

The Molecular formula of TH5 ($C_{25}H_{23}FN_6O_4$) and molecule weight was 490.18, Reddish brawn solid , the percentage of obtained was 93% and melting point was observed between104-107 ℃ . the solvent of system in TLC was (9:1) (acetone /hexane) and the R_f was 0.72 .

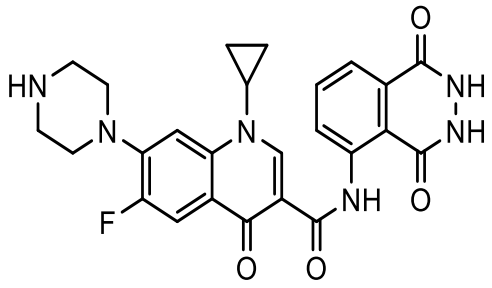

Compound TH6:

The Molecular formula of TH6 ($C_{23}H_{20}N_4O_3$) and molecule weight was 400.44 , dark brawn solid , the percentage of obtained was 87% and melting point was observed between 215-217 ℃ . the solvent of system in TLC was (9:1) (acetone /hexane) and the R_f was 0.46 .

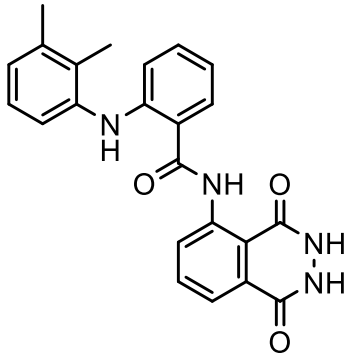

Compound TH7:

The Molecular formula of TH7 ($C_{26}H_{23}N_{11}O_8S_3$) and molecule weight was 713.09, Brawn solid , the percentage of obtained was 78% and melting point was observed between 245-246 ℃. the solvent of system in TLC was (9:1) (acetone /hexane) and the R_f was 0.65.

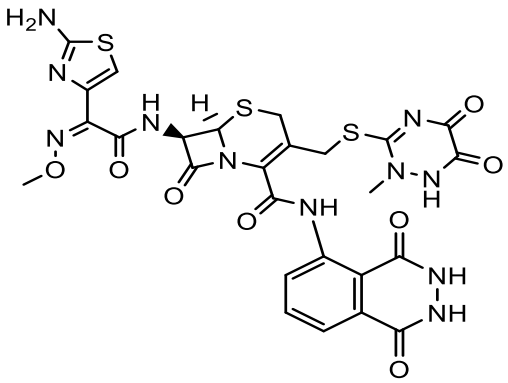

Compound TH8:

The Molecular formula of TH8 ($C_{24}H_{24}N_6O_5S$) and molecule weight was 508.55 , Brawn solid , the percentage of obtained was 83% and melting point was observed between 249-252 % .the solvent of system in TLC was (9:1) (acetone /hexane) and the RF was 0.63.

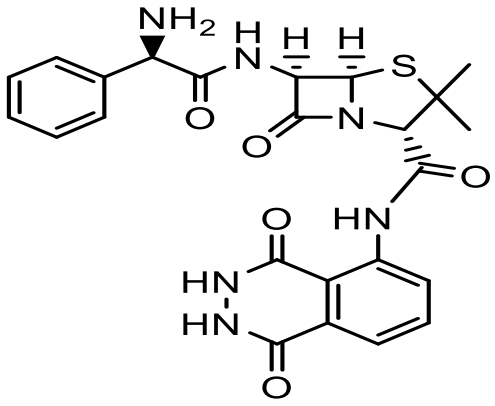

Compound TH9:

The Molecular formula of TH9 ($C_{24}H_{22}N_8O_8S_2$) and molecule weight was 614.10, dark brawn solid , the percentage of obtained was 91 % and melting point was observed between 231-234 ℃ .the solvent of system in TLC was (9:1) (acetone /hexane) and the R_f was 0.77.

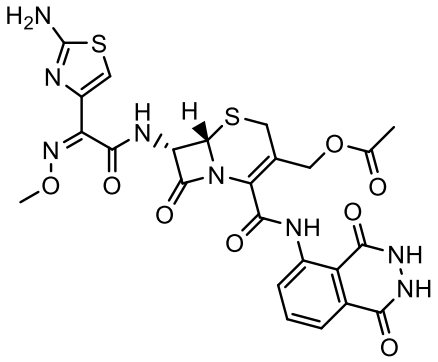

2.3.5. Synthesis of derivatives (TH10-TH15)

Luminol (1mmol ,0.2 g.) and (1mmol ,0.1g.) of succinic anhydride were dissolved in(10 ml)of DMSO .The mixture was left at 50 ℃ for (2 hrs.) with stirring. after that, The mixture of the reaction was added thionyl chloride (0.12g,1mmol) at room temperature for (30 min.) . 1mmol of amino drugs: cephalexin (0.32 g), Mefenamic acid (0.26 g), paracetamol(0.15 g), theophylline(0.18 g), amoxicillin (0.36 g), ampicillin (0.34 g) dissolved in 10ml of DMSO were added to the above the mixtures and heated for (3hrs.) at (50-60 ℃) with stirring . Triethylamine (TEA)(0.087 g., 3.0 mmol) was added and the mixtures were heated again for (30 min). The progress of reactions was monitored by TLC. Then, the mixture was cooled by ice bath until the precipitate was appeared, filtered and dried the product[123].

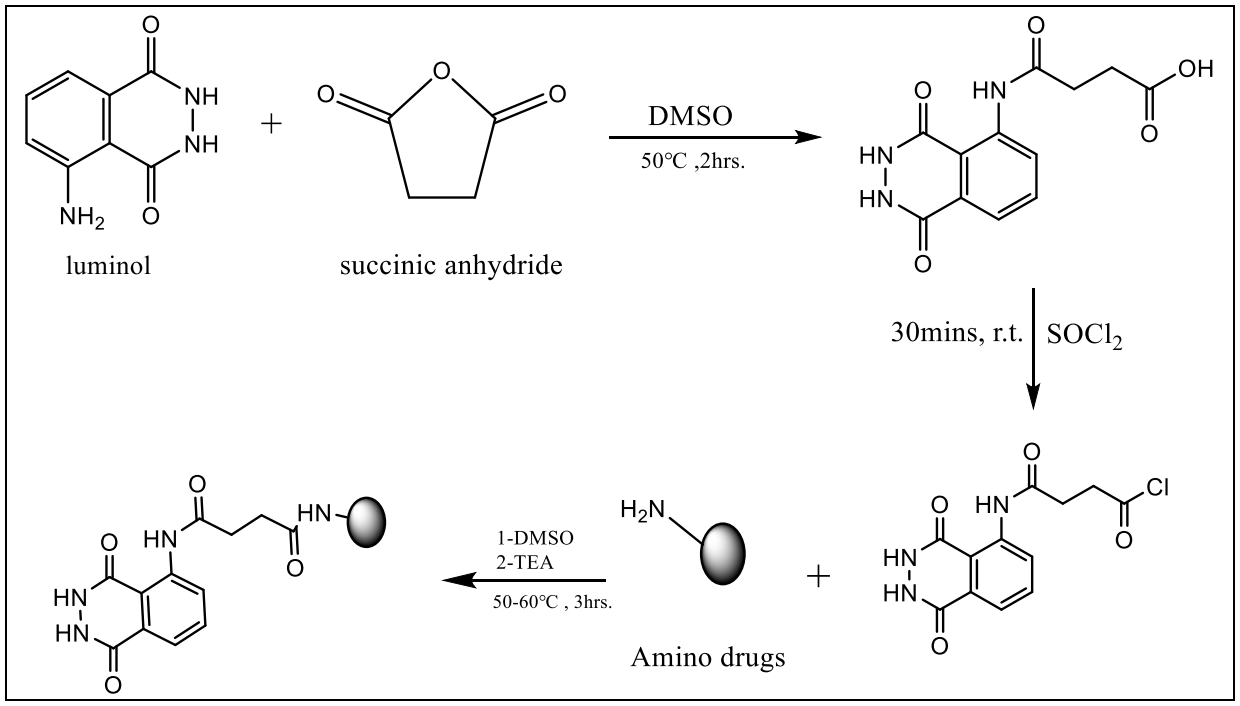

Equation 3: Schematic description for synthesis compounds (TH10-TH15)

2.3.6. Chemical structure and physical data for prepared compounds(TH10-TH15).

Compound TH10:

The Molecular formula of TH10 ($C_{29}H_{28}N_6O_8S$) and molecule weight was 620.64, Brawn solid , the percentage of obtained was 90 % and melting point was observed between 260-263 ℃ .the solvent of system in TLC was (9:1) (acetone /hexane) and the R_f was 0.62.

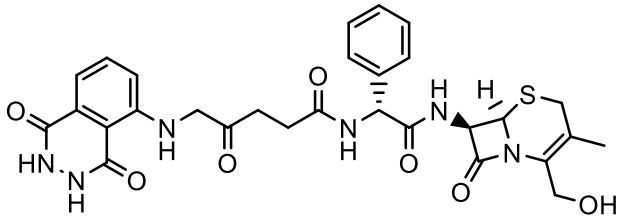

Compound TH11:

The Molecular formula of TH11 ($C_{27}H_{24}N_4O_6$) and molecule weight was 500.51, light Brawn solid , the percentage of obtained was 85 % and melting point was observed between 210-212 ℃ . The solvent of system in TLC was (8:2) (acetone /hexane) and the R_f was 0.75.

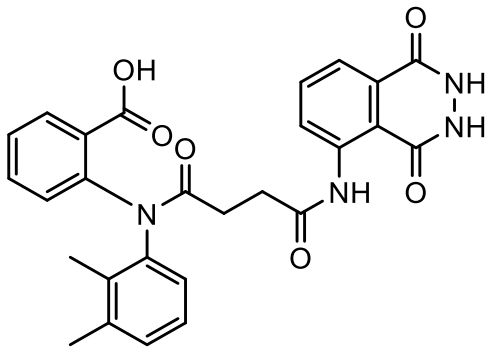

Compound TH12:

The Molecular formula of TH12 ($C_{20}H_{18}N_4O_6$) and molecule weight was 410.39, dark Brawn solid , the percentage of obtained was 90 % and melting point was observed between 223-225 ℃. The solvent of system in TLC was (8:2) (acetone /hexane) and the R_f was 0.69.

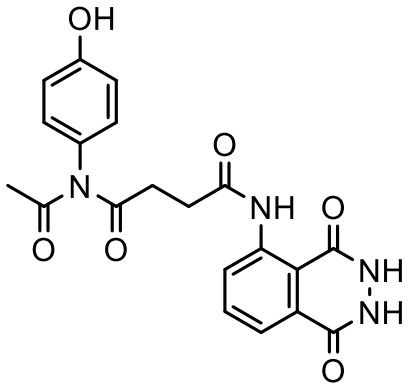

Compound TH13:

The Molecular formula of TH13 ($C_{19}H_{17}N_7O_6$) and molecule weight was 439.39, Brawn solid , the percentage of obtained was 82 % and melting point was observed between 110-113℃ . The solvent of system in TLC was (9:1) (acetone /hexane) and the R_f was 0.74.

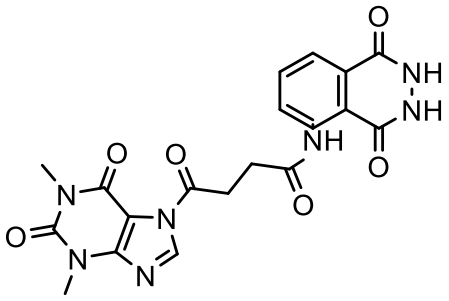

Compound TH14:

The Molecular formula of TH14 ($C_{28}H_{28}N_6O_9S$) and molecule weight was 624.63, dark Brawn solid , the percentage of obtained was 88 % and melting point was observed between245-247 ℃ . the solvent of system in TLC was (9:1) (acetone /hexane) and the R_f was 0.61.

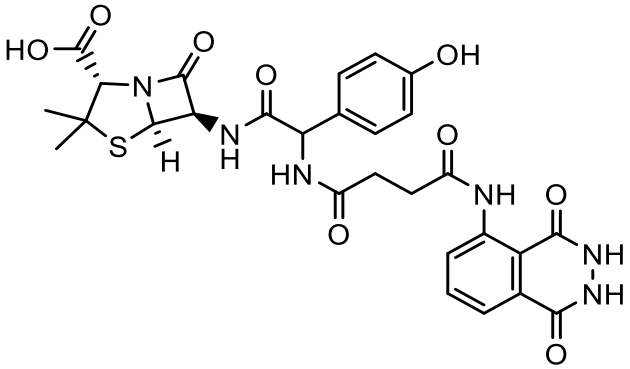

compound TH15:

The Molecular formula of TH15 ($C_{28}H_{28}N_6O_8S$) and molecule weight was 608.63 , Brawn solid , the percentage of obtained was 93 % and melting point was observed between 122-125℃ . The solvent of system in TLC was (9:1) (acetone /hexane) and the R_f was 0.79.

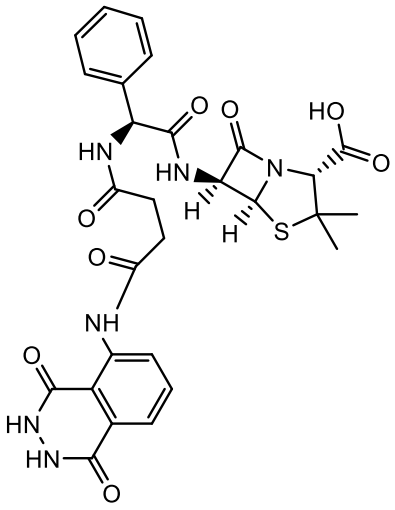

2.4. The solubility:

The solubility in different solvents (Water, DMSO, Ethanol, Acetone, Dichloromethane (DCM) , petroleum ether, diethyl ether, and ethyl acetate) for all synthesized derivatives was studied at room temperature and the results were recorded in a Table 3 page 94.

2.5 Biological activity:

Anti-bacterial activity:

For each of the synthesized compounds , biological activity was investigated using diffusion agar method for each of positive gram bacteria and negative gram bacteria. The antibacterial activity of these materials was performed using agar diffusion method. Both pathologic isolates E. coli and Staphylococcus aureus were employed in the current study and provided by biology department, University of Babylon, Iraq. The method used to estimate the inhibitory effect of prepared compounds on these types of bacteria is agar diffusion method; it includes the work of drilling in the dishes planted with bacteria to put the prepared derivatives

in the excavation of cultivars planted with bacteria in concentrations (1 mg/mL).The dishes were put in an incubator at temperature of (37 °C) for 24 hours, and then the inhibition zone was measured for each case. All samples were dissolved in DMSO. The results of the antibacterial activity test were recorded in Table 4 page 96.

2.6. Photolysis reactions

At room temperature, a volume of (100 ml) and a concentration of (80 ppm) of the two solutions: (TH2,TH11) were taken and exposed to ultraviolet irradiation with stirring at 25,30 and 35 ℃ after that a volume of (3 ml) were taken after every half hour for (250 min) , λ max was measured and UV were also taken . Photoreaction unit is shown in Figure 26 .

Figure 26 : Photoreaction unit setup.

2.7. Photo catalytic breakdown of the material

0.1 g of cobalt oxide is added to the sample solution in a volume of (100 ml) and a concentration of (80 ppm) from TH2 and TH11 with continuous stirring of the A suspension and irradiation at 25 ,30 and 35 ℃ after that were taken (3 ml) of the reaction mixture is withdrawn at times (0,15,30,60,90,120 min) , a centrifuge is made For drawn samples, taking the tracer and measuring its absorbance . This experiment was repeated with different weight of cobalt oxide(0.15 g.) and (0.20 g.) .

CHAPTER THREE

RESULTS AND DISCUSSION

3. Results and Discussion

Synthesis of new compounds based on luminol and its interaction with amino-containing drugs, and carboxyl-containing drugs were synthesized by formation of amide bonds and modulating the properties of luminol . The LM compound was synthesized by reacting of 3-nitro-phthalic acid with hydrazine in the presence of diethylene glycol and sodium dithionate. Synthesis of LM compound is shown in the following Scheme:-

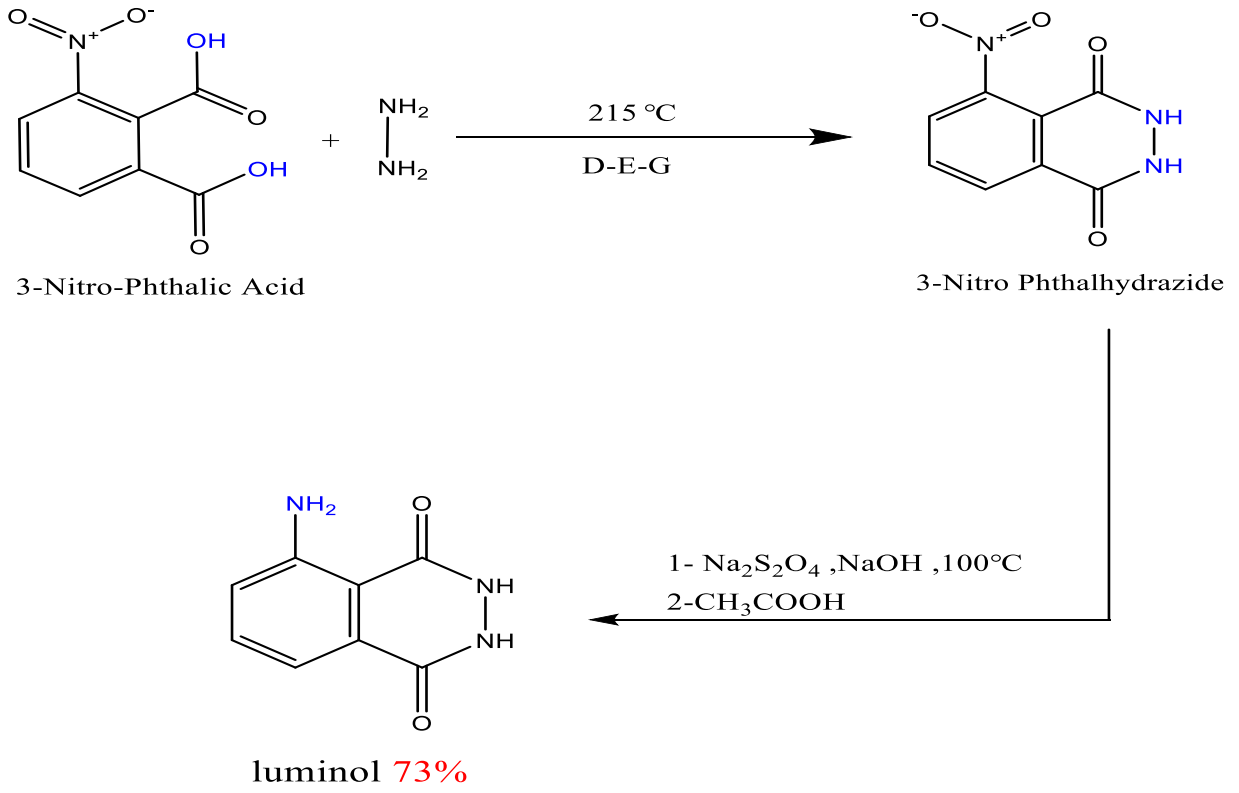

Scheme 1: Schematic description of synthesis of LM compound

The FT-IR spectrum of Luminol showed the following values (V_{max} in cm^{-1}):3466-3329 (N-H str. groups) , 3161 (CH str. Ar.) , 1653-1647 (C=O str. amid) , 1492(C=C str. Ar.) , 1323 (C-N) Figure 27 .

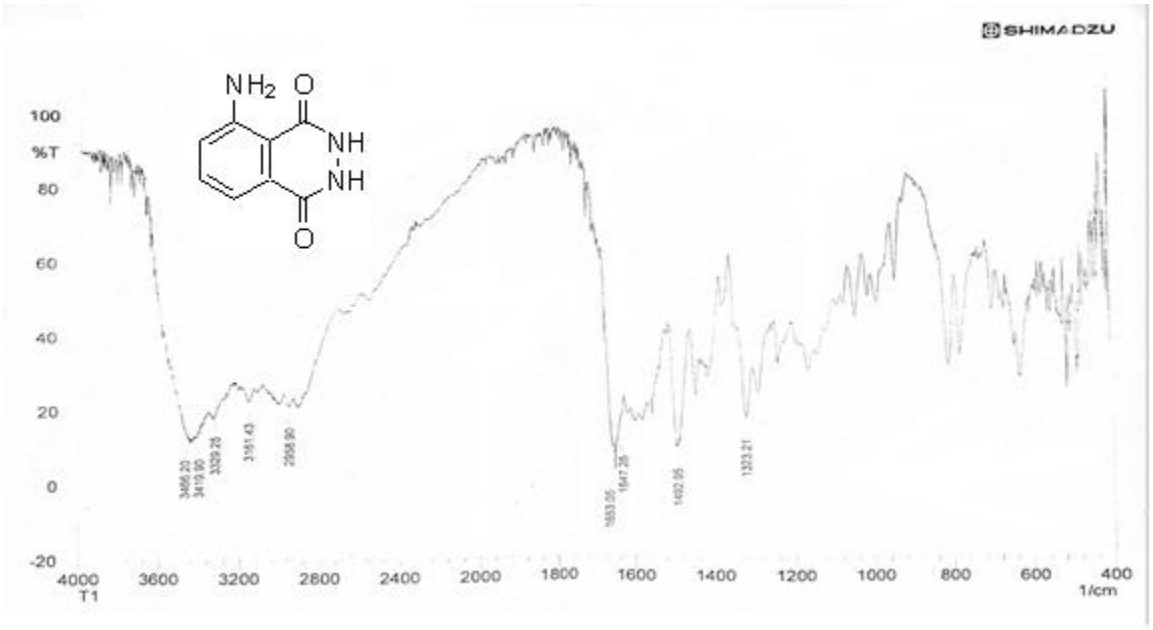

Figure 27 : FT-IR spectrum for Luminol

The compound LM was used as a starting material for synthesis of derivatives (TH1-TH9) by reacting of LM with different carboxyl drugs (Naproxen, Ibuprofen, Diclofenac Acid, Cephalexin, Ciprofloxacin, Mefenamic Acid , Ceftriaxone, Ampicillin , Cefotaxime) respectively. On another hand, the (LM) was used as starting material with succinic anhydride to produced (LS) and the last one was reacted with different amino drugs (cephalexin, Mefenamic acid , paracetamol , theophylline , amoxicillin , ampicillin) to synthesis (TH10-TH15). All synthesized derivatives were characterized and confirmed with FT-IR, ^{1}HNMR, ^{13}CNMR, and C.H.N.S.

3.1. Synthesis of acid chloride :

Acid chloride derivatives of (T1-T9) were synthesized by reacting of the carboxyl-containing drugs with Thionyl chloride . The FT-IR spectrum of (T1-T9) showed completely absence of hydroxyl group of carboxyl drugs as shown in Figures 28 to 36.

The compound T1 was synthesized from a reaction of Naproxin with Thionyl chloride as shown in equation 4.

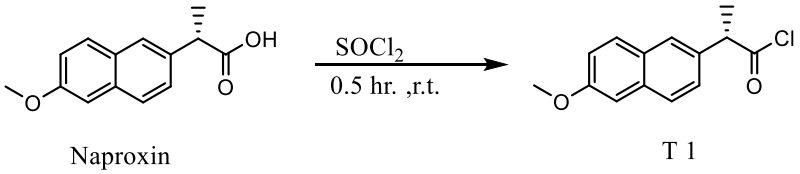

Naproxin T 1

The equation 4: Synthesis for T1 .

The FT-IR spectrum of T1 showed the following values (V_{max} in cm^{-1}):3167 (CH str. Ar.), 2939 (CH str. Al.), 1668 (C=O str. acid chloride) , 1486 (C=C str. Ar.) ,1323 (CH_3) , 1011 (C-O str. ketone) , 767 (C-Cl str.) Figure 28.

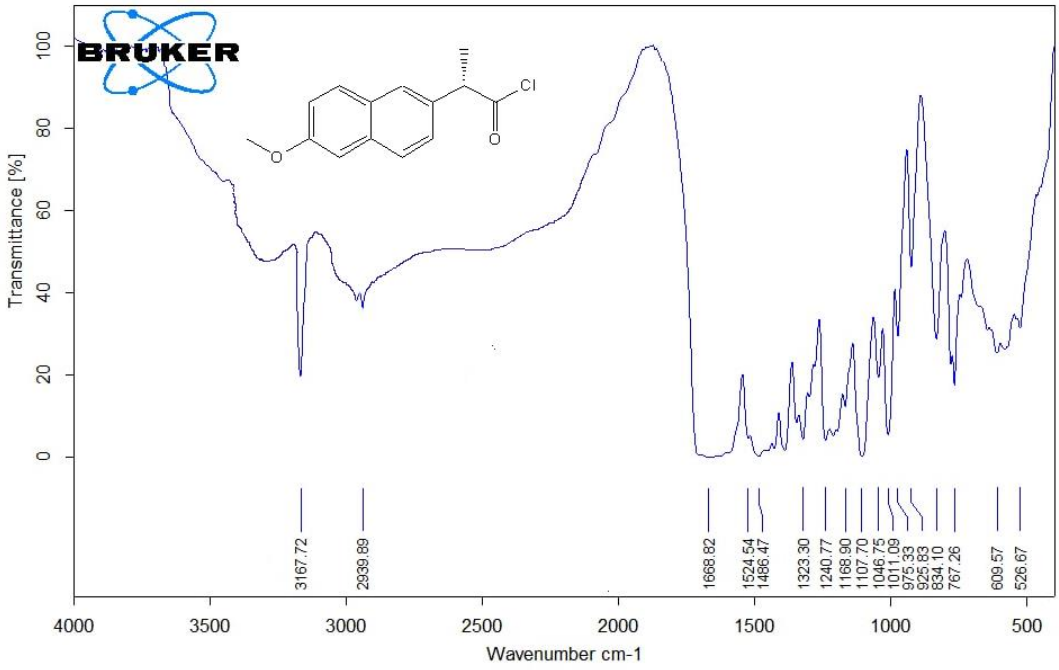

Figure 28: FT-IR spectrum for T1

Ibuprofen was reacted with Thionyl chloride to produced T2 as explained in equation 5.

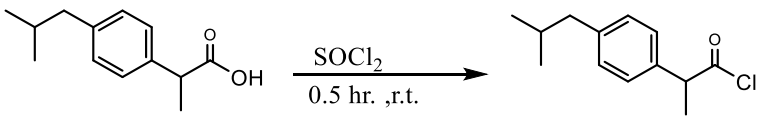

Ibuprofen T 2

The equation 5: Synthesis for T2 .

The FT-IR spectrum of T2 showed the following values (V_{max} in cm^{-1}) : 3012 (CH str. Ar.), 2920 ; 2956 (CH str. Al.), 1718 (C=O str. acid chloride), 1491-160(C=C str. Ar.), 1323;1379 (CH_3), 700 (C-Cl str.) Figure 29.

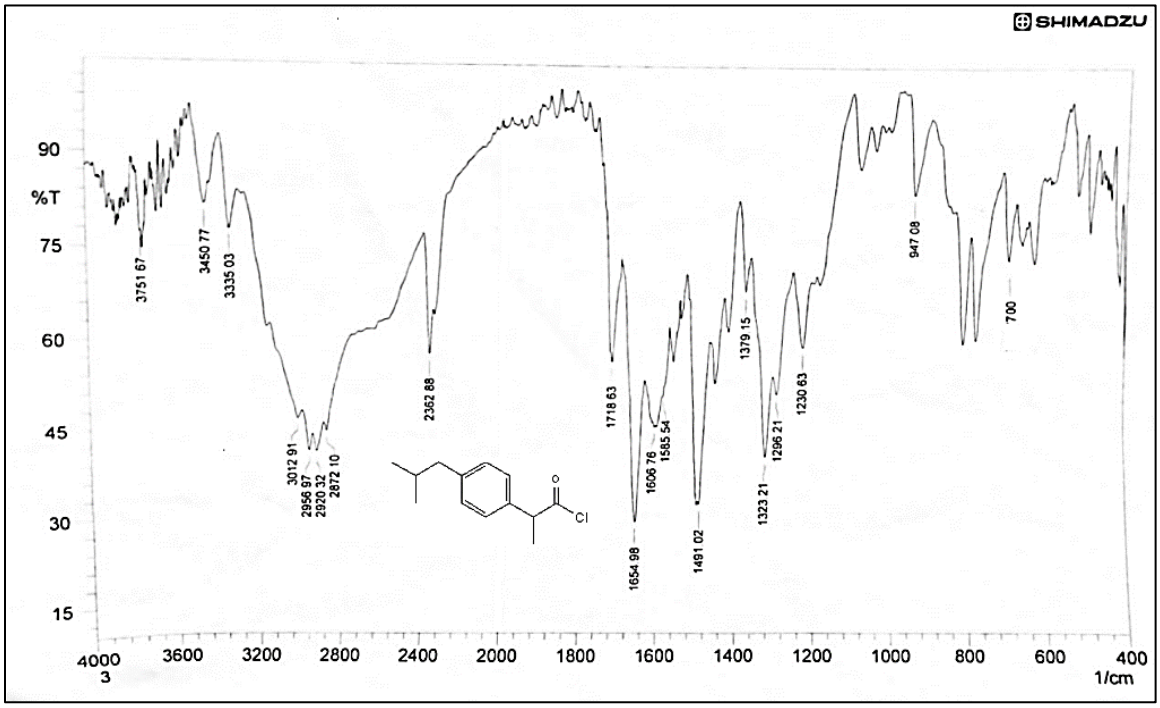

Figure 29: FT-IR spectrum for T2

The T3 was synthesized by reacting Diclofenac acid with Thionyl chloride as explained in the equation 6.

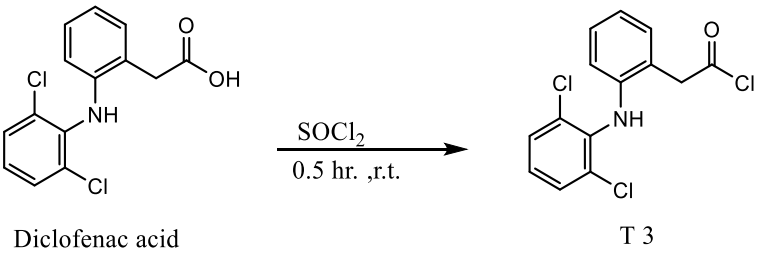

Diclofenac acid T 3

The equation 6 : Synthesis for T3.

The FT-IR spectrum of T3 showed the following values (V_{max} in cm^{-1}):3394 (NH str.) , 3074 (CH str. Ar.), 1707 (C=O str. acid chloride) , 1600 (C=C str. Ar.) ,1465 (CH_2) , 1301 , 1361 (C-N) , 786 (C-Cl str.) figure 30.

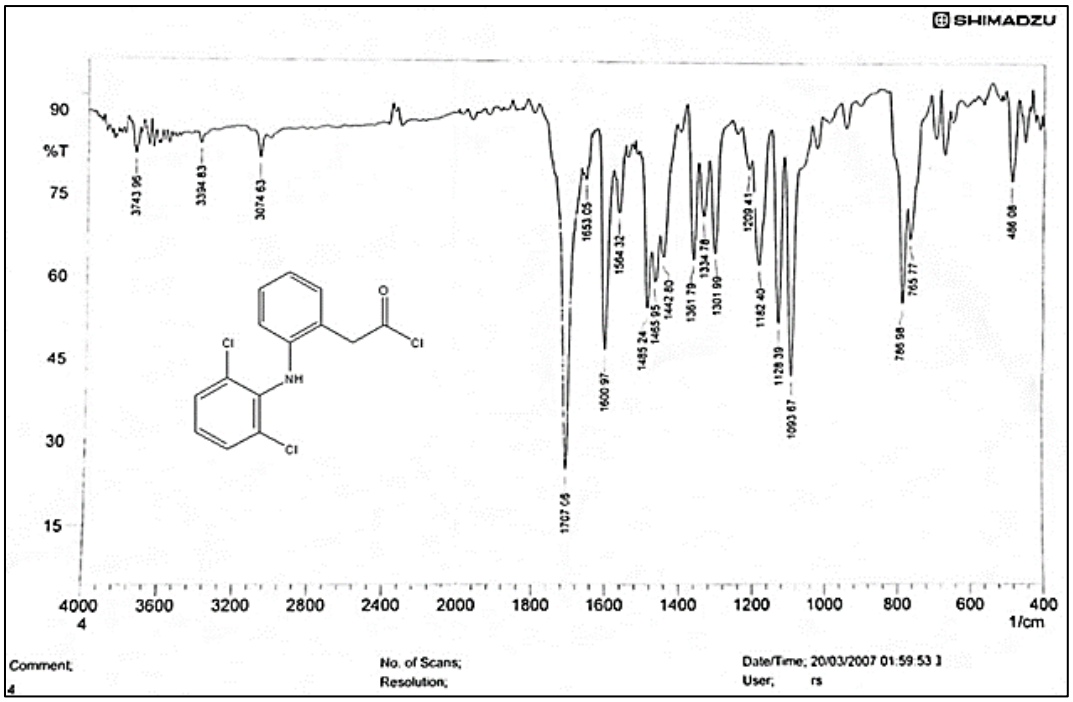

Figure 30: FT-IR spectrum for T3

T4 was prepared by the reaction of cephalxine with Thionyl chloride as shown in the following equation.

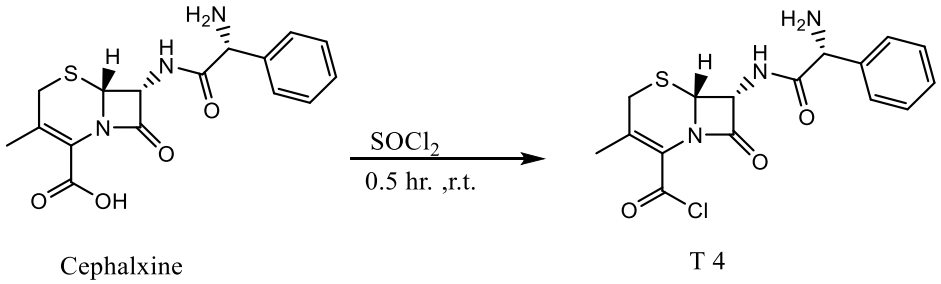

The equation 7: Synthesis for T4 .

The FT-IR spectrum of T4 shows the following values (V_{max} in cm^{-1}):3178 (NH str.) , 2978, 2939 (CH str. Al.) , 3111 (CH str. Ar.), 1828 (C=O str. acid chloride), 1678 (C=O str. β-lactam ring) ,1653 (C=O str. amide) , 1506 (C=C str. Ar.) , 1396 (C-N) , 698 (C-Cl str.) Figure 31 .

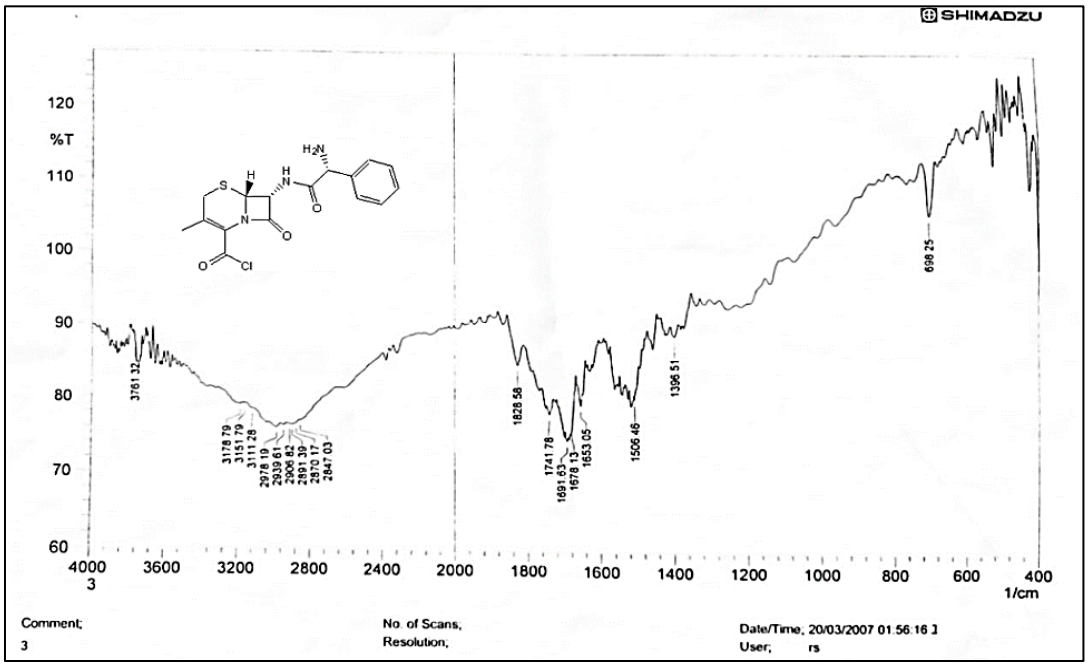

Figure 31: FT-IR spectrum for T4 derivative

To synthesis T5 , ciproflaxine was reacted with Thionyl chloride as showed in equation 8.

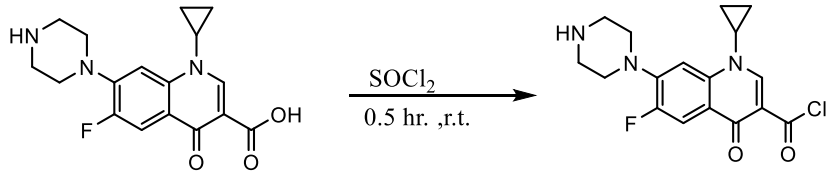

Ciproflaxine T 5

The equation 8: Synthesis for T5.

The FT-IR spectrum of T5 shows the following values (V_{max} in cm^{-1}): 3399(NH str.) , 3010 (CH str. Ar.) , 2928 (CH str. Al.) , 1716 (C=O str. acid chloride) , 1628 (C=O str.) , 1516 (C=C str. Ar.) , 1034-1203 (C-N) , 669 (C-Cl str.) Figure 32 .

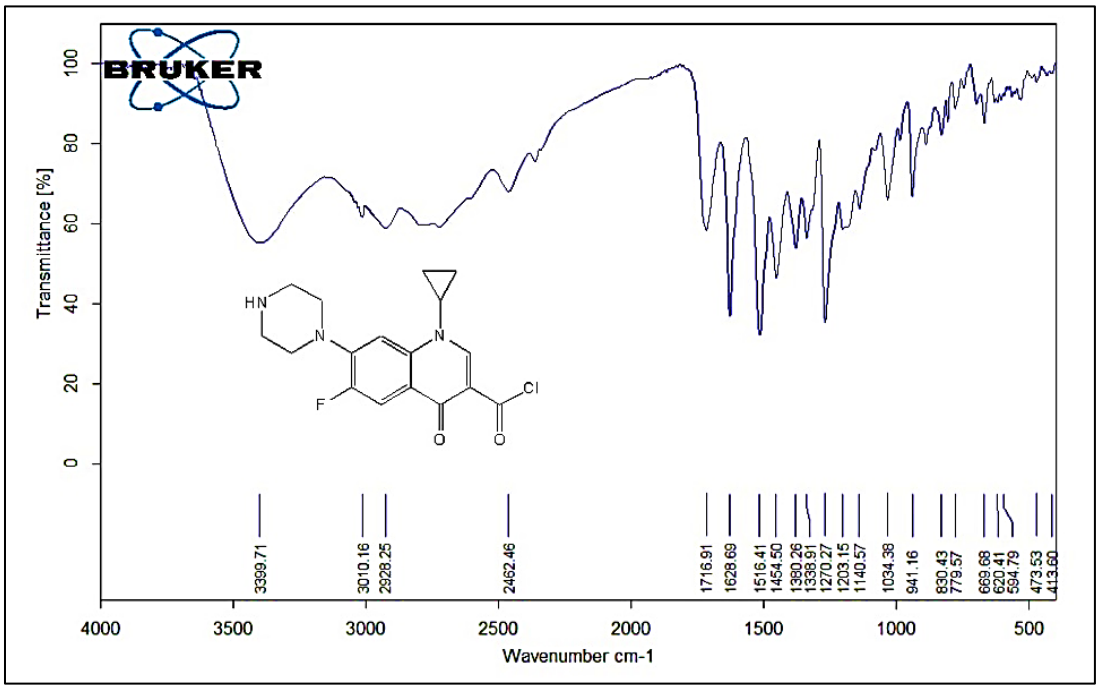

Figure 32: FT-IR spectrum for T5 derivative

The T6 produced by reacted Mefenamic acid with Thionyl chloride as explained in the equation 9.

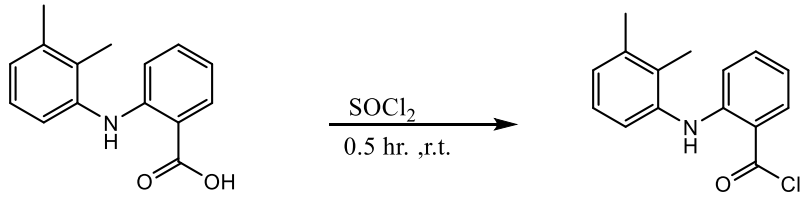

Mefenamic acid T 6

The equation 9: Synthesis for T6.

The FT-IR spectrum of T6 shows the following values (V_{max} in cm^{-1}): 3335(NH str.) , 3060 (CH str. Ar.) , 2850 - 2919 (CH str. Al.) , 1710,1761 (C=O str. acid chloride) , 1607 (C=C str. Ar.) , 1375 (CH_3) ,1304 ,1325 (C-N) , 557-668 (C-Cl str.). This spectrum is presented in Figure 33 .

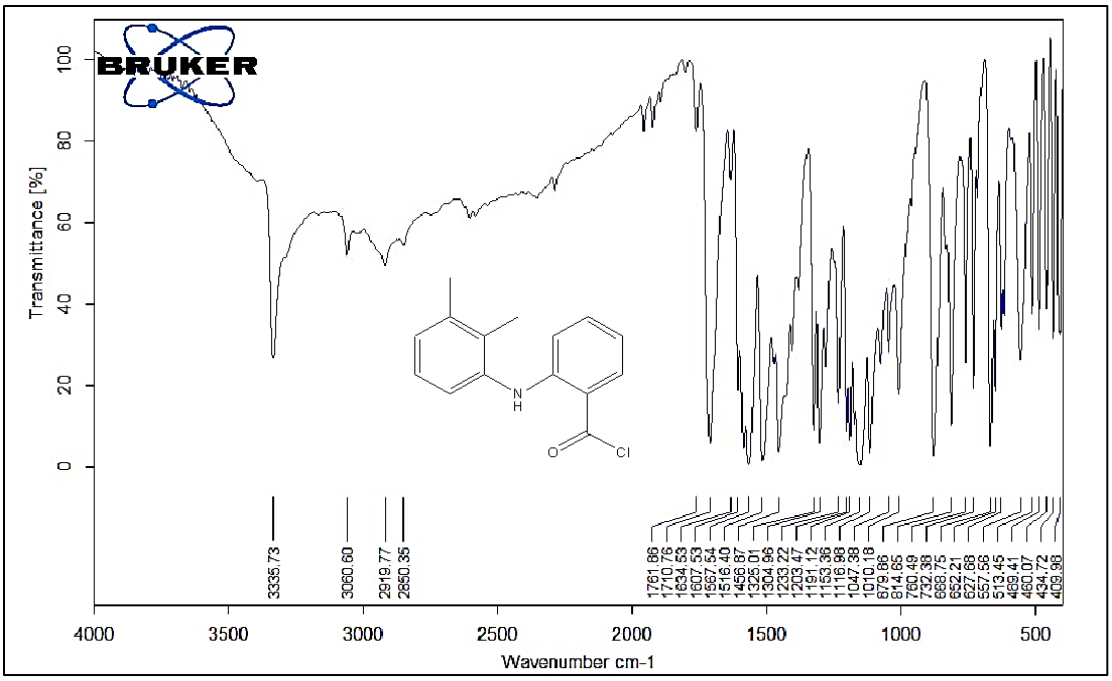

Figure 33: FT-IR spectrum for compound T6.

Ceftriaxone was reacted Thionyl chloride to produced T7 as explained in equation 10.

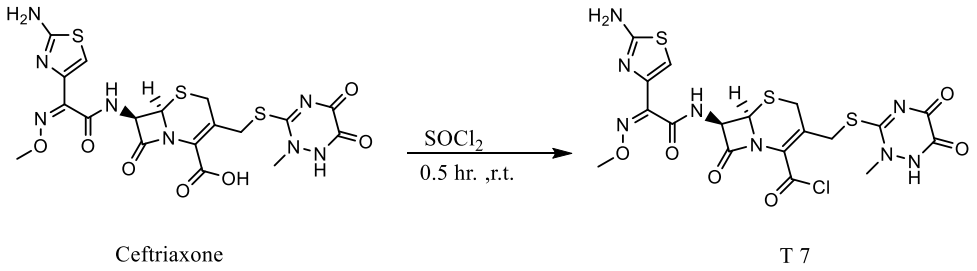

Ceftriaxone T 7

The equation 10: Synthesis for T7.

The FT-IR spectrum of T7 shows the following values (V_{max} in cm^{-1}): 3446 (NH str. Amid) , 3290 (NH str.) , 3028 (=CH str.), 2945 (CH str. Al.), 1772 (C = O str. β-lactam ring), 1712 (C=O acid chloride) , 1631-1680 (C = O str. amid) , 1560 (C = N str.), 1456 (C = C str.) , 1045 (C-N) , 690 (C-Cl). This spectrum is presented in Figure 34 .

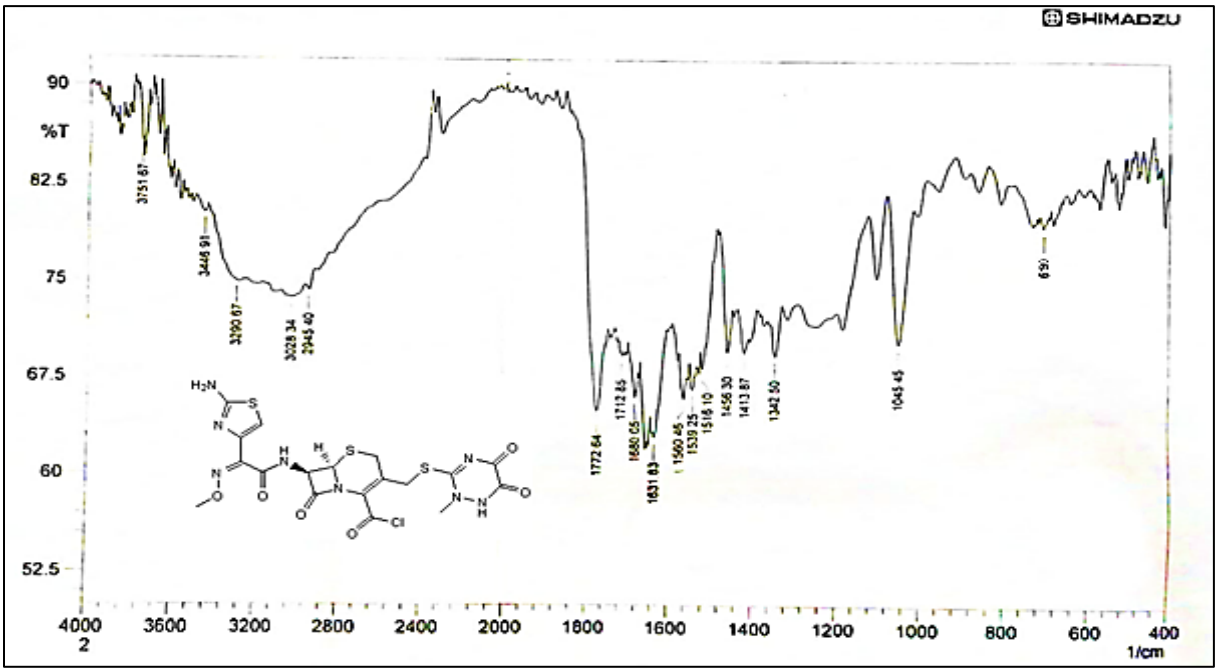

Figure 34: FT-IR spectrum for T7.

T8 was synthesized by the reaction of Ampicillin with Thionyl chloride as shown in equation 11.

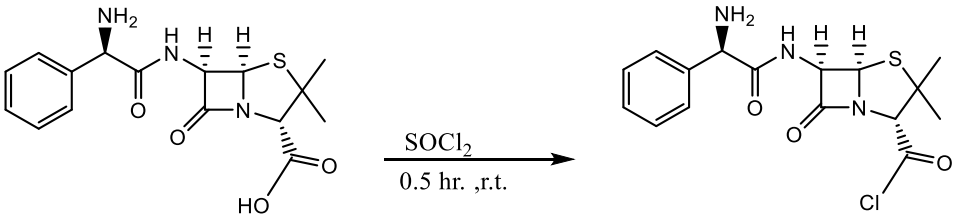

Ampicilline T 8

The equation 11: Synthesis of compound T8.

The FT-IR spectrum of T8 shows the following values (V_{max} in cm^{-1}): 3392 -3198 (NH str. Amid), 3009-3053 (CH str. Ar.) , 2970 (CH str. alkane), 1735 (C = O str. β-lactam ring),1699 (C=O acid chloride) , 1604 (C = O str. Amide) , 1462 (C = C str. Ar.) , 1195 (C - N str.) , 580-698 (C-Cl). This spectrum is presented in Figure 35 .

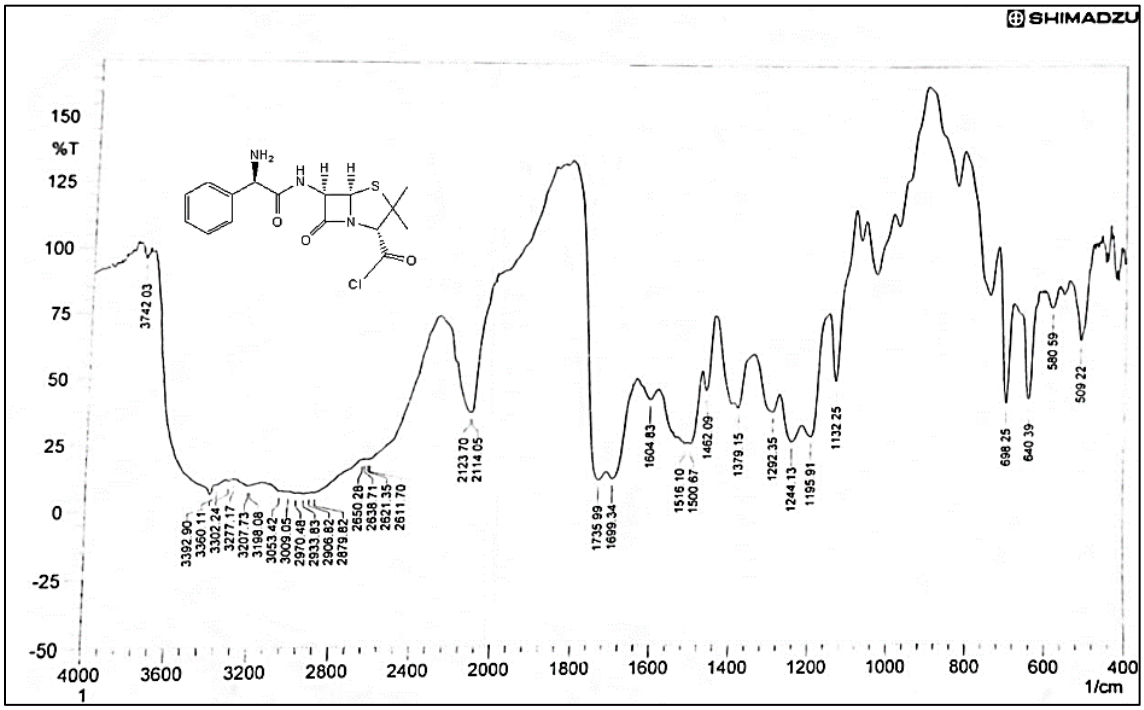

Figure 35: FT-IR spectrum for compound T8.

Cefotaxime was reacted with Thionyl chloride to form T9, the chemical equation for the preparation of T9 is explaining in the equation 12.

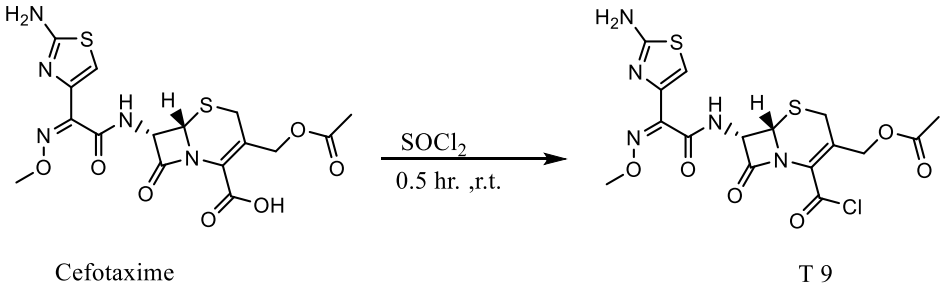

The equation 12: Synthesis for T9.

The FT-IR spectrum of T9 shows the following values (V_{max} in cm^{-1}): 3137 (NH amid str.) , 3076 (=CH str.), 2943 (CH str. alkane), 1752 (C = O str. β-lactam ring , C=O acid chloride and C=O ester) (overlap), 1631 (C = O str. amid) , 1426 (C = C str. Ar.), 1530 (C = N str.) , 1036 - 1153 (C-N str.), 566-716 (C=Cl) This spectrum is presented in Figure 36 .

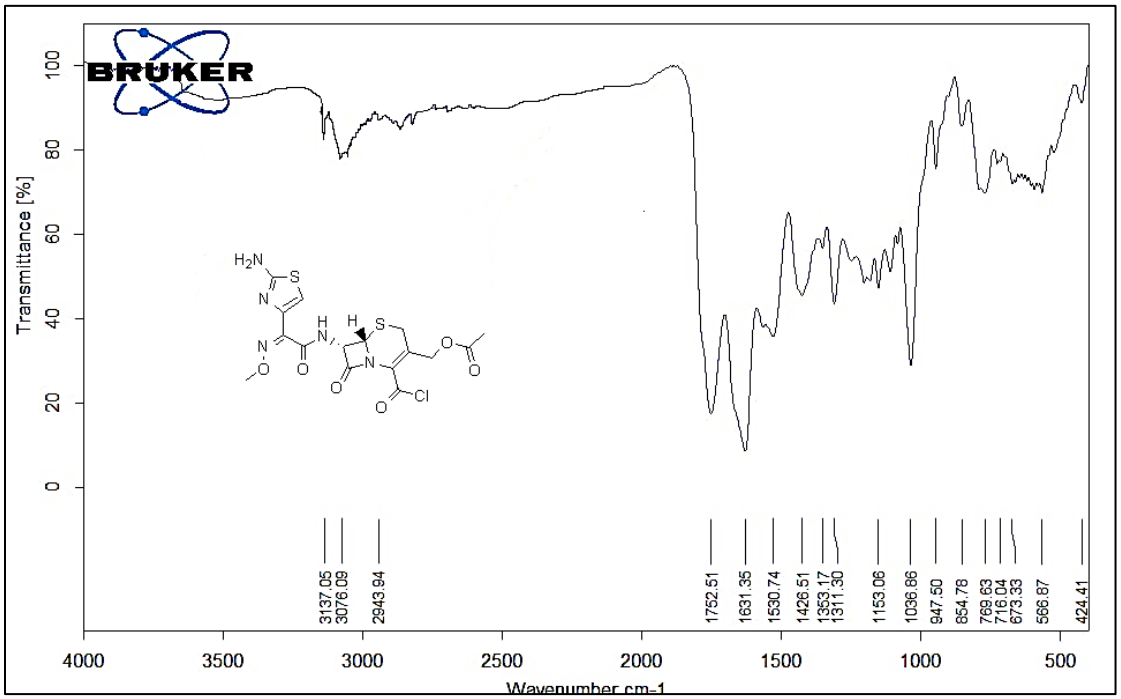

Figure 36: FT-IR spectrum for T9

3.2 synthesis of Compounds (TH1-TH9) :

These compounds were synthesized from the reaction of Luminol (LM) with acid chloride for drugs that Prepared in advance (T1-T9) respectively as shown in Figures (37) and (38). Reaction mechanism of this reaction is shown in Figure 39.

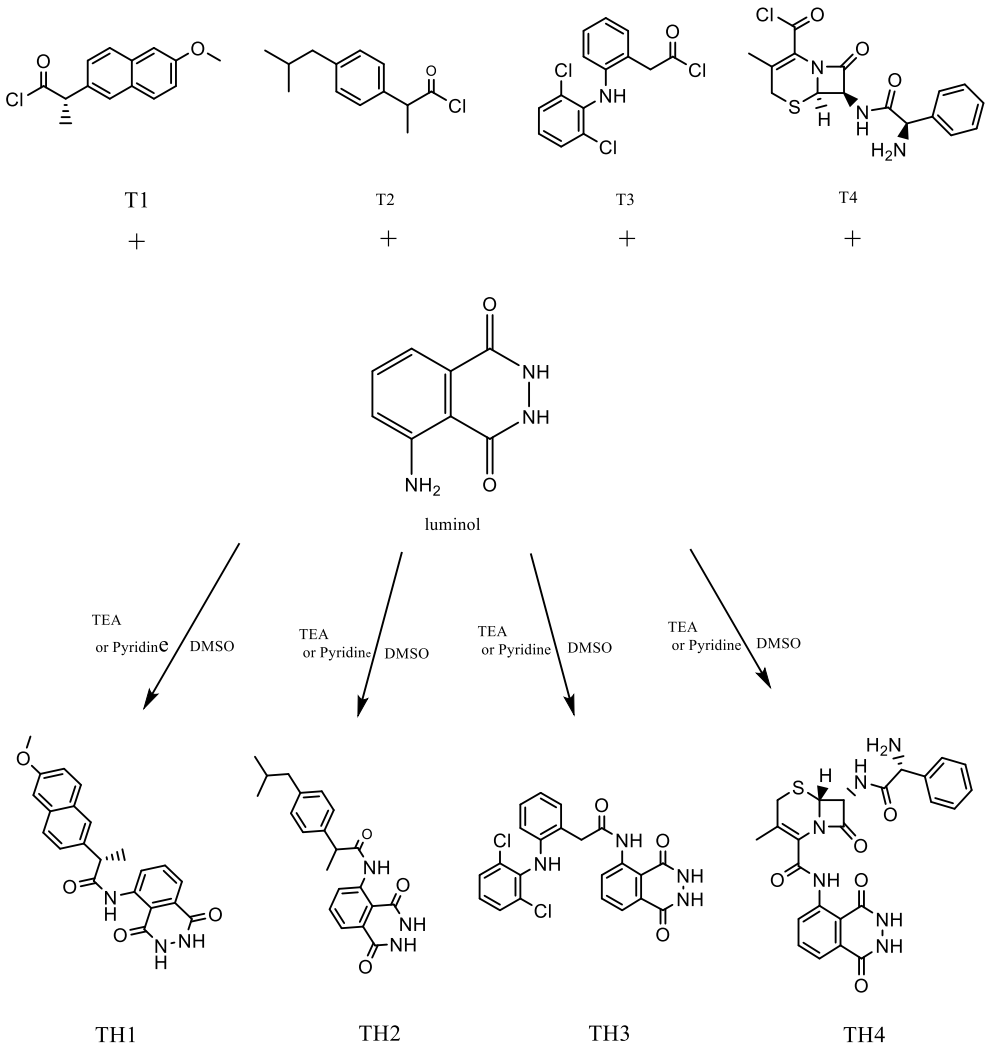

Figure 37: Schematic description for Synthesis of Compounds (TH1-TH4).

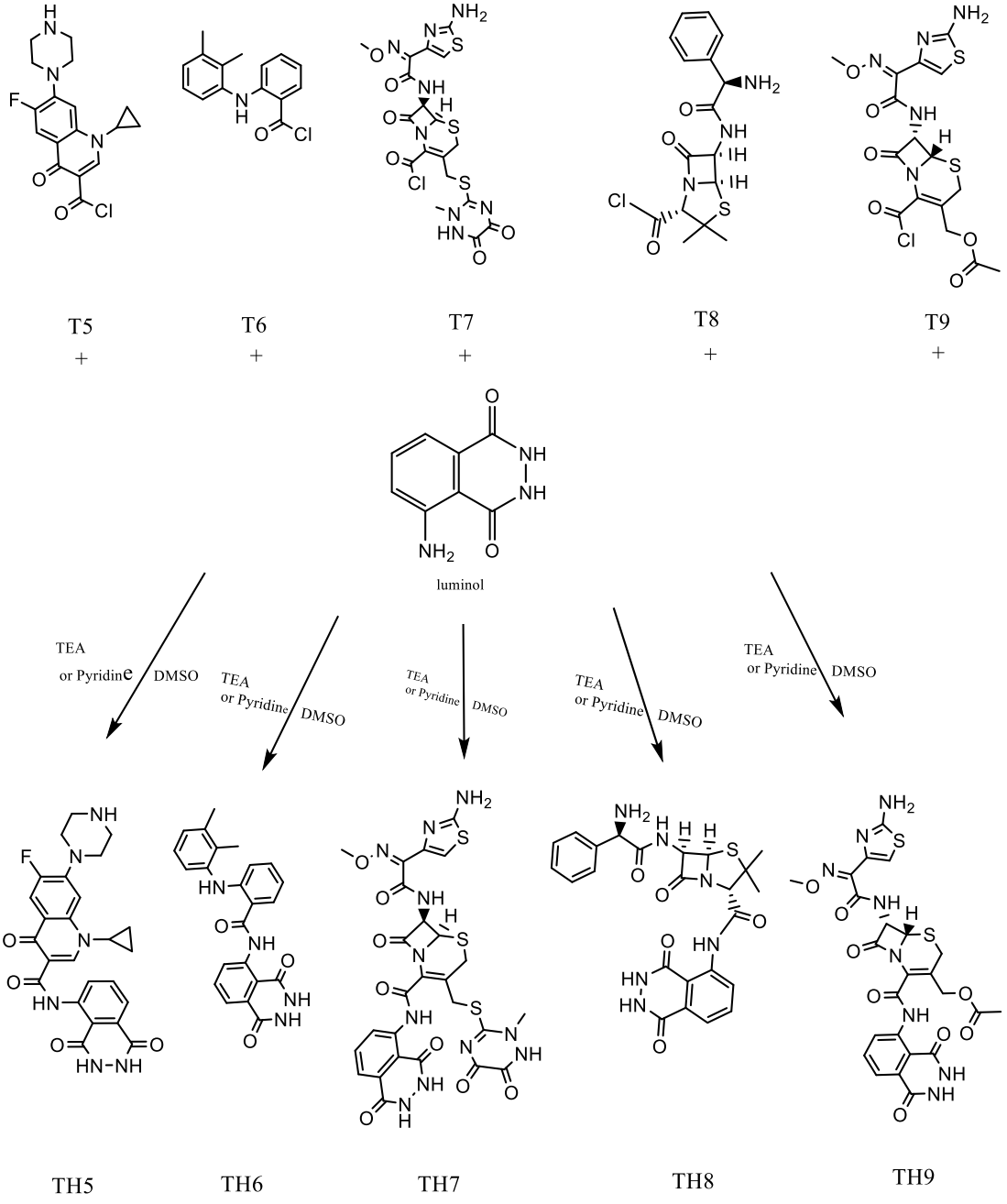

Figure 38: schematic description for synthesis of Compounds (TH5-TH9).

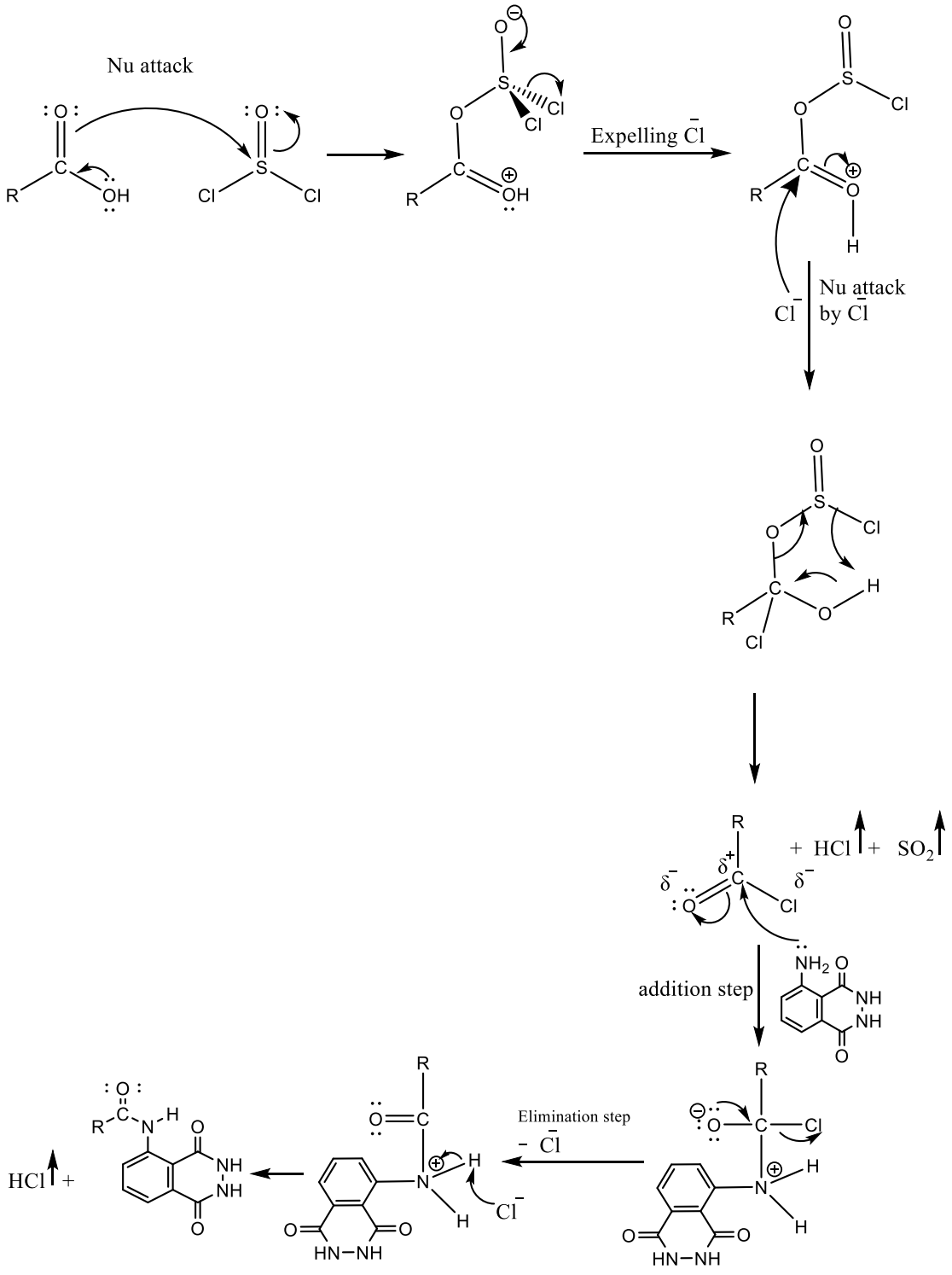

Figure 39: A general mechanism for producing the compounds (TH1-TH9).

The equation 13 represents the synthesis equation for TH1.

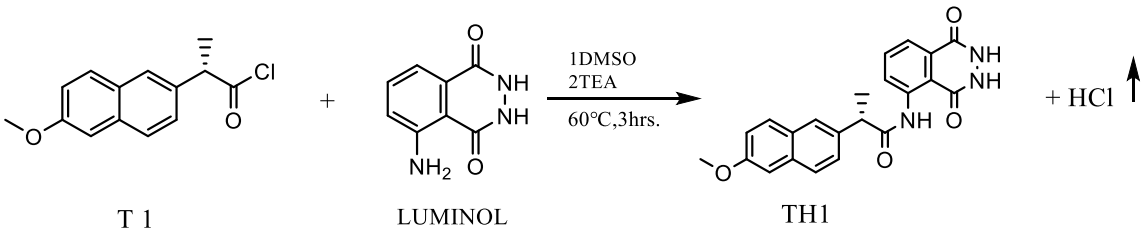

The equation 13: synthesis for TH1 .

Figure 40, showed the FT-IR spectrum for **TH1 [(S)-N-(1,4-dioxo-1,2,3,4-tetrahydrophthalazin-5-yl)-2-(6-methoxynaphthalen-2-yl)propanamide]** (V_{max} in cm^{-1}): 3169 -3439 (NH str. amid) , 3012 (CH str. Ar.), 2972 (C-H str. alkane), 1647 (C=O str. amide), 1537 -1566 (C=C str. Ar.), 1321 (C-N str.), 1053-1222 (C-O str.) . ^{1}H-NMR (500 MH, δ ppm): 10.79 ; 9.92 (N-H, sec. amide), 8.07-6.82 (C-H, benzene) , 3.79 (C-H, methyl), 3.61 (C-H, methine) , 2.49 (DMSO) , 1.19 (C-H methyl) Figure 41.

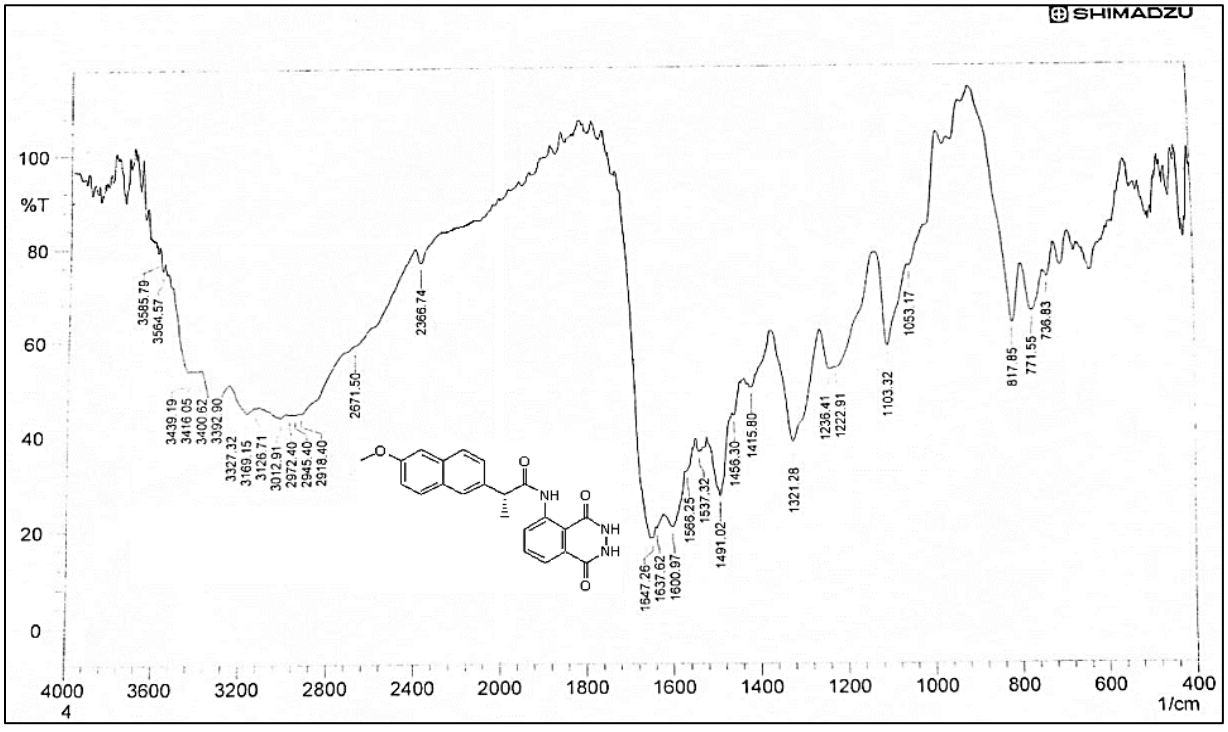

Figure 40: FT-IR spectrum for TH1

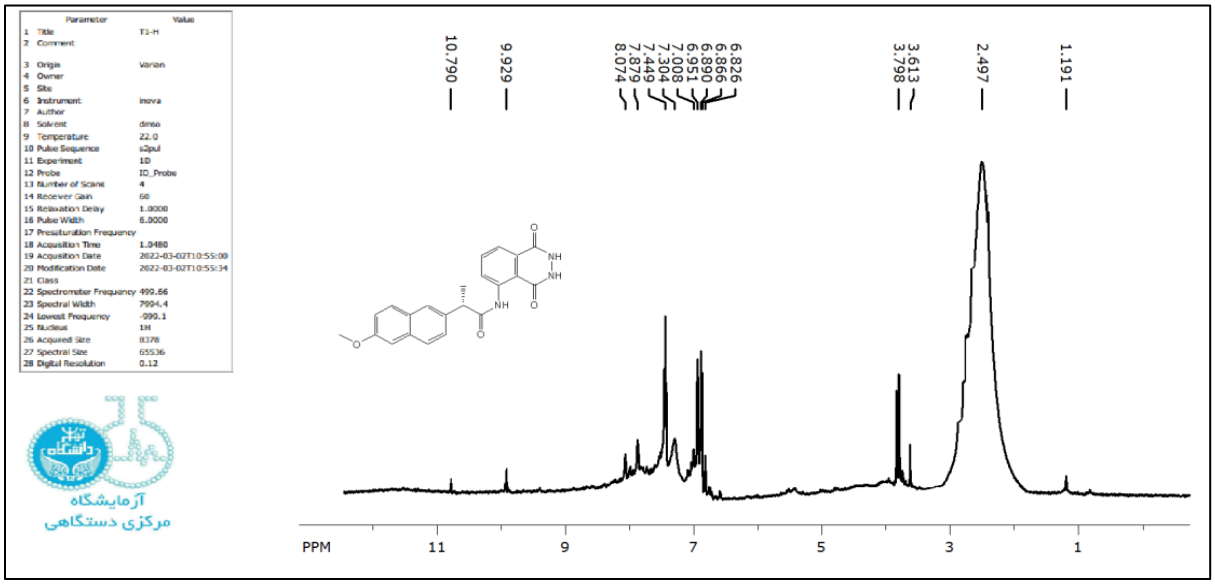

Figure 41: ^{1}H-NMR spectrum for TH1

Ibuprofen acid chloride was reacted with luminol to produce new derivative TH2 as explained in equation 14.

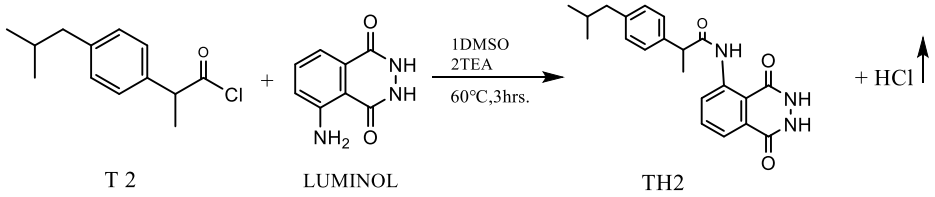

The equation 14 : Synthesis for TH2 .

FTIR spectrum for **TH2 [N-(1,4-dioxo-1,2,3,4-tetrahydrophthalazin-5-yl)-2-(4-isobutylphenyl)propanamide]** presented in Figure 42, this spectrum shows the following values ((V_{max} in cm^{-1}): 3454 (NH) , 3014-3161 (CH aromatics), 2918-2962 (CH str.), 1654 (C=O amid), 1496 (C=C aromatics) , 1296 _1323 (C-N). ^{1}H NMR (500 MH, δ ppm) : 0.84-1.78 (CH_3), 2.38 (CH aliphatic), 2.49 (DMSO), 3.6 (CH_2 aliphatic) , 6.87 -8.05 (CH benzene), 10.02 ; 11.31(NH amid) Figure 43. ^{13}C NMR (125 MH, δ ppm): 15.4_22.8 (CH_3), 29.0_42.5 (CH), 40.3 (DMSO), 44.5(CH_2), 119.3_140.3 (benzene), 167.3-172.2 (C=O amid). This spectrum is presented in Figure 44.

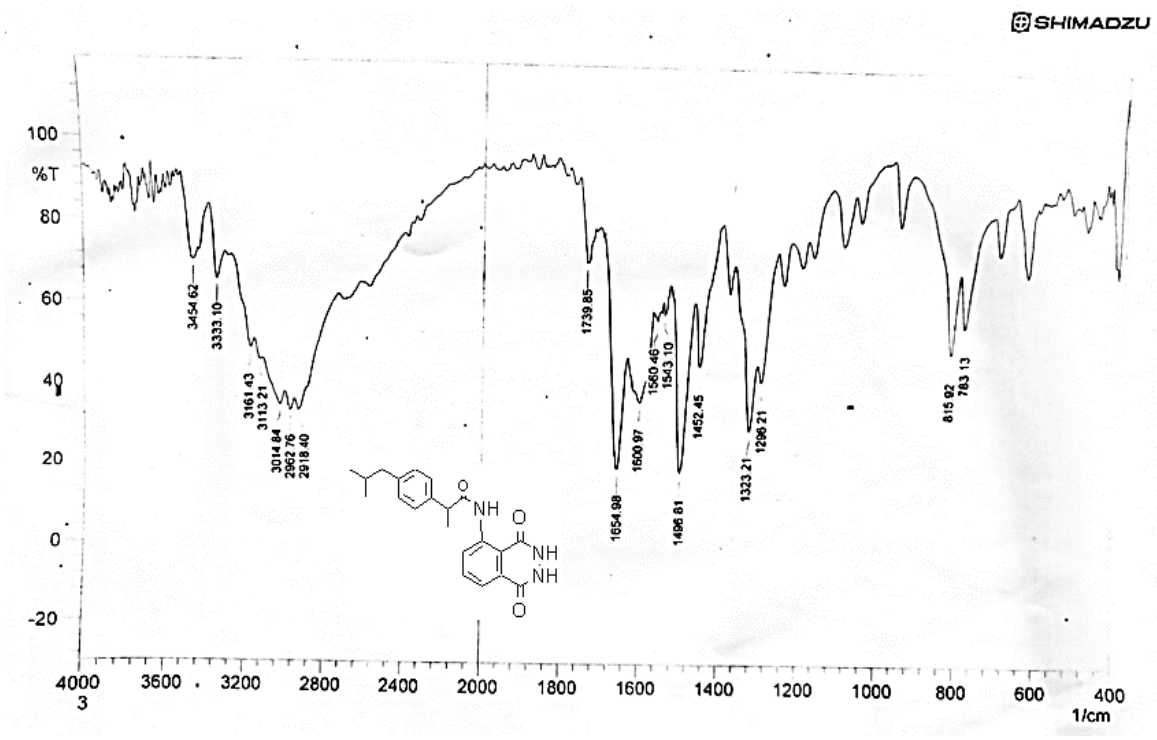

Figure 42: FT-IR spectrum for TH2

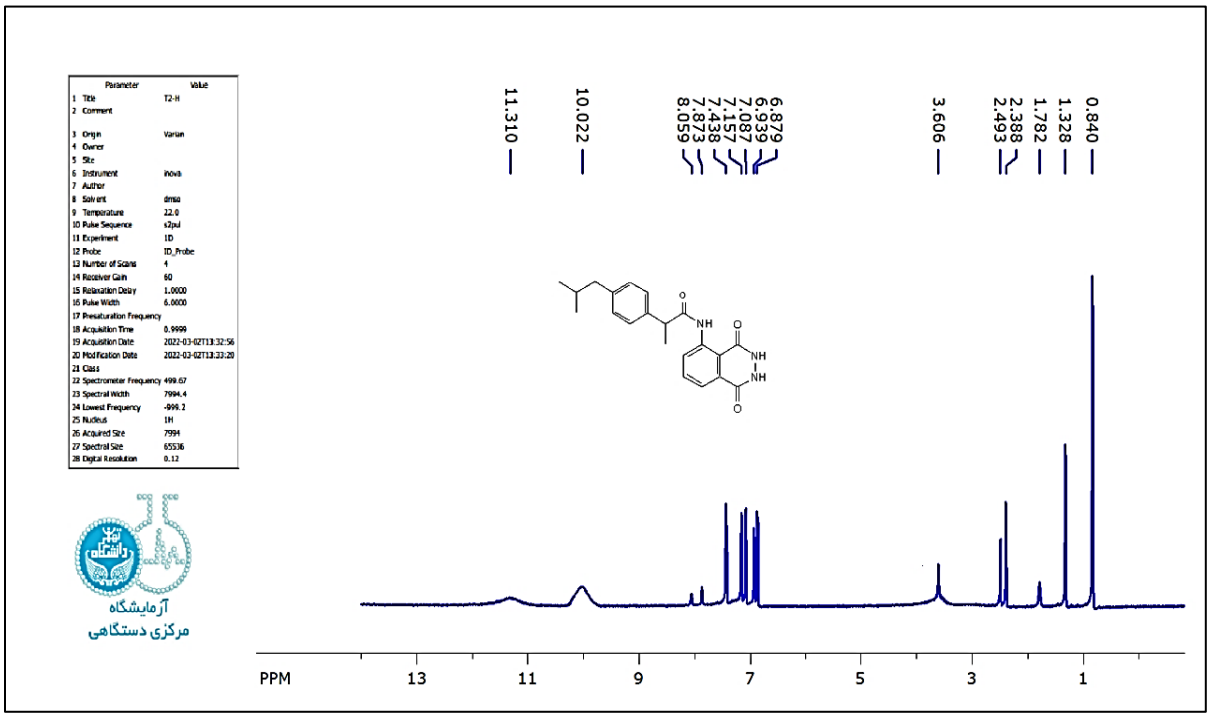

Figure 43: ^{1}H-NMR spectrum for TH2

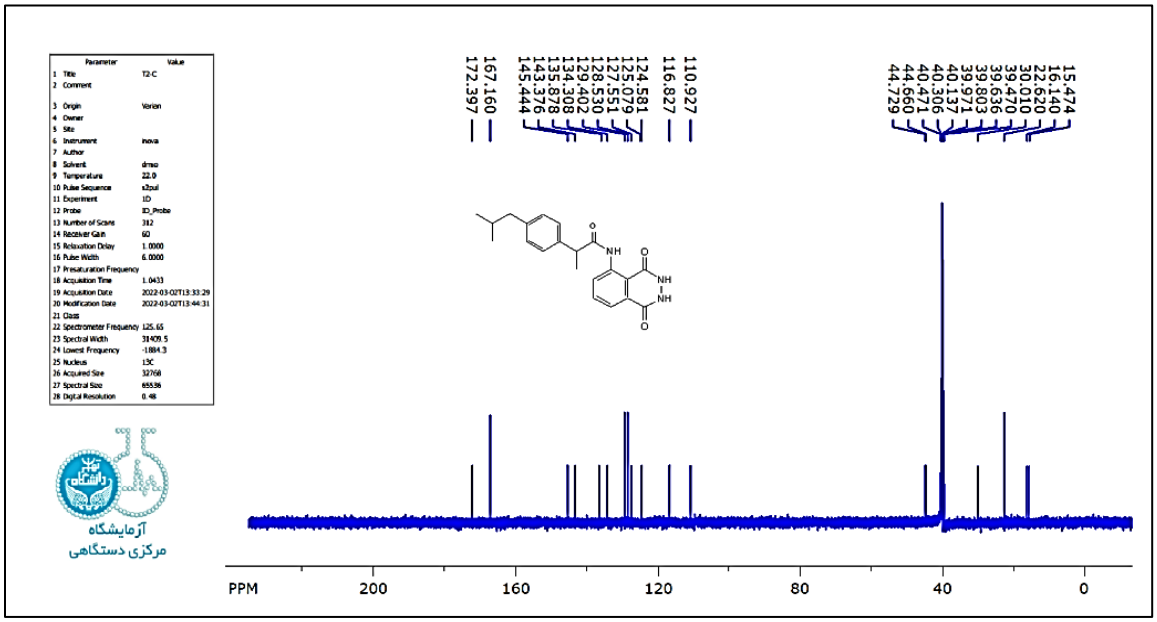

Figure 44: ^{13}C-NMR spectrum for TH2

The derivative TH3 was synthesized by reacting Diclofenac acid chloride with luminol as explained in the equation 15.

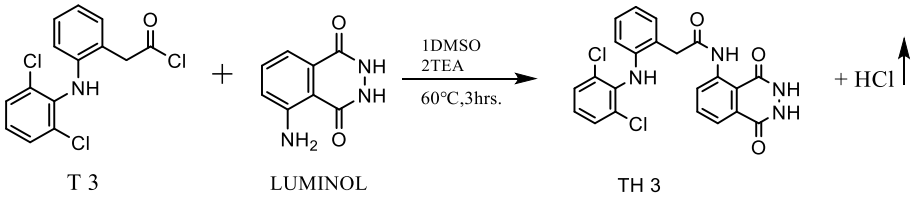

The equation 15 : Synthesis for TH3.

FTIR spectrum for **TH3[2-(2-((2,6-dichlorophenyl)amino)phenyl)-N-(1,4-dioxo-1,2,3,4-tetrahydrophthalazin-5-yl)acetamide]** derivative shows the following values (V_{max} in cm^{-1}) : 3340-3471 (NH amine and amide), 3028-3167 (CH aromatics), 2918-2968 (CH str.), 1654 (C=O str.), 1492 (C=C aromatics), 1240-1321 (C-N str.), 609 (C- Cl) Figure 45. ^{1}H NMR (500 MH, δ ppm): 11.63,10.33 (NH amide), 9.22(NH amine), 7.73-6.37(CH benzene), 3.86(CH_2) , 2.49 (DMSO) Figure 46 . ^{13}C NMR : (125 MH, δ ppm): 167.88-163.02 (C=O amide), 148.46 (C-N amide), 143.32(C-Cl benzene), 134.89-108.95(1benzene), 39.89(DMSO), 35.53(CH_2). This spectrum is presented in Figure 47.

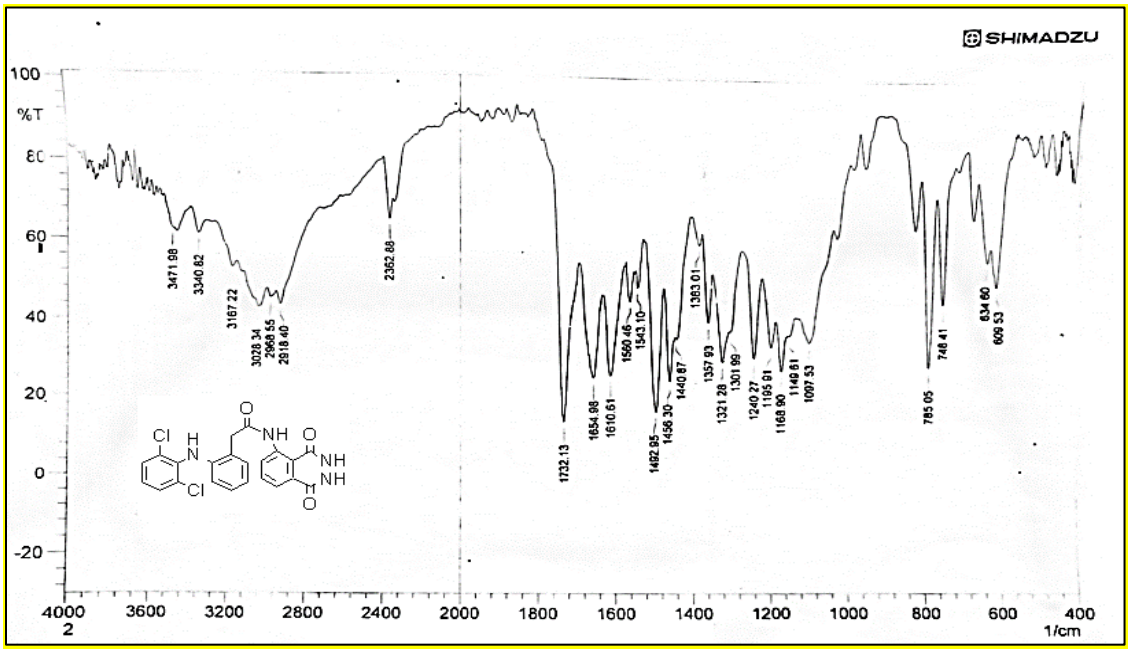

Figure 45: FT-IR spectrum for TH3.

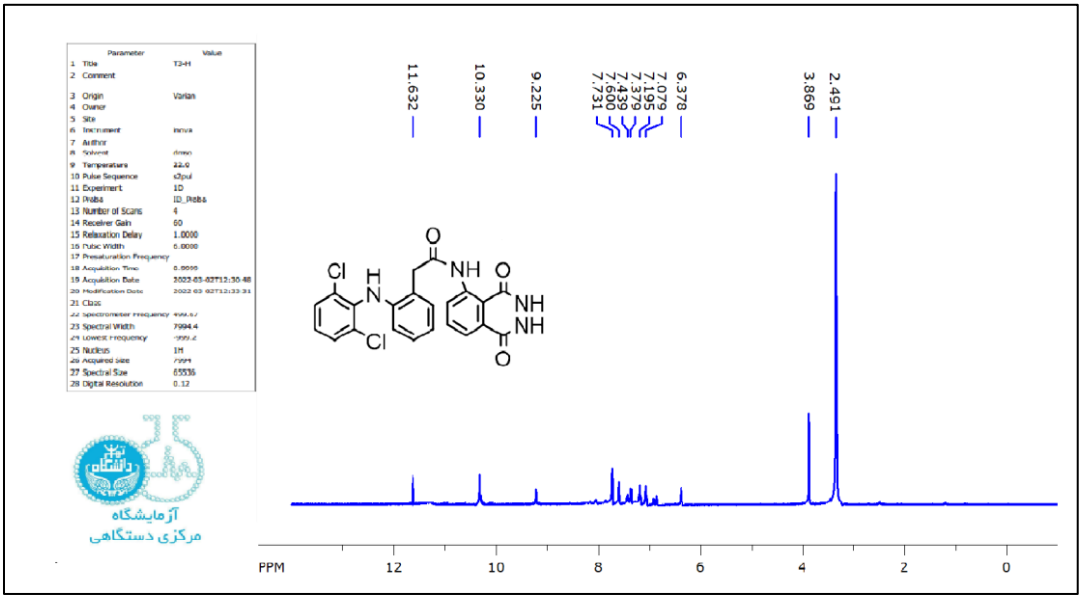

Figure 46: ^{1}H-NMR spectrum for TH3

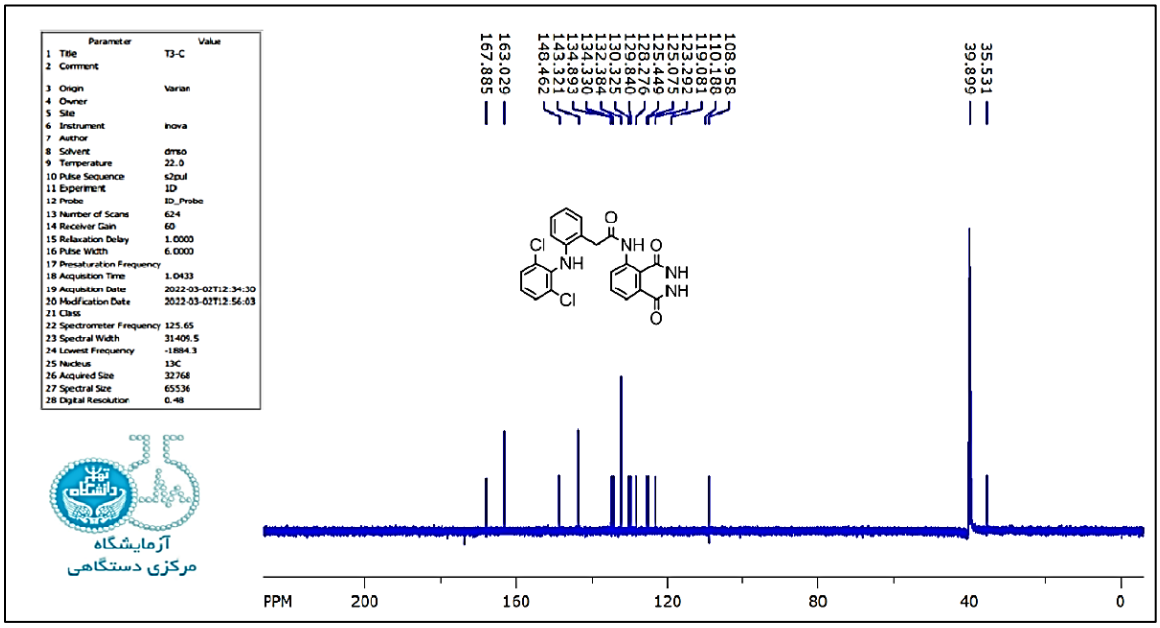

Figure 47: ^{13}C-NMR spectrum for TH3

TH4 was synthesized by the reaction of cephalxine acid chloride with luminol as shown in the following equation.

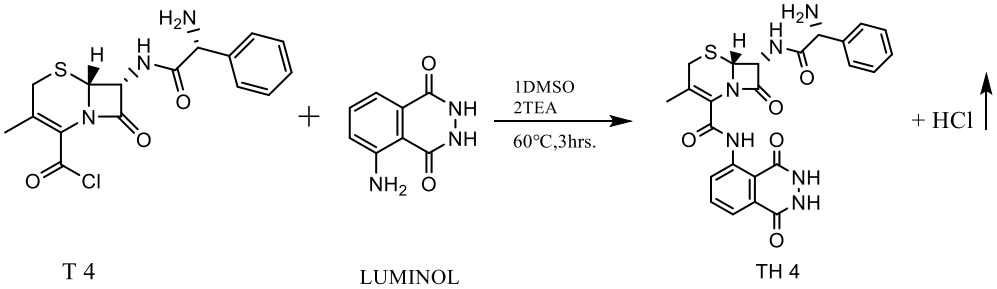

The equation 16: Synthesis for TH4 .

The FT-IR spectrum of **TH4 [(6R,7R)-7-((R)-2-amino-2-phenylacetamido)-N-(1,4-dioxo-1,2,3,4-tetrahydrophthalazin-5-yl)-3-methyl-8-oxo-5-thia-1-azabicyclo[4.2.0]oct-2-ene-2-carboxamide]**showed the following values (V max in cm-1):3394 (NH str. amine and NH amide) , 3074 (CH str. Ar.) , 2920 ; 2956 (CH str. Al.), 1772; 1751 (C=O str. β-lactam ring) ,1683 (C=O str. amide) , 1670 (C=C str. Ar.) , 1496 (C-N) Figure 48 . 1H-NMR (500 MH, δ ppm) : 10.45 ; 9.95 ; 9.53 (NH, sec. amide), 8.73-6.88 (CH, benzene) , 5.68 (CH, propiolactam)

, 5.53 (H, propiolactam) , 4.97 (NH, amine) , 3.77 ; 3.40 (CH2, methylene) , 2.53 (DMSO) , 2.33 (CH ,methine) , 1.96 (CH, methyl). This spectrum is presented in Figure 49 .

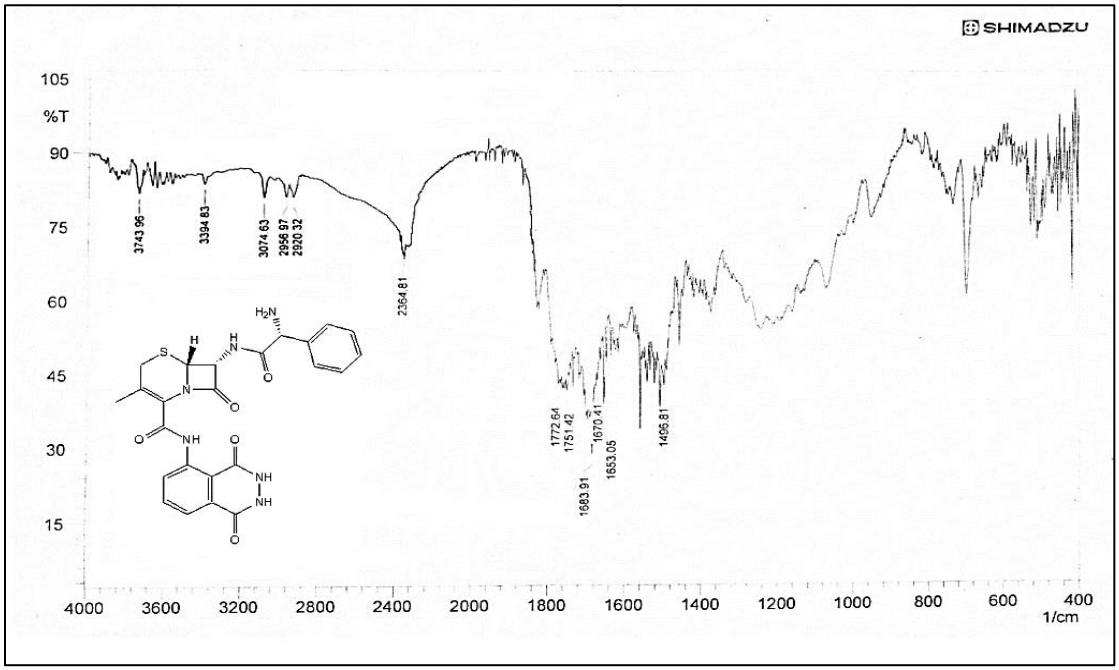

Figure 48: FT-IR spectrum for TH4

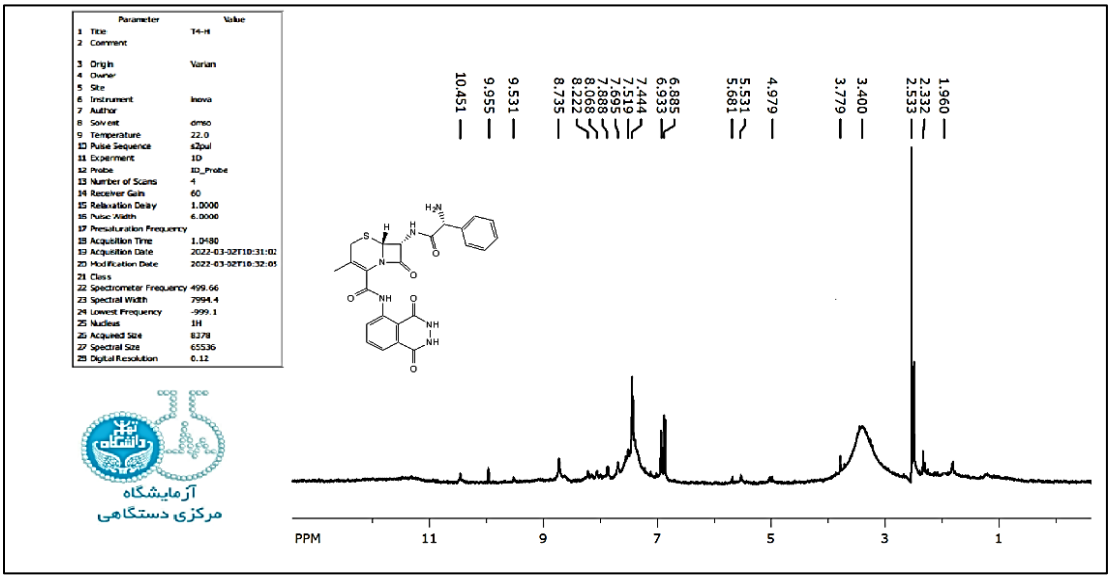

Figure 49: ^{1}H-NMR spectrum for TH4

To synthesize TH5, ciproflaxine acid chloride was reacted with luminol as shown in equation 17.

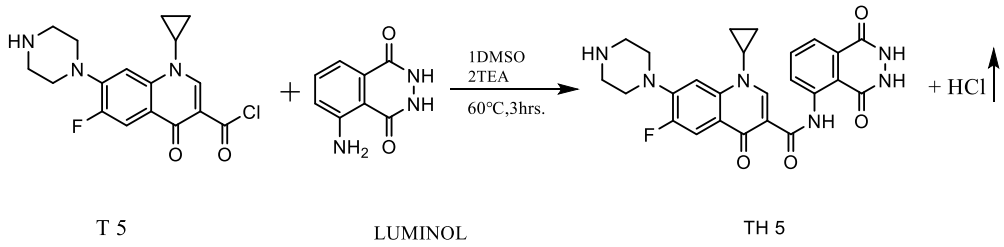

The equation 17: Synthetic route for compound TH5

The FT-IR spectrum for **TH5 [1-cyclopropyl-N-(1,4-dioxo-1,2,3,4-tetrahydrophthalazin-5-yl)-6-fluoro-4-oxo-7-(piperazin-1-yl)-1,4-dihydroquinoline-3-carboxamide]** showed the following values (V max. cm-1): 3439 ; 3479 (NH str. amine and amide) overlap, 3020 (CH str., Ar.), 2916 (CH str., alkane), 1651 ; 1626 (C=O str., ketone, amide), 1454-1560 (C=C str., Ar.), 1440 (C-F str.), 1261 (C-N str. ar.) ,1008 (C-N str., alkyl) Figure 50. 1H-NMR (500 MH, δ ppm): 10.81 , 10.50 , 10.26 (N-H, sec. amide), 8.86 (C-H, ethylene), 8.11- 6.92 (C-H, benzene) , 4.65 (N-H, aromatic amine), 4.06 (C-H, cyclopropane), 3.80 ,2.72 (CH2, methylene), 1.22 (CH2, cyclopropane), 2.49 (DMSO). This spectrum is presented in Figure 51.

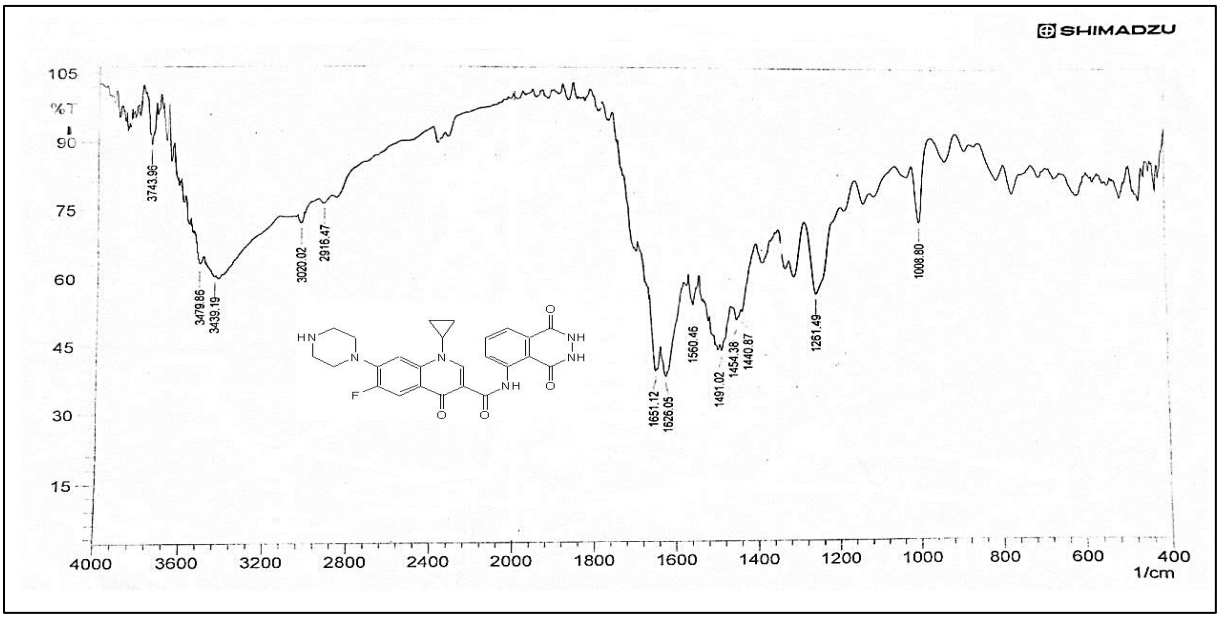

Figure 50: FT-IR spectrum for TH5

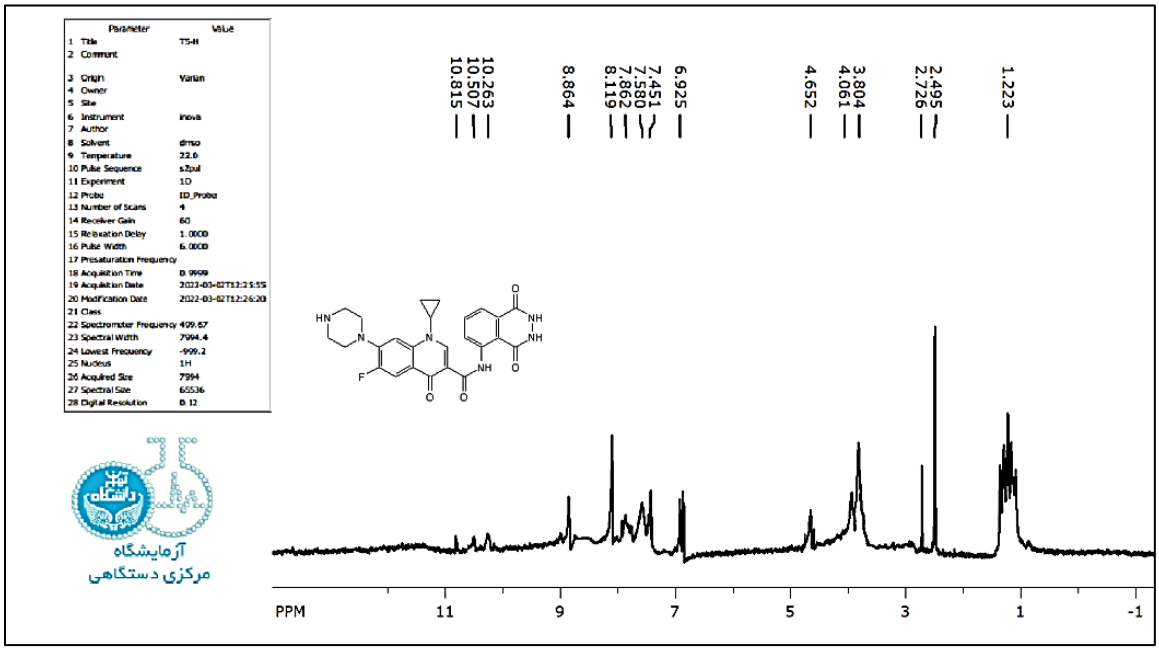

Figure 51: ^{1}H-NMR spectrum for TH5

Compound TH6 prepared from the reaction of Mefenamic acid chloride and luminol as the following equation 18.

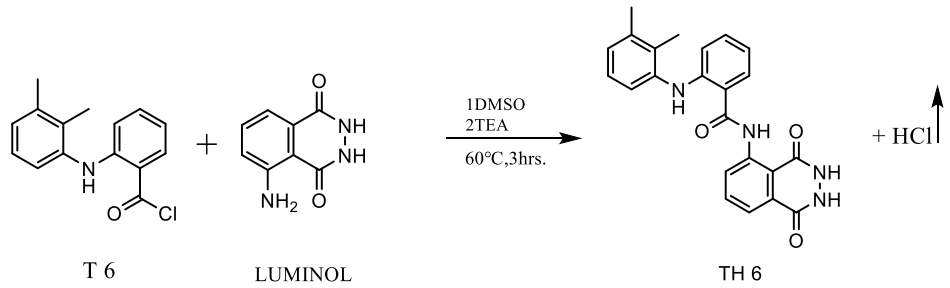

The equation 18 : Synthesis of TH6 .

FTIR spectrum for the derivative **TH6 [2-((2,3-dimethylphenyl)amino)-N-(1,4-dioxo-1,2,3,4-tetrahydrophthalazin-5-yl)benzamide]** shows the following values (V max., cm-1):3163.36-3443.05(NH amine and amid), 3012.91 (CH aromatic) , 1656.91(C=O amid),1498.74(C=C aromatic),1323.21(CH_3), 1240.27(C-N str.) Figure 52 .^{1}HNMR (500 MHz, δ ppm) for the derivative shows the following chemical shifts:11.83-11.51(NH amid),9.83(NH amine),8.92-6.69(CH benzene) ,2.49(DMSO),2.09-1.19(CH_3). This spectrum is presented in Figure 53.^{13}C NMR spectrum for the derivative shows the following chemical shifts: (125 MHz, δ ppm):168.64-167.18(C=O amide),155.90-144.41(C-N amide)

143.39-109.95(1-benzene),39.94(DMSO),21.27-15.68(CH_3). This spectrum is presented in figure 54.

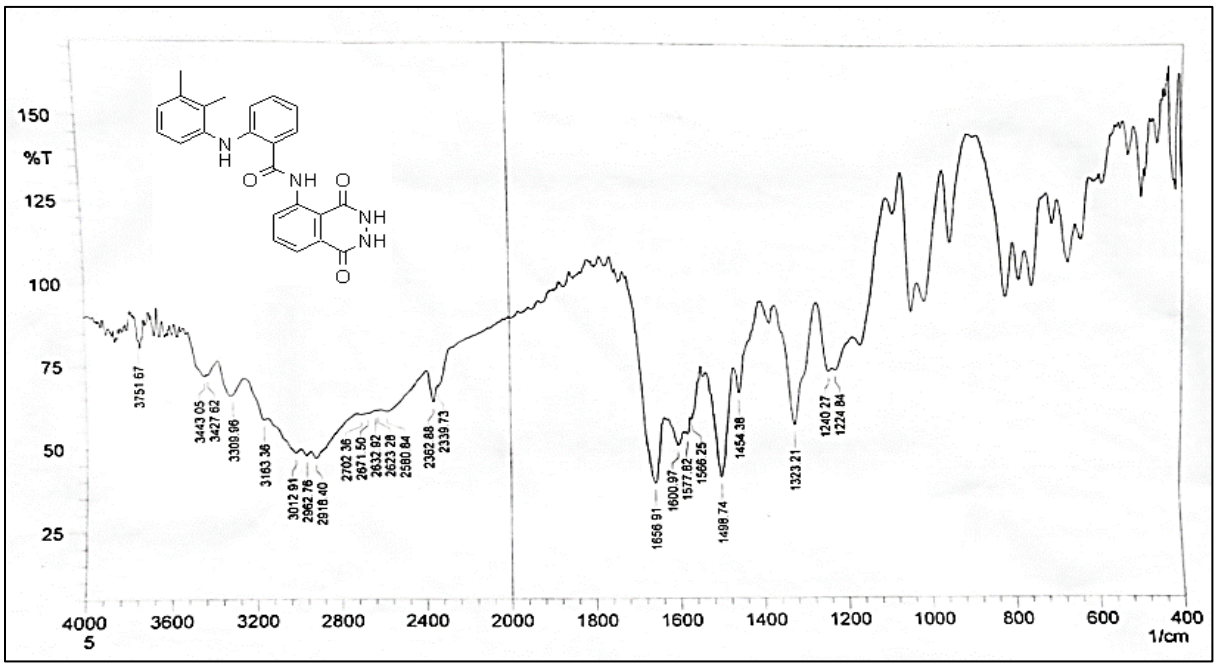

Figure 52: FT-IR spectrum for TH6

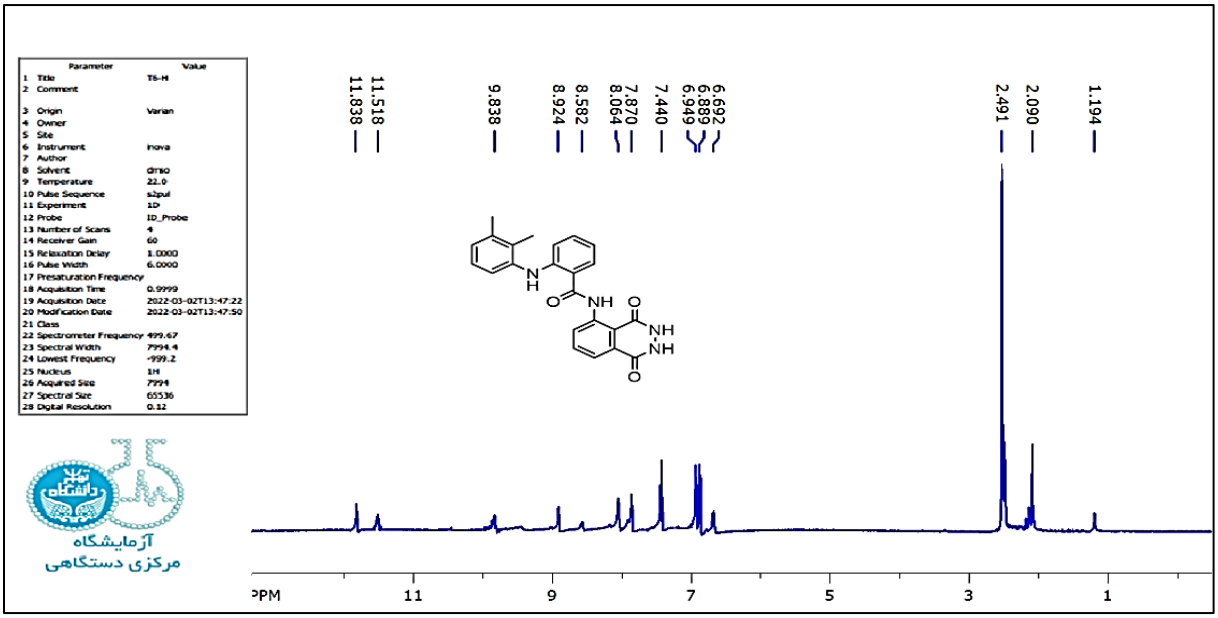

Figure 53: ^{1}H-NMR spectrum for TH6.

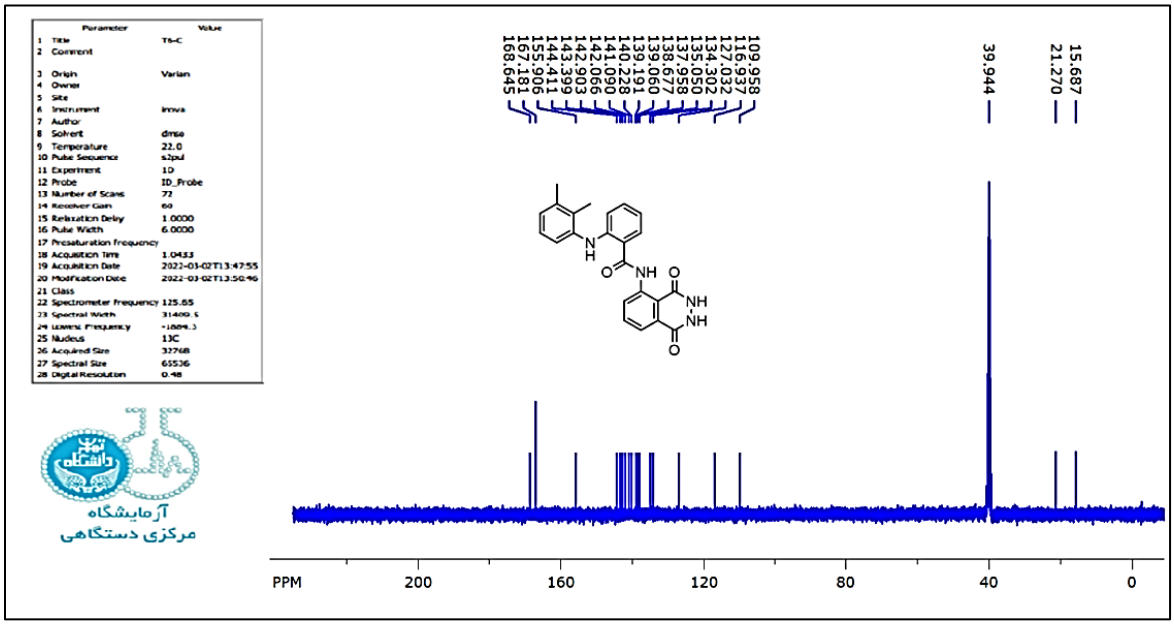

Figure 54: ^{13}C-NMR spectrum for TH6

Ceftriaxone acid chloride was reacted with luminol for producing TH7 as explaining in equation .

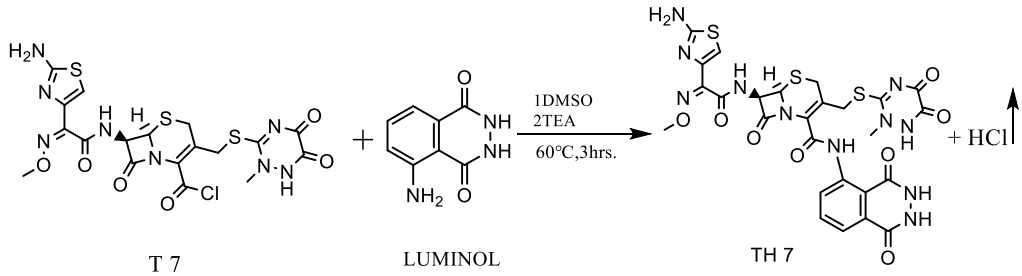

The equation 19: Synthesis of TH7 .

FTIR spectrum for **TH7 [(6R,7R)-7-((Z)-2-(2-aminothiazol-4-yl)-2-(methoxyimino)acetamido)-N-(1,4-dioxo-1,2,3,4-tetrahydrophthalazin-5-yl)-3-(((2-methyl-5,6-dioxo-1,2,5,6-tetrahydro-1,2,4-triazin-3-yl)thio)methyl)-8-oxo-5-thia-1-azabicyclo[4.2.0]oct-2-ene-2-carboxamide]** showed the following values (V max., cm-1): 3444-3119 (NH groups str.) , 3067; 3030 (CH str. Ar.), 2987 ; 2939 (CH str. alkane), 1768 (C = O str. β-lactam ring), 1678; 1600 (C = O

str., C = C str.), 1581; 1489 (C = C str. Ar.) , 1506 (C = N str.), 1319 (C-N str. aryl), 1035 (C-O str.) . This spectrum is presented in Figure 55 .1H-NMR (500 MH, δ ppm):10.74; 9.58 ; 9.28 (NH, sec. amide), 8.07 (CH,thiazole) , 7.44-6.94 (CH, benzene), 5.12 (CH, propiolactam), 5.03 (H, propiolactam) 4.26 (CH_2, methylene), 3.80 (NH, Aromatic amine),3.38 (CH_2, methylene), 2.53 (DMSO), 2.06 ;1.88 (CH, methyl) Figure 56 .

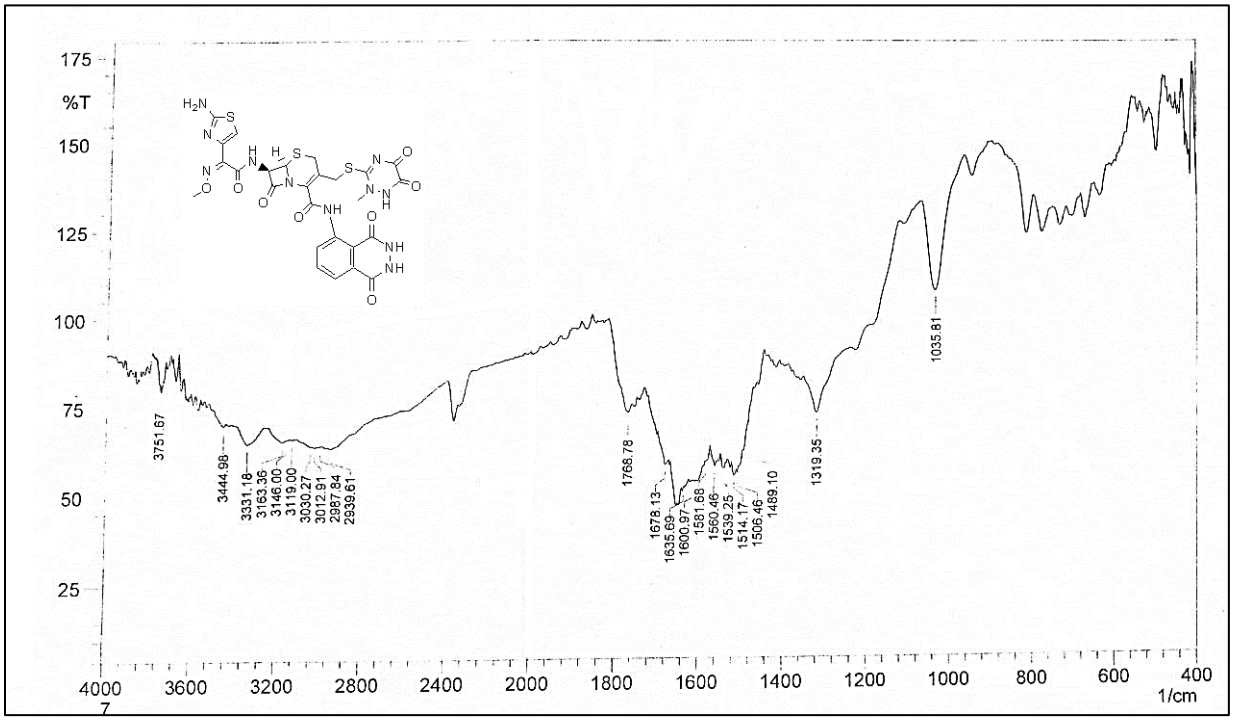

Figure 55: FT-IR spectrum for TH7

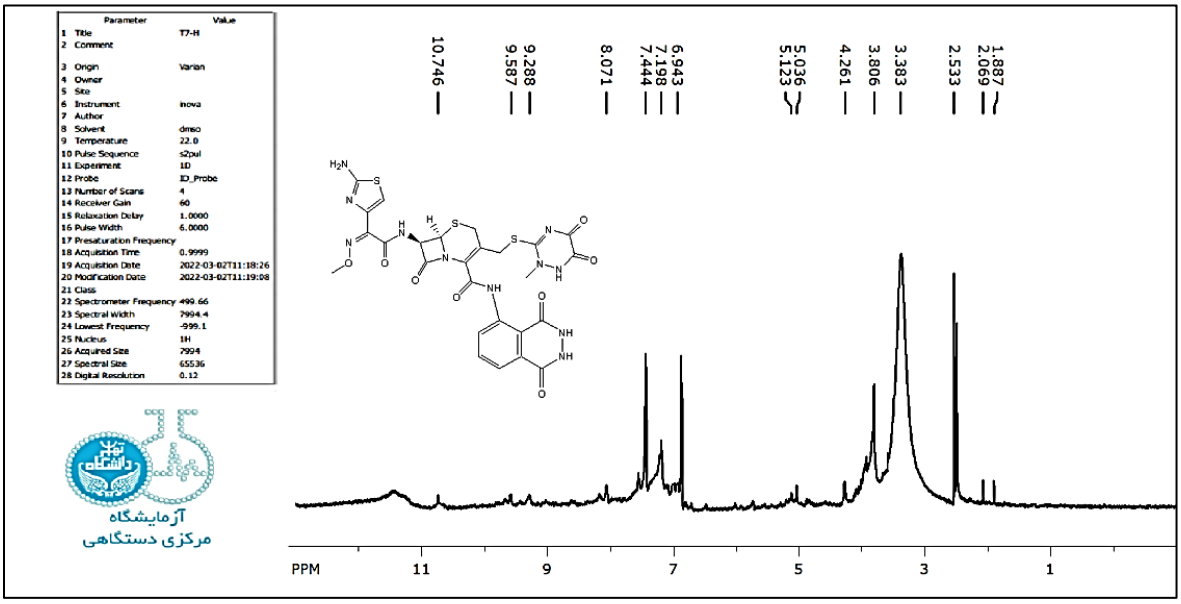

Figure 56: ^{1}H-NMR spectrum for TH7

TH8 was synthesized by the reaction of luminol with ampicillin acid chloride as shown in equation 20.

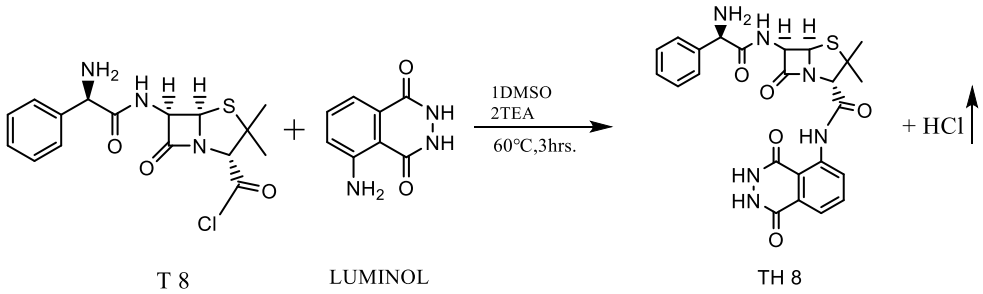

The equation 20 : Synthesis of TH8 .

FT IR spectrum for the derivative **TH8 [(2S,5R,6R)-6-((R)-2-amino-2-phenylacetamido)-N-(1,4-dioxo-1,2,3,4-tetrahydrophthalazin-5-yl)-3,3-dimethyl-7-oxo-4-thia-1-azabicyclo[3.2.0]heptane-2-carboxamide]** shows the following values (V max., cm-1):3161.43 ,3329.25(NH amine and amid),3010.98 (CH aromatics) , 2964.69(CH aliphatic) , 2582.77(S-H str., mercaptans) ,1647.26(C=O str., amid), 1600.97(C=C str., aromatic),1379.15 (CH_3), 1321.28

(C-N str.) Figure 57. ^{1}H NMR (500 MH, δ ppm) for the derivative shows the following chemical shifts:11.44,10.37,8.05 (NH amide),8.27 (NH amine),7.87-6.88(1benzene), 3.35(H propiolactam) , 2.47(DMSO), 2.33-1.89(CH methine),0.87(CH_3) Figure 58. ^{13}C NMR (125 MH, δ ppm) spectrum for the derivative shows the following chemical shifts:174.80-166.21(C=O amide),153.32(C-N amide),136.48-111.96(1benzene) ,82.50-71.60 (CH aliphatic), 62.36-57.15(CH_2, aliphatic),42.12(DNSO) , 29.58(CH_3). This spectrum is presented in Figure 59.

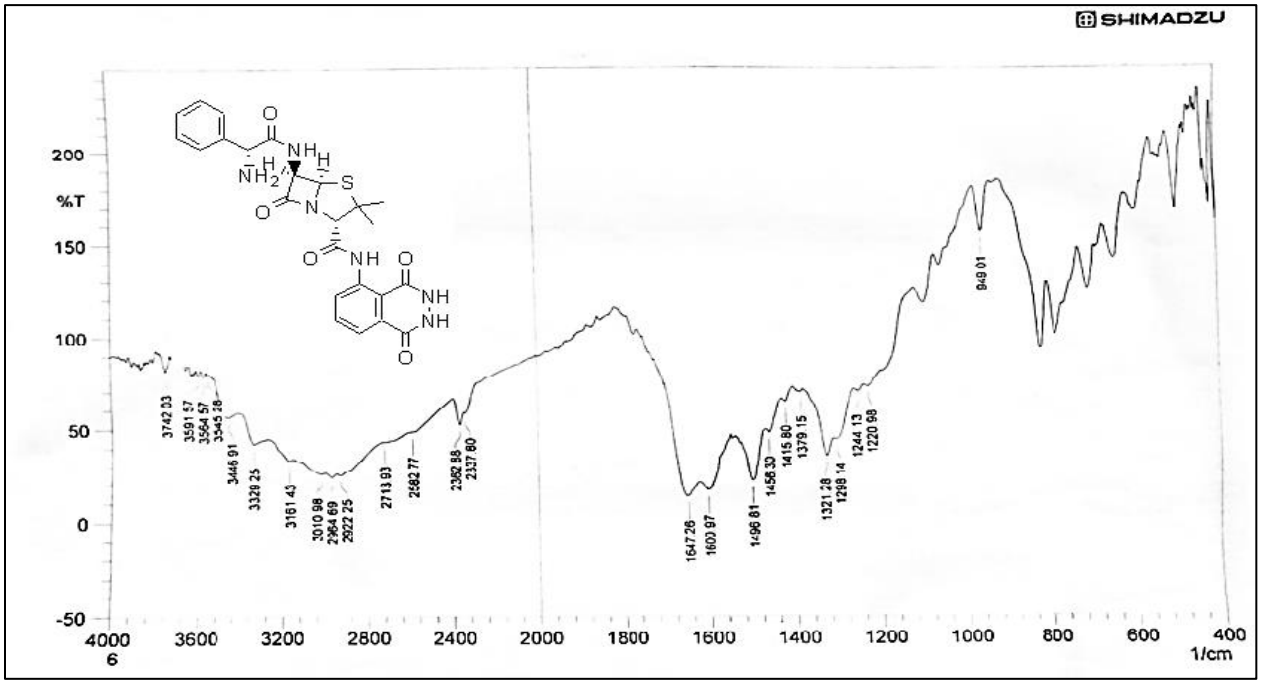

Figure 57: FT-IR spectrum for TH8

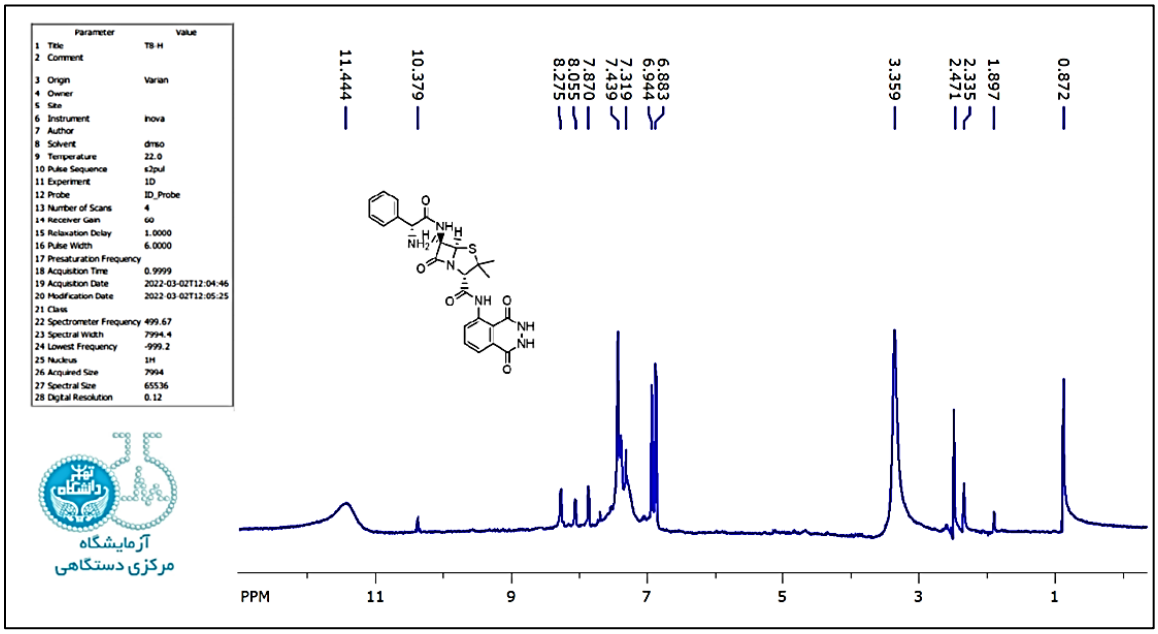

Figure 58: ^{1}H-NMR spectrum for TH8.

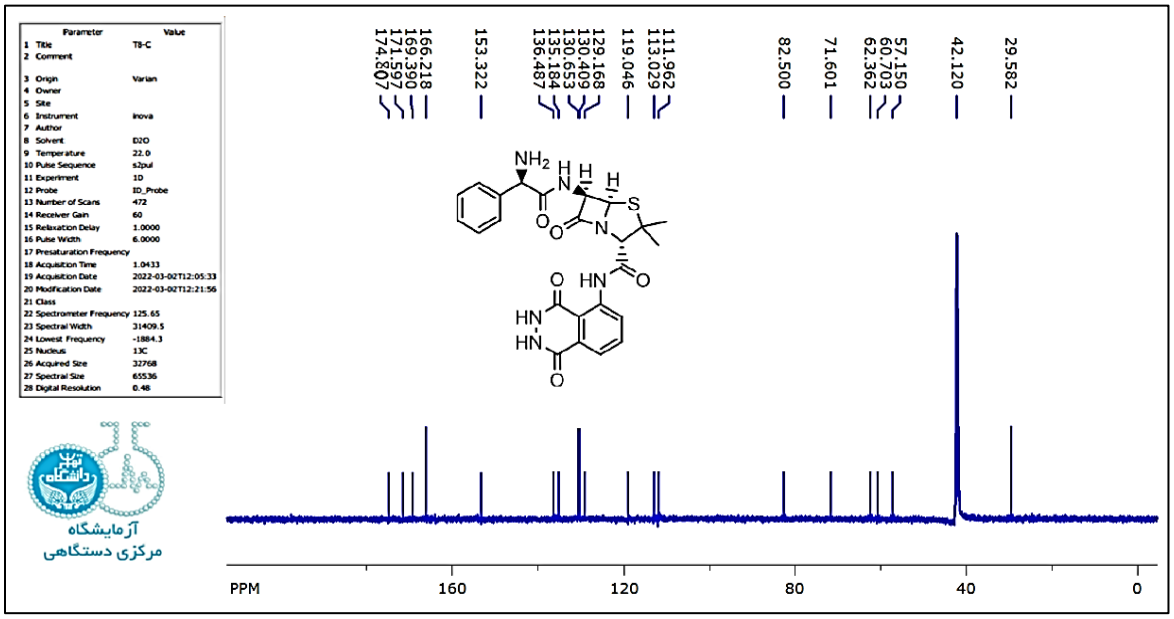

Figure 59: ^{13}C-NMR spectrum for TH8 .

Cefotaxime acid chloride was reacted with luminol to form TH9, the chemical equation for the preparation is explaining in equation 21.

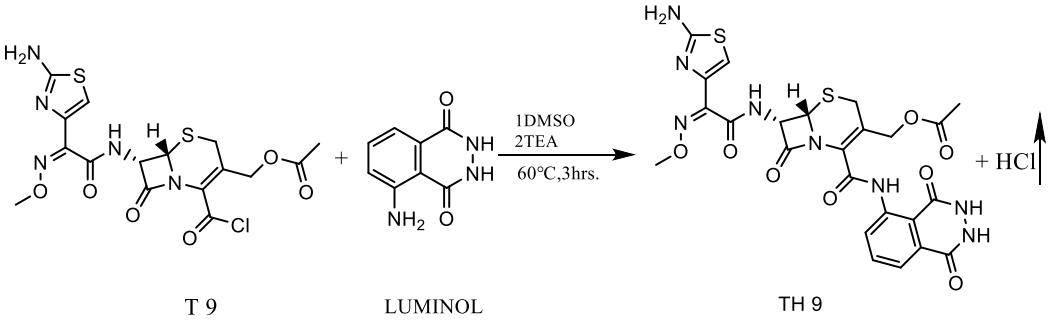

The equation 21 : Synthesis for TH9 .

FTIR spectrum for **TH9 [((6S,7S)-7-((Z)-2-(2-aminothiazol-4-yl)-2-(methoxyimino) acetamido)-2-((1,4-dioxo-1,2,3,4-tetrahydrophthalazin-5-yl)carbamoyl)-8-oxo-5-thia-1-azabicyclo[4.2.0]oct-2-en-3-yl)methyl acetate]** showed the following values (V max., cm-1): 3317 (NH groups str.) , 3171 (CH str. Ar.), 2939 (CH str. alkane), 1751 (C = O str. β-lactam ring , C=O str. ester), 1647;1637 (C = O str., C = C str.), 1606 (C = C str. Ar.) , 1537-1504 (C=N str.) , 1325 (C-N str. aryl), 1221 (C-O str.) , 1031 (C-N str. alkyl) Figure 60 . ^{1}H NMR (500 MH, δ ppm) for the derivative shows the following chemical shifts : 9.60 ;9.30 ;9.03;8.69 (NH, sec. amide), 8.07 (CH, thiazole), 7.88-7.21 (CH, benzene), 5.12 (CH, propiolactam), 5.04 (H, propiolactam) 4.27 (CH_2, methylene) , 4.09 (NH, Aromatic amine),3.80 (CH_2, methylene),3.65 (CH, methyl), 2.49 (DMSO), 1.90(CH, methyl). This spectrum is presented in Figure 61.

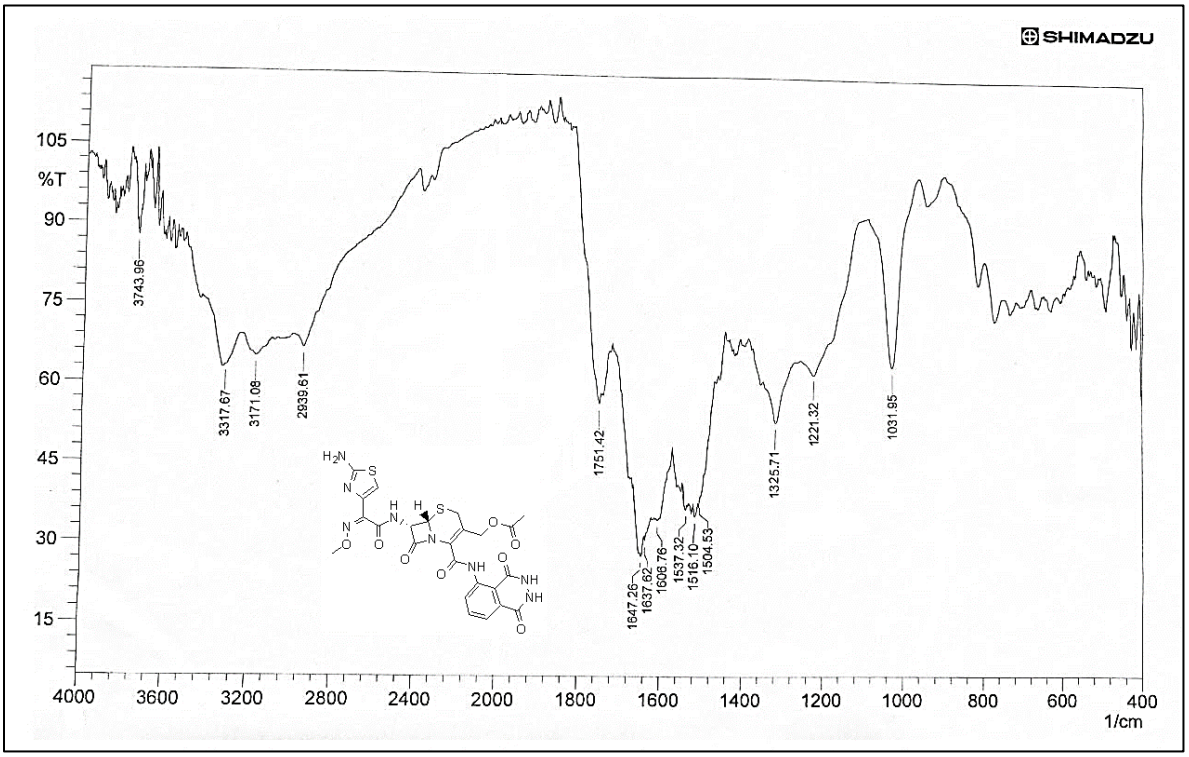

Figure 60: FT-IR spectrum for TH9

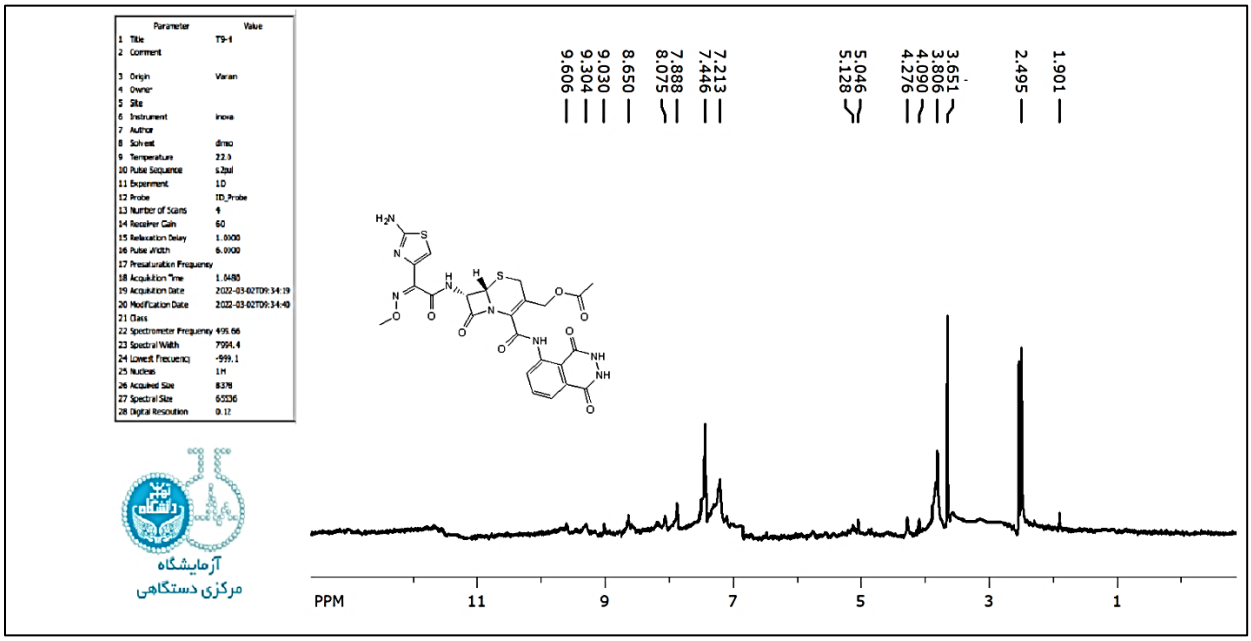

Figure 61: ^{1}H-NMR spectrum for TH9

3.3 synthesis of Compounds (TH10-TH15) :

LS was prepared by reaction luminol with succinic anhydride, Equation 22 is illustrated the preparation reaction for LS .

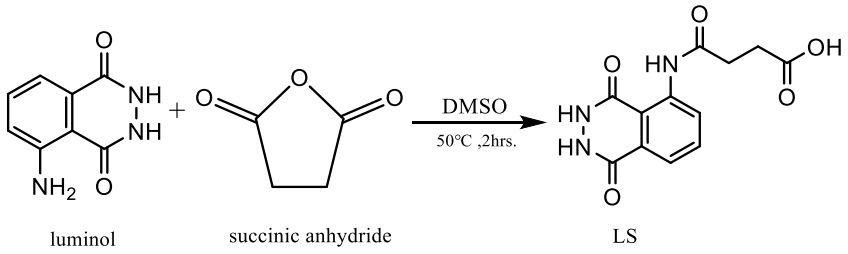

The equation 22 : Synthesis of LS

FTIR spectrum **for LS [4-((1,4-dioxo-1,2,3,4-tetrahydrophthalazin-5-yl)amino)-4-oxobutanoic acid]** showed the following values ($\bar{V}$., cm-1): 3452-2679 (OH, carboxylic acid) , 3331;3159 (NH str. amide) overlap, 3012 (CH str. Ar.), 2960,2914 (CH str. alkane), 1656(C=O str. carboxyl), 1610 (C = O str. amide), 1599 (C = C str. Ar.) , 1491,1446 (C = N str.), 1321 (C-N str.), 1091 (C-O str. carboxyl). This spectrum is presented in Figure 62.

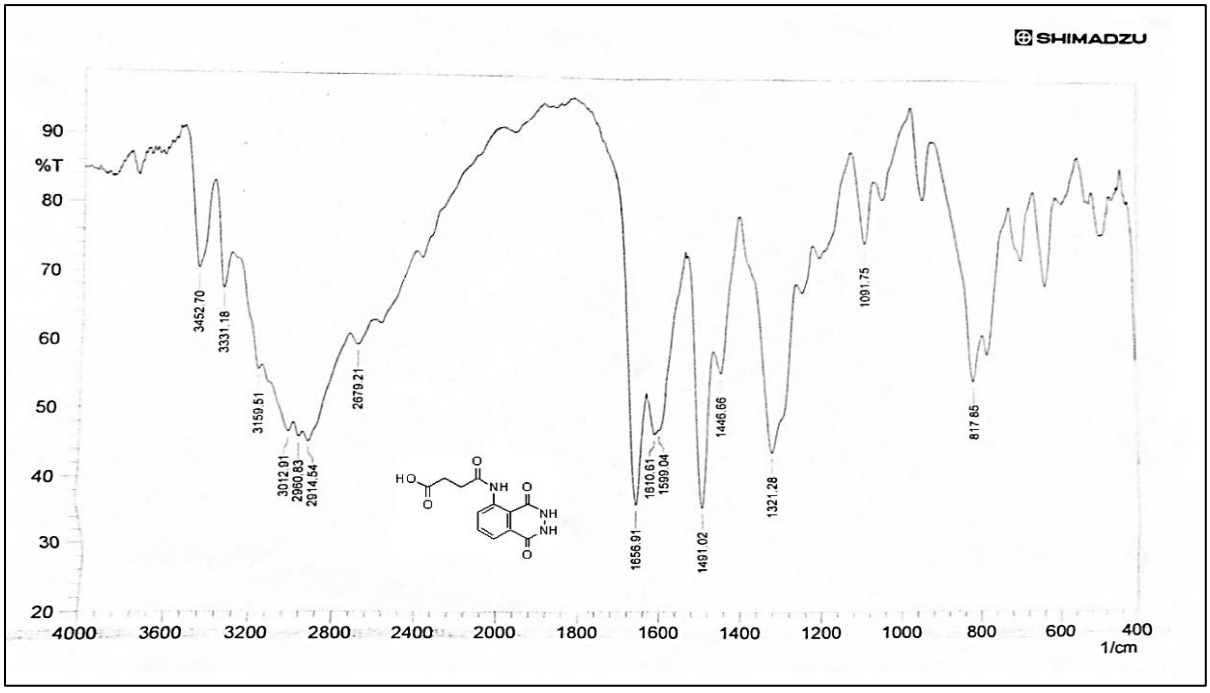

Figure 62 : FT-IR spectrum for LS

Then LS-carboxylic group was converted to chloride after that ,the last one was reacted with different amino-containing drugs (Cephalxine , Mefenamic , Paracetamol ,Theophylline ,Amoxicillin ,Ampicillin) to produce the compounds (TH10-TH15) respectively as shown in the general equation 23. The mechanism for the equation 23 is illustrated in Figure 63.

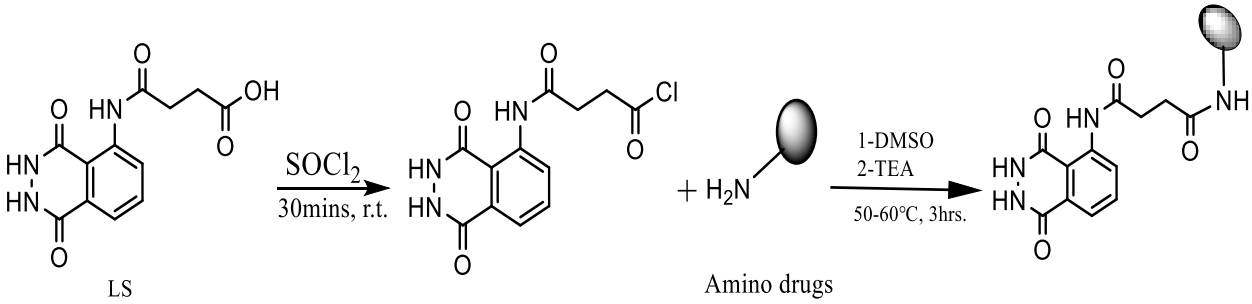

Equation 23 : general equation for synthesis (TH10-TH15).

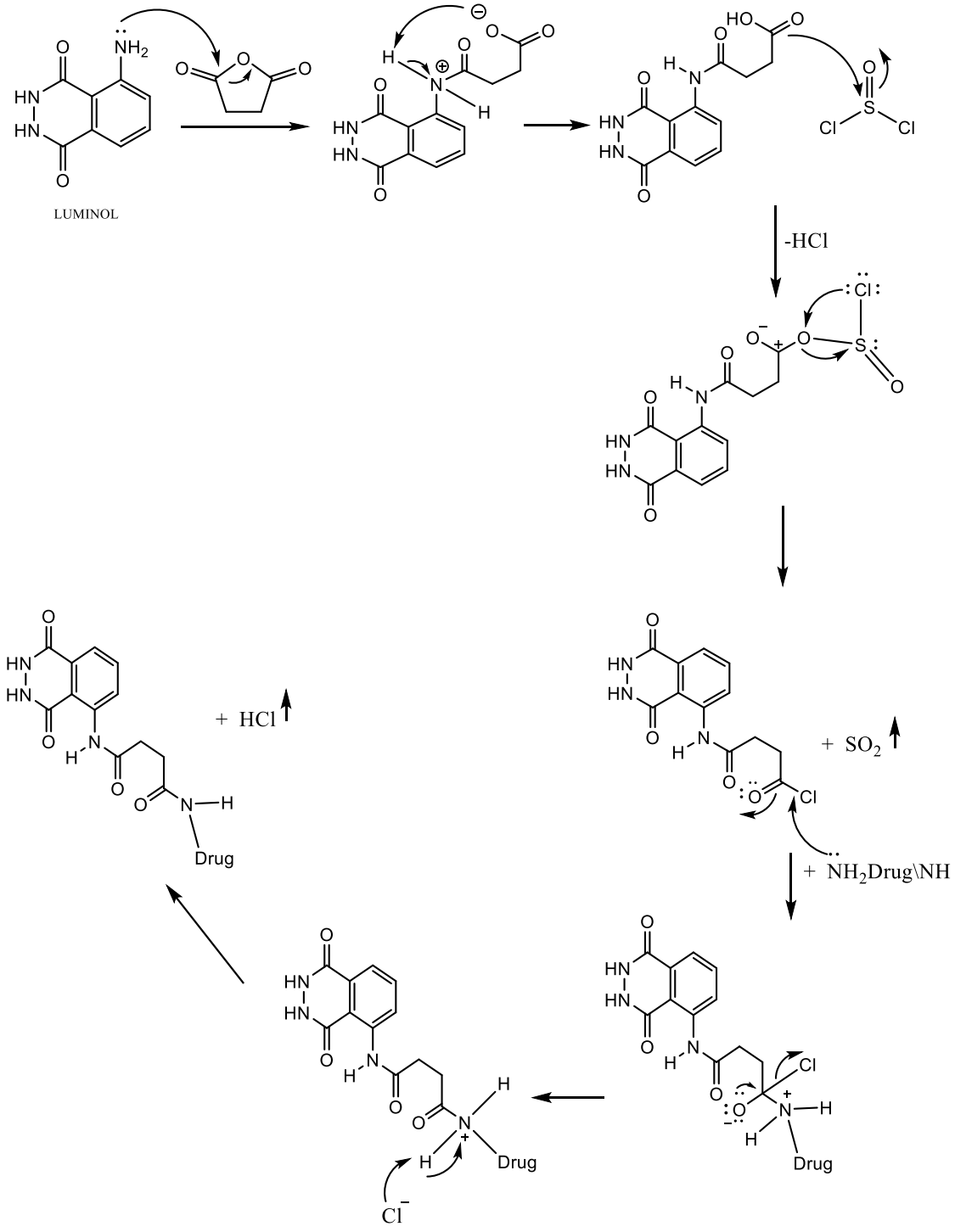

Figure 63 : Mechanism for synthesis of compounds (TH10-TH15)

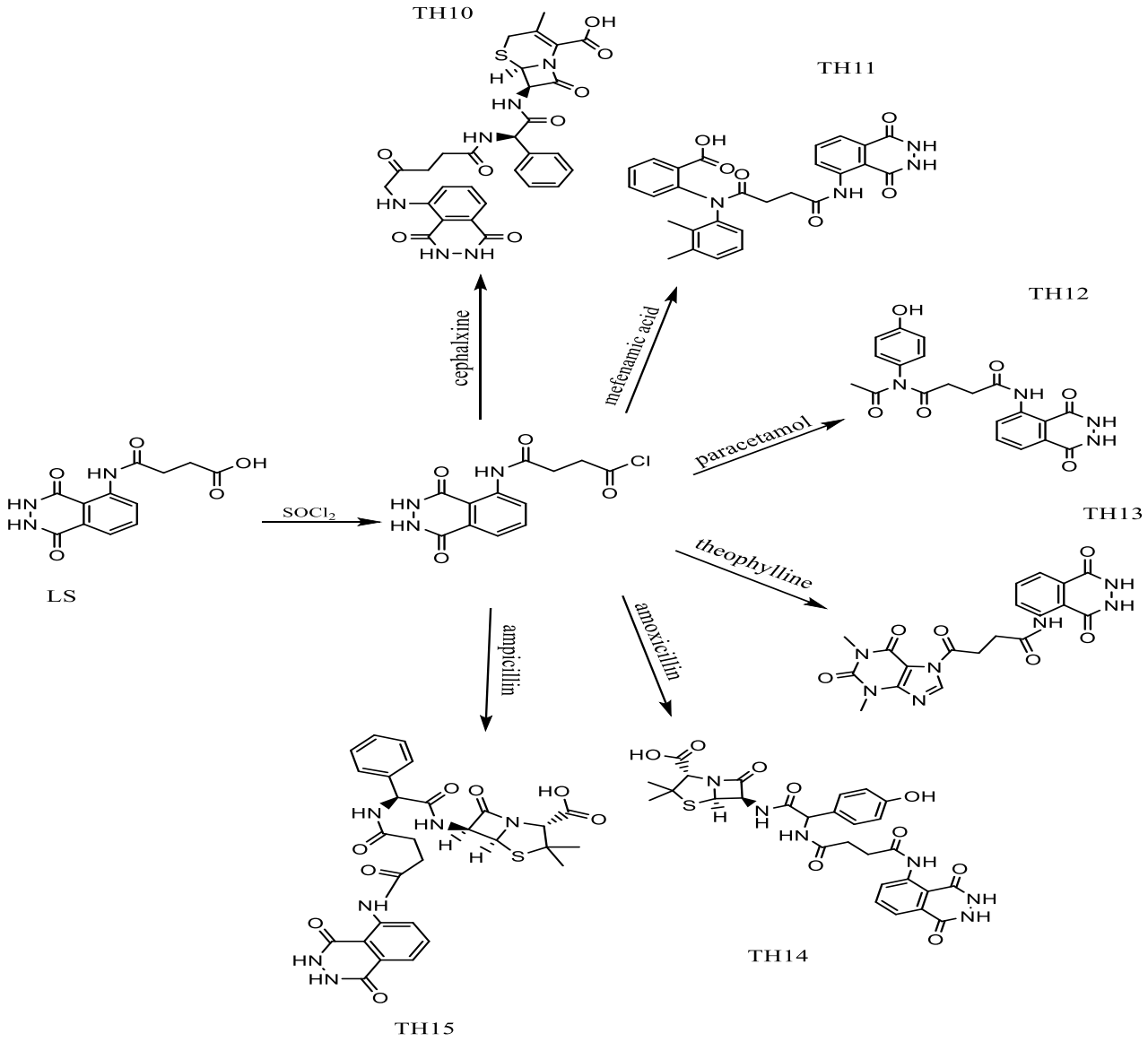

Figure 64 : Synthesis of compounds (TH10-TH15).

Equation 24 shows the reaction that happened between the Cephalexin and LS to form TH10.

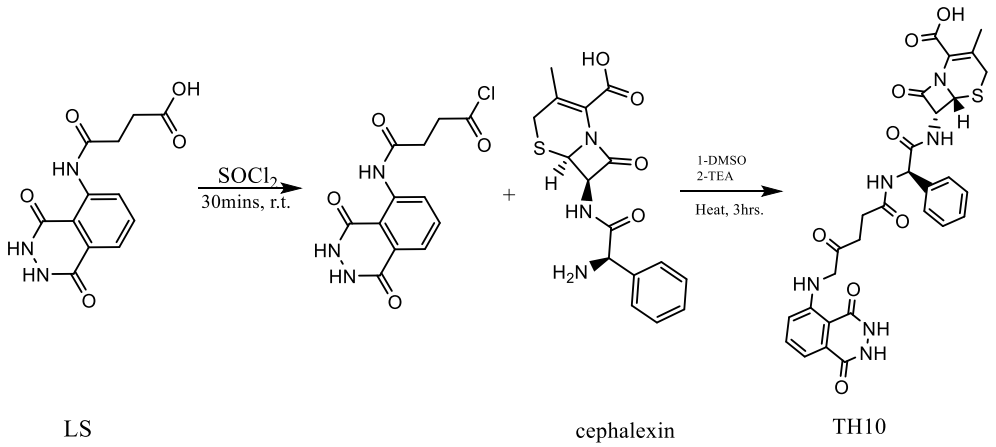

The equation 24 : Synthesis of TH10

FTIR spectrum for **TH10 [(6R,7R)-7-((R)-2-(5-((1,4-dioxo-1,2,3,4-tetrahydrophthalazin-5-yl)amino)-4-oxopentanamido)-2-phenylacetamido)-3-methyl-8-oxo-5-thia-1-azabicyclo[4.2.0]oct-2-ene-2-carboxylic acid]** showed the following values (V max., cm-1): 3390-2924 (OH, str. carboxylic acid) , 3390 -3182 (NH ,str. groups), 3061-3032 (CH str. Ar.), 2978 (CH str. alkane), 1836(C = O str. β-lactam ring), 1622-1610 (C=O str. groups), 1575 -1404 (C = C str. Ar.), 1298 (C-N str. aryl), 1259 (C-O str. carboxyl) , 1109 (C-N str. alkyl)Figure 65. ^{1}H NMR (500 MH, δ ppm) for the derivative shows the following chemical shifts:12.89 (OH ,carboxylic acid) , 10.0-8.87 (NH, sec. amide), 8.11-7.12 (CH, benzene), 5.73 (CH ,methine) , 5.52 **(C**H, propiolactam) , 5.30 **(**H, propiolactam), 4.93 (NH ,amine), 4.65- 2.64 (CH_2, methylene) , 2.53 (DMSO), 2.01 (CH, methyl)Figure 66. ^{13}CNMR (125 MH, δ ppm) : 195.18 (C, carbonyl), 175.29 (C=O ,carboxyl) , 170.42 ;163.89 (C=O amide) , 138.08 ;120.19 (CH-benzene), 63.91 – 59.59. (CH, aliphatic) , 39.51 (DMSO), 31.63-25.82 (CH_2, aliphatic), 18.86 (CH_3). This spectrum is presented in Figure 67.

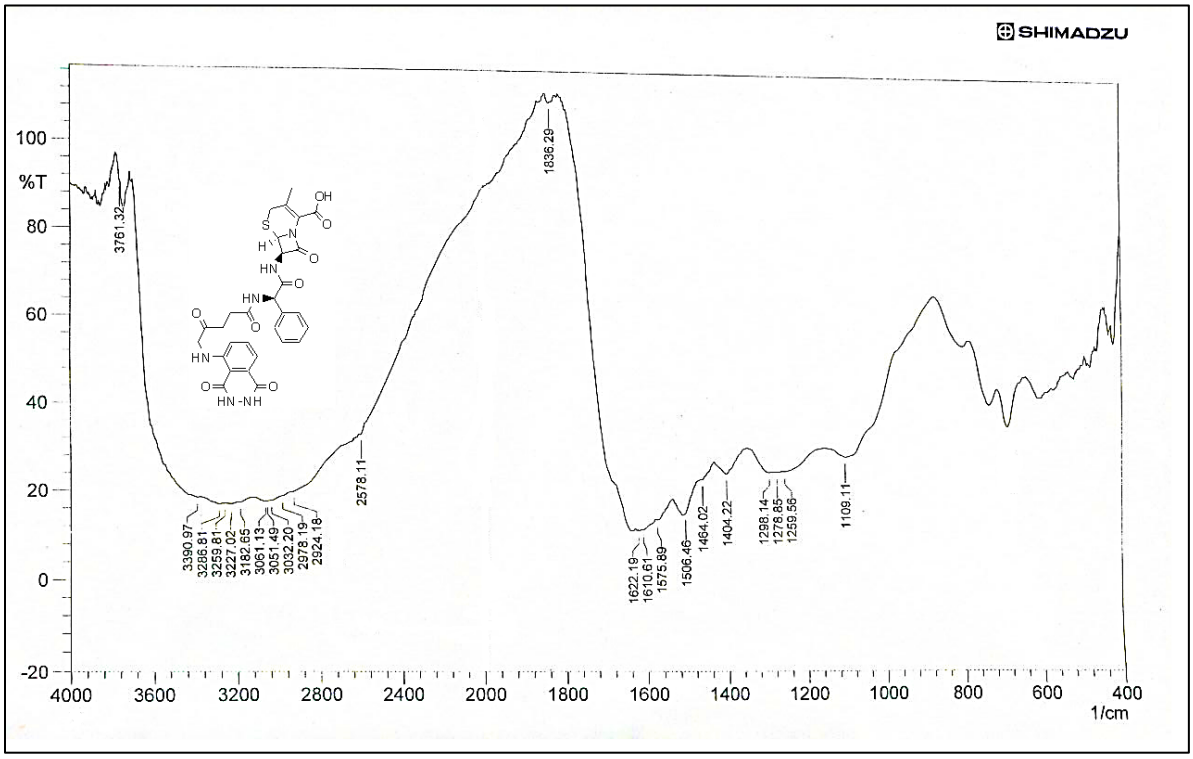

Figure 65: FT-IR spectrum for TH10

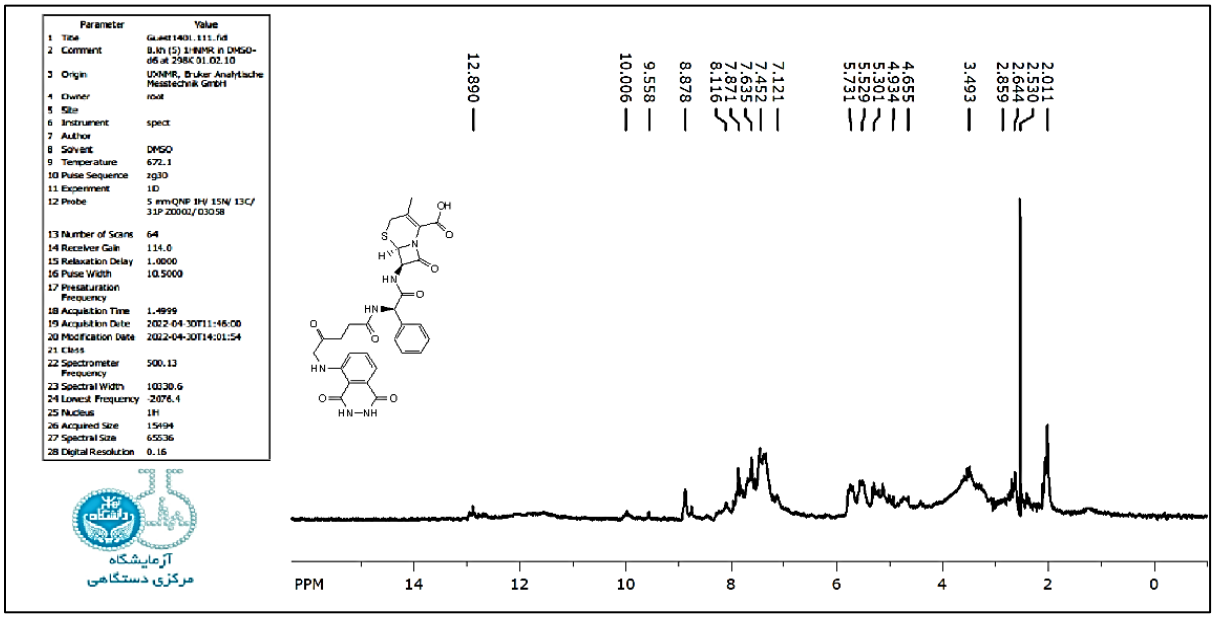

Figure 66: ^{1}H-NMR spectrum for TH10.

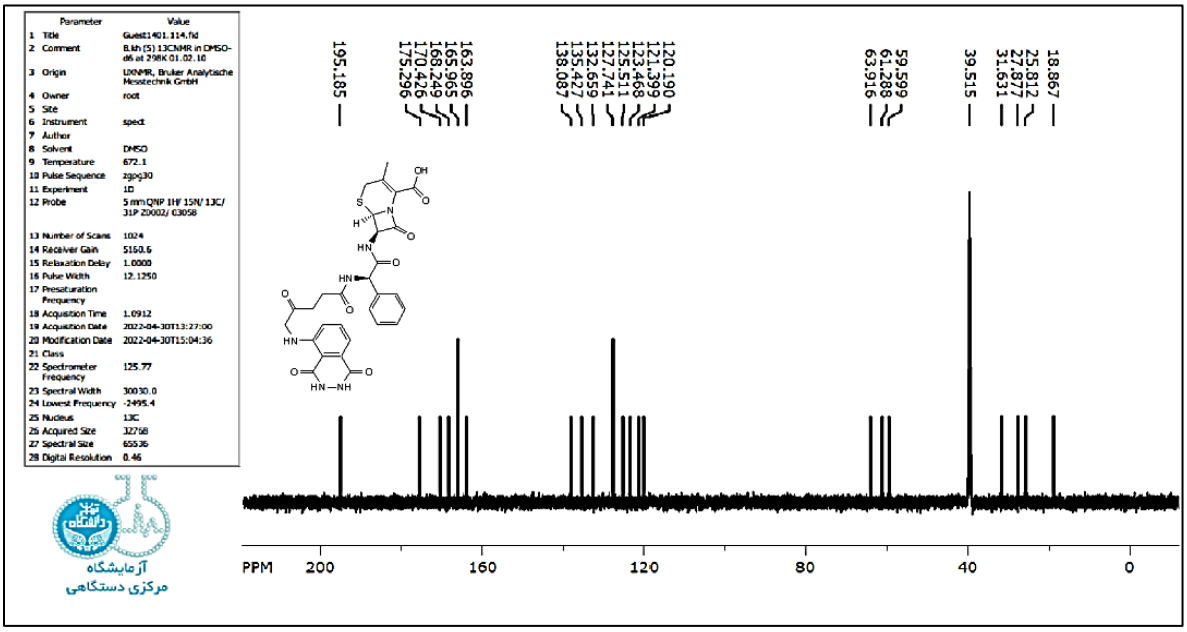

Figure 67 : ^{13}C-NMR spectrum for TH10

TH11 was synthesized from the reaction of mefenamic acid with LS as shown in equation 25 .

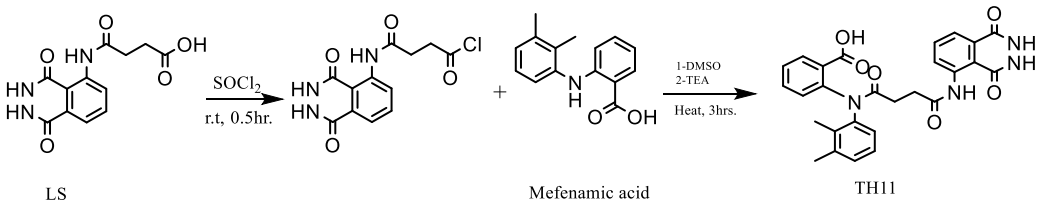

Equation 25 : Synthesis of TH11

FTIR spectrum for **TH11 [2-(N-(2,3-dimethylphenyl)-4-((1,4-dioxo-1,2,3,4-tetrahydrophthalazin-5-yl)amino)-4-oxobutanamido)benzoic acid]** showed the following values (V max., cm-1): 2640- 3344 (OH ,carboxylic acid) , 3061;3005 (CH str. Ar.), 2939-2916 (CH str. alkane), 1722 (C=O str. carboxyl), 1651 (C = O str. amid), 1437-1610 (C = C str. Ar.) , 1329(C-N str.), 1247 (C-O str. carboxyl) Figure 68 . ^{1}HNMR (500 MHz, δ ppm) for the derivative shows the following chemical shifts:13.81 (OH, carboxylic acid), 10.66-10.00(NH amide) , 8.50-6.83 (CH, benzene) , 2.73 (CH_2, methylene), 2.53 (DMSO), 2.38 -2.20 (CH_3,methyl) Figure 69. ^{13}CNMR (125 MH, δ ppm) : 179.47 (C=O ,carboxyl) , 170.84- 160.11

(C=O amide) , 140.56- 115.65 (CH-benzene) , 39.56 (DMSO), 33.81;29.60 (CH_2, aliphatic), 16.76;13.88(CH_3, aliphatic). This spectrum is presented in Figure 70.

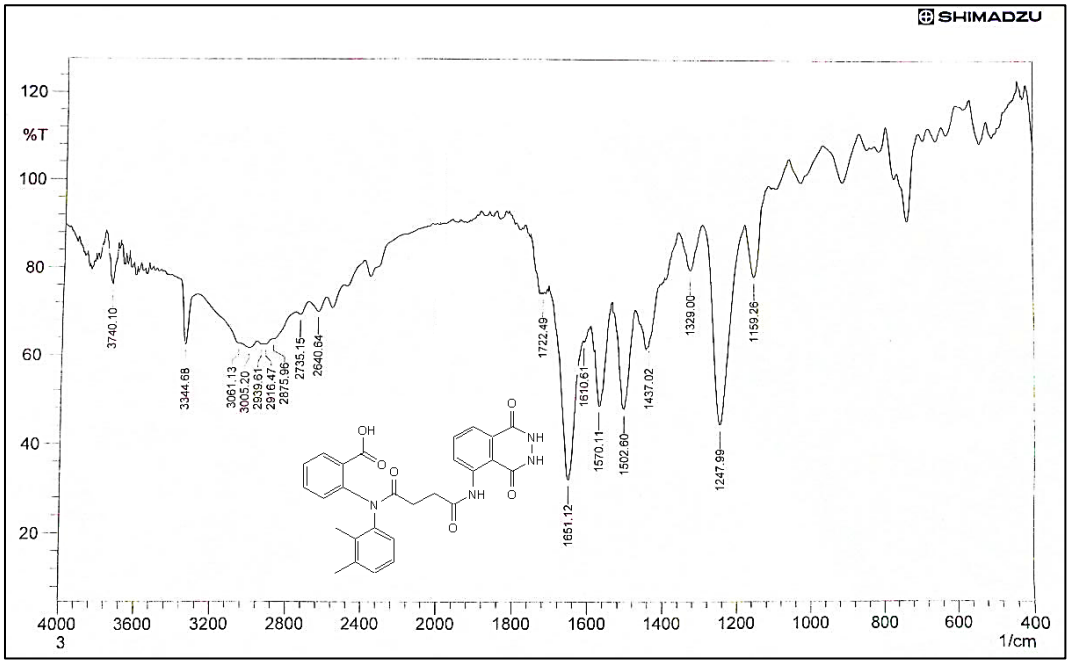

Figure 68: FT-IR spectrum for TH11

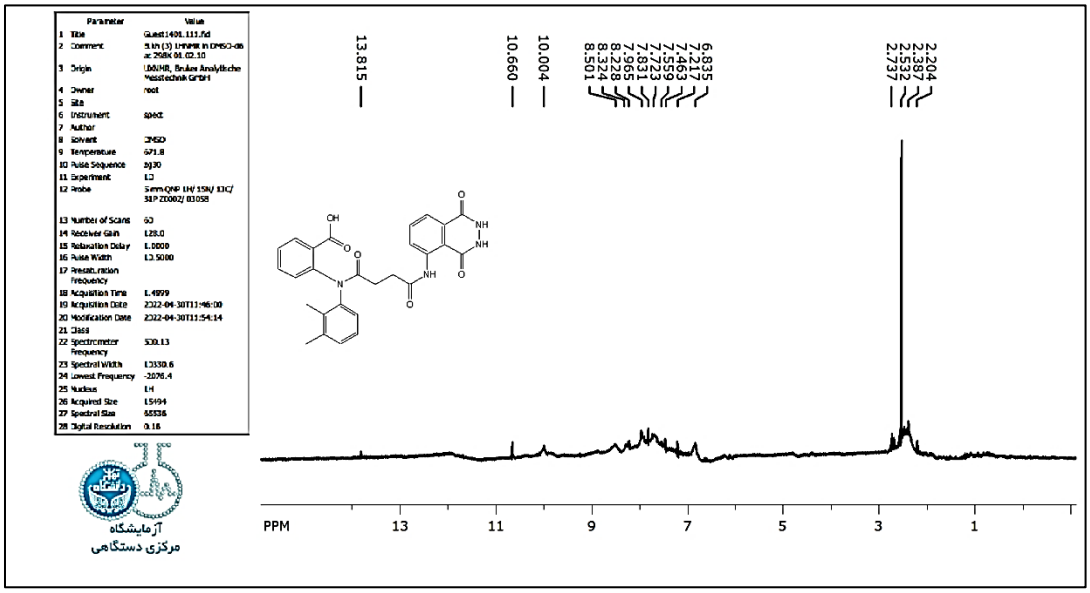

Figure 69 : ^{1}H-NMR spectrum for TH11

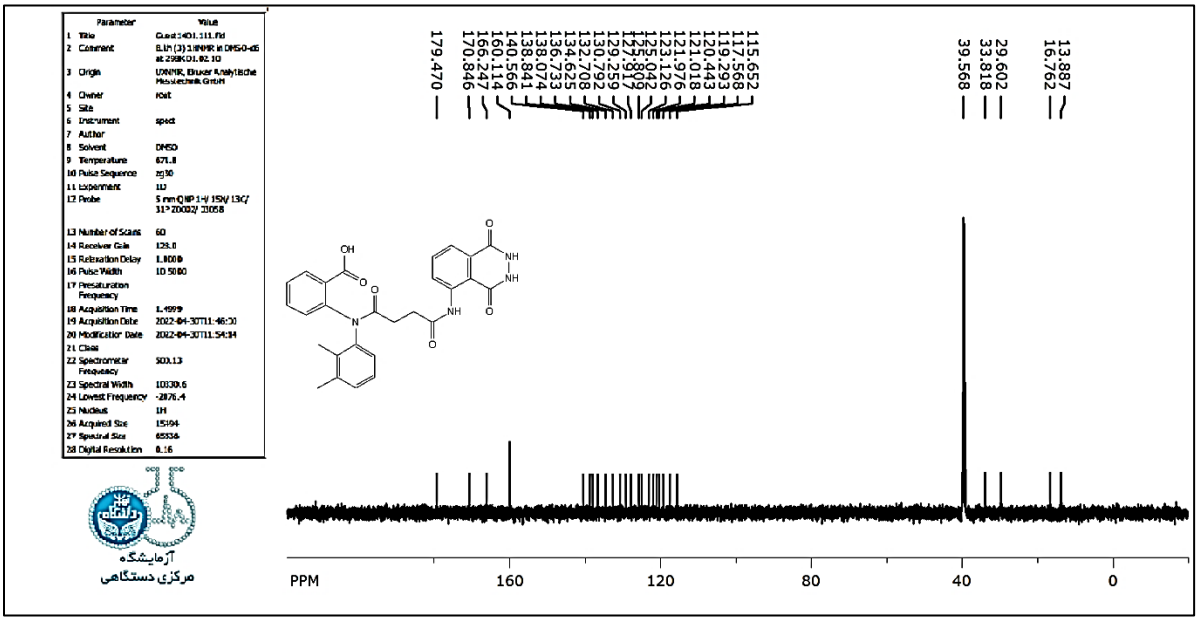

Figure 70: ^{13}C-NMR spectrum for TH11.

The paracetamol was reacted with LS to form TH12, the equation 26 explaining how this reaction happened.

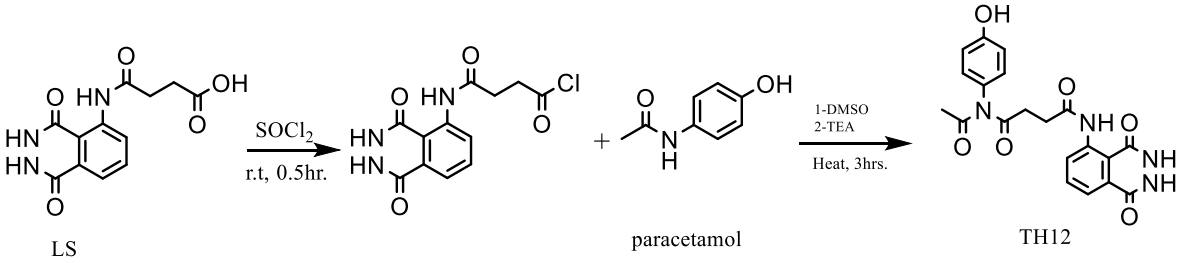

The equation 26: Synthesis for TH12 .

FTIR spectrum for **TH12 [N1-acetyl-N4-(1,4-dioxo-1,2,3,4-tetrahydrophthalazin-5-yl)-N1-(4-hydroxyphenyl)succinamide]** showed the following values (V max., cm-1): 3406;3394 (OH groups ,NH groups) overlap , 3014 (CH str. Ar.), 2931 (CH str. alkane), 1722 (C=O str. carboxyl), 1649 (C = O str. amide), 1606-1423 (C = C str. Ar.) , 1294(C-N str.), 1203 (C-O str. carboxyl) Figure71 . ^{1}HNMR (500 MHz, δ ppm) for the derivative shows the following chemical shifts: 9.14 ;8.21 (NH amide) ,7.99 (OH, alcohol), 7.65-5.56 (CH, benzene) , 2.50 (DMSO), 2.10 (CH_2, methylene), 1.26 (CH_3, methyl) Figure 72. ^{13}CNMR (125 MH, δ ppm) : 177.22- 162.08 (C=O amide) , 149.80- 120.44 (CH-

benzene) , 39.57(DMSO), 35.42;31.27 (CH_2, aliphatic), 26.17(CH_3, aliphatic). This spectrum is presented in Figure 73.

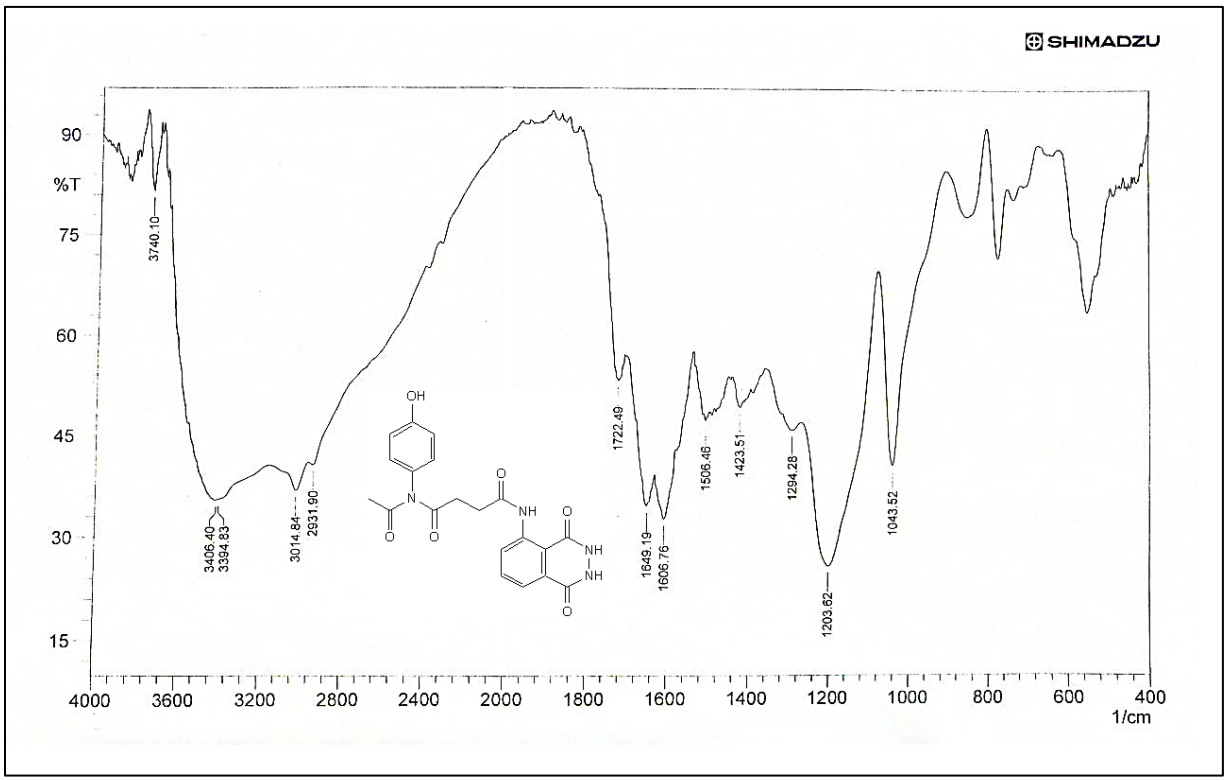

Figure 71: FT-IR spectrum for TH12

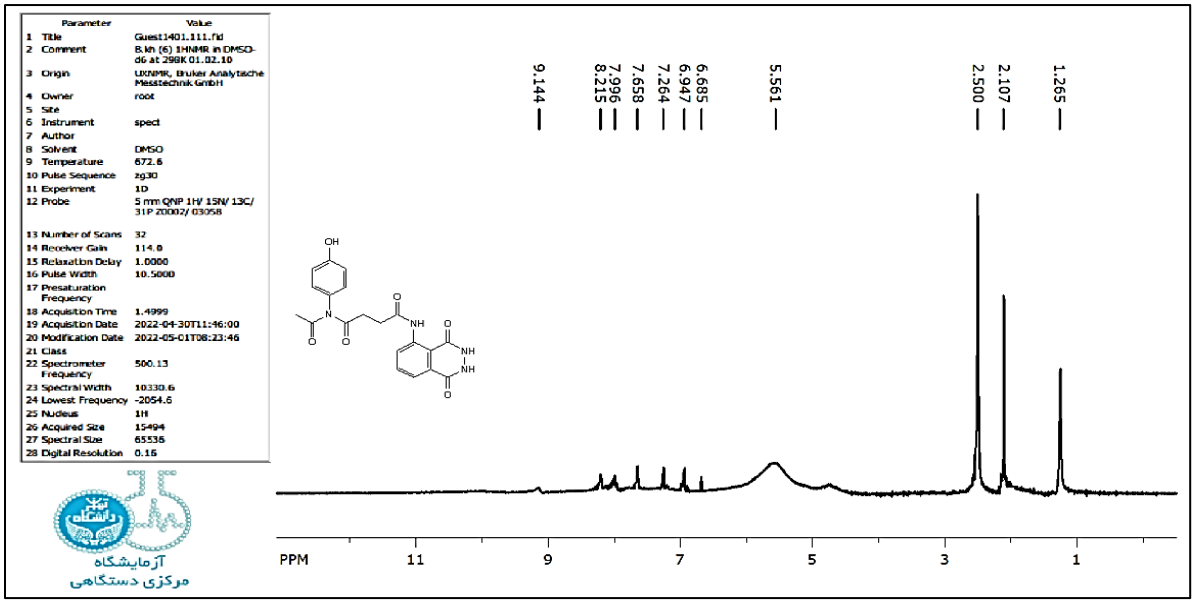

Figure 72: ^{1}H-NMR spectrum for TH12

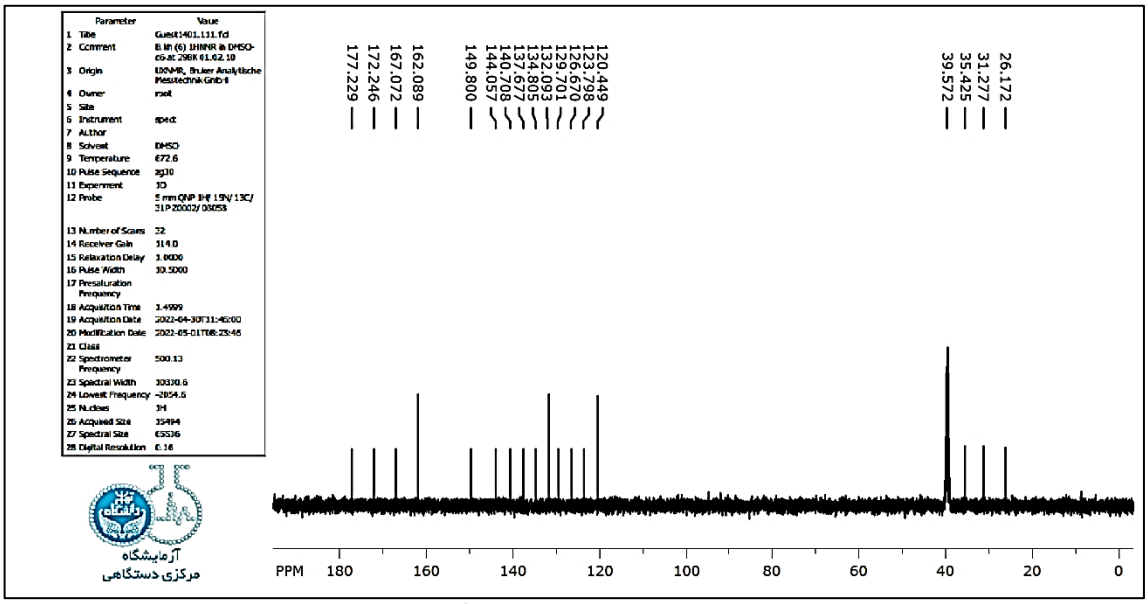

Figure 73: ^{13}C-NMR spectrum for TH12

TH13 was prepared by the reaction of theophylline with LS as shown in the equation .

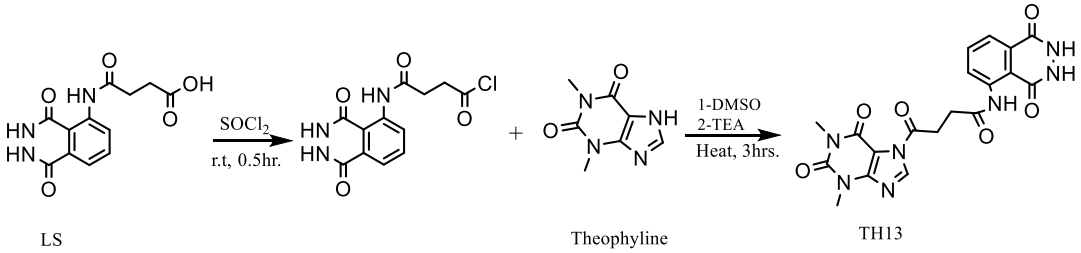

The equation 27: Synthesis for TH13 .

FTIR spectrum for **TH13 [4-(1,3-dimethyl-2,6-dioxo-1,2,3,6-tetrahydro-7H-purin-7-yl)-N-(1,4-dioxo-1,2,3,4-tetrahydrophthalazin-5-yl)-4-oxobutanamide]** showed the following values (V max., cm-1): 3333;3302 (NH groups) , 3080 (CH str. Ar.), 2918 (CH str. alkane), 1654 (C = O str. amide), 1612 (C = C str. Ar.) , 1454 (C=N) , 1394;1301(C-N str.) Figure 74 . ^{1}HNMR (500 MHz, δ ppm) for the derivative shows the following chemical shifts: 9.62 ;9.24 (NH, amide) ,8.19 (CH, imidazole), 8.01-7.73 (CH, benzene) , 3.28;2.77 (CH_3, methyl), 2.62 (DMSO), 2.50;2.42 (CH_2, methylene) Figure 75.

^{13}CNMR (125 MH, δ ppm) : 174.16 -154.04 (C=O amide) , 147.90 (N, urea) ,138.51-132.38 (CH , imidazole) , 131.42-122.03 (CH-benzene) , 39.62 (DMSO), 36.17 ,33.49 (CH_2, aliphatic), 26.17(CH_3, aliphatic). This spectrum is presented in Figure 76.

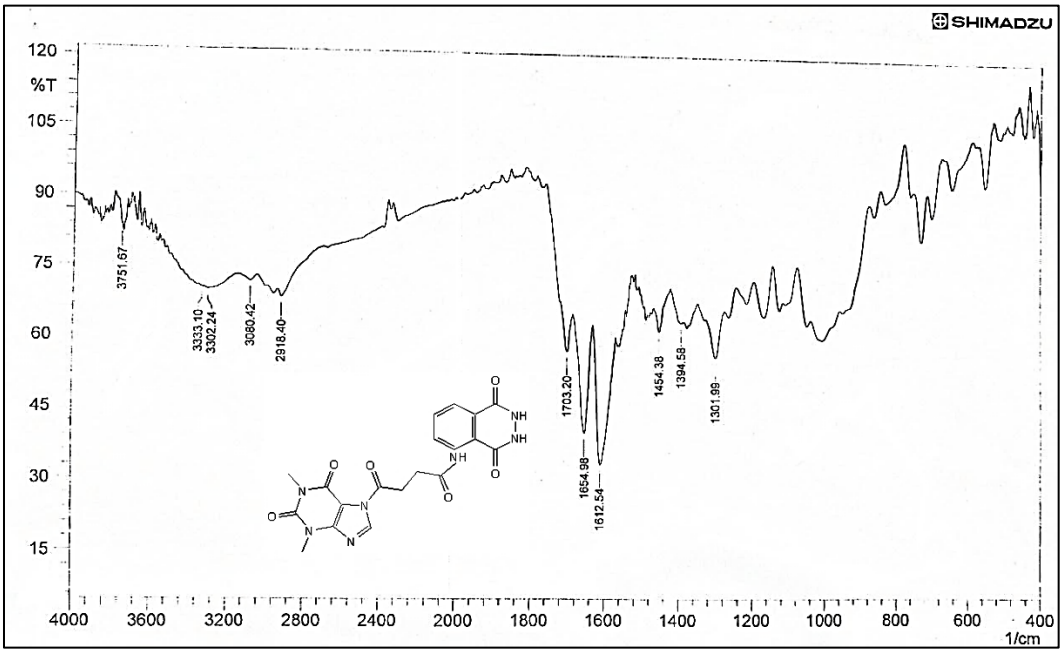

Figure 74: FT-IR spectrum for TH13

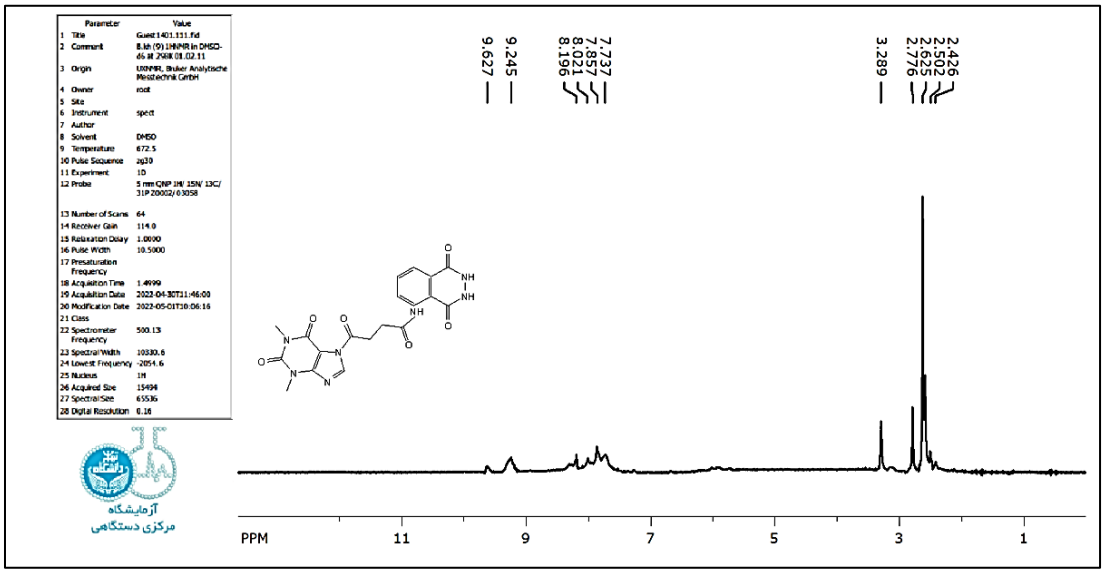

Figure 75: ^{1}H-NMR spectrum for TH13

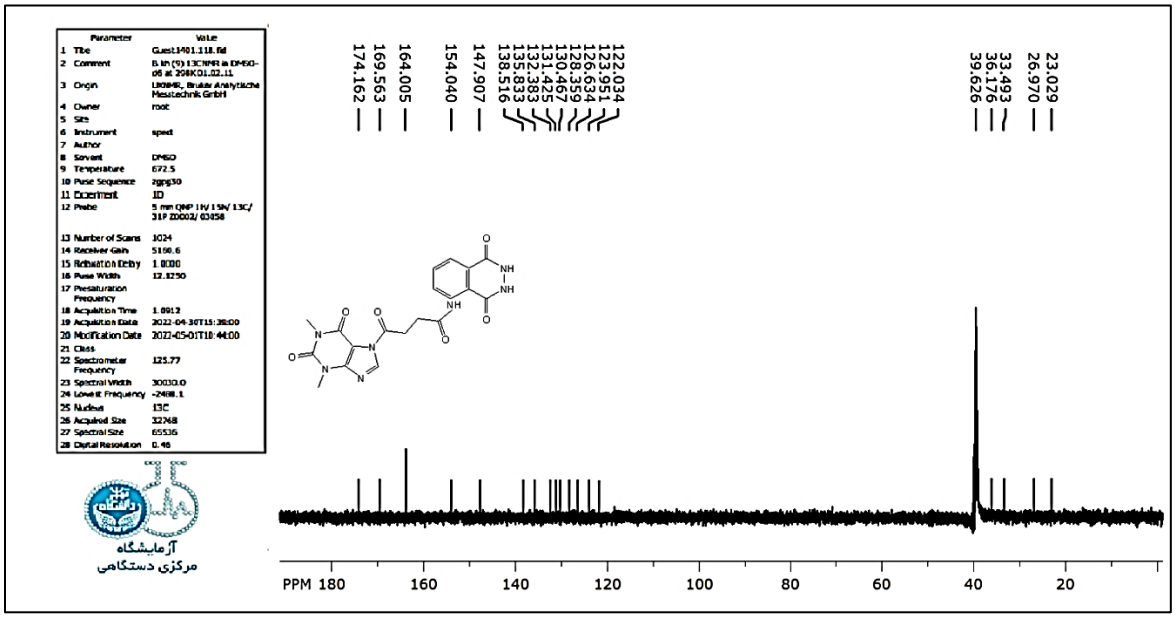

Figure 76: ^{13}C-NMR spectrum for TH13

Amoxicillin was reacted with LS to form TH14 as shown in the following equation.

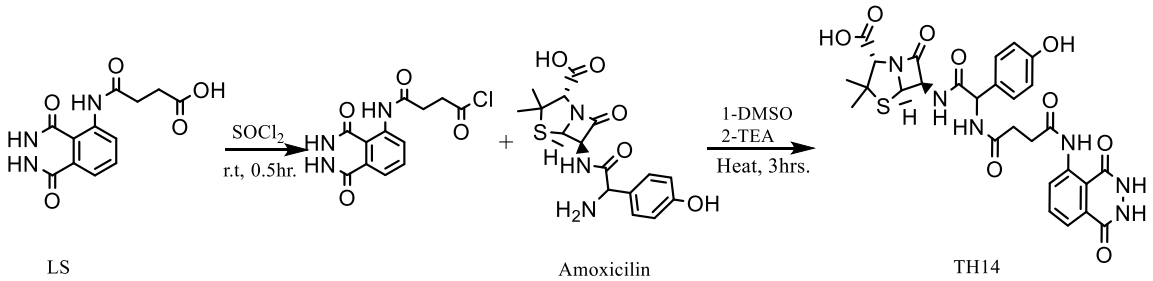

The equation 27 : Synthesis for TH14.

FTIR spectrum for **TH14 [(2S,5R,6R)-6-(2-(4-((1,4-dioxo-1,2,3,4-tetrahydrophthalazin-5-yl)amino)-4-oxobutanamido)-2-(4-hydroxyphenyl) acetamido)-3,3-dimethyl-7-oxo-4-thia-1-azabicyclo[3.2.0]heptane-2-carboxylic acid]** showed the following values (V max., cm-1): 3454-2690(OH, carboxylic) , 3454 -3230 (NH ,amine) , 3086 (CH str. Ar.), 2931 (CH str. alkane) , 1720(C = O str. β-lactam ring ,C=O str. carboxylic acid) overlap , 1602 (C = O str. amide), 1508;1462 (C = C str. Ar.) , 1390 (C-N str.), 1267;1224 (C-O str. carboxyl)

Figure 77 . [1]HNMR (500 MHz, δ ppm) for the derivative shows the following chemical shifts:13.86 (OH, carboxylic acid), 10.78-8.23 (NH, amide) ,8.0-6.85 (CH, benzene) , 5.73 (OH ,alcohol), 5.47 (CH, propiolactam) ,5.23 (H, propiolactam) , 4.35 ;4.08 (CH, methine), 2.54 (DMSO), 2.09 , (CH_2, methylene) ,1.37(CH_3, methyl) Figure 78. [13]CNMR (125 MH, δ ppm) : 177.28 (C ,carboxyl) , 173.33- 164.66 (C=O amide) , 139.71-128.0 (CH-benzene) , 78.10 -64.11 (CH ,aliphatic) , 39.46 (DMSO), 34.50 (CH_2, aliphatic), 25.47(CH_3, aliphatic). This spectrum is presented in Figure 79 .

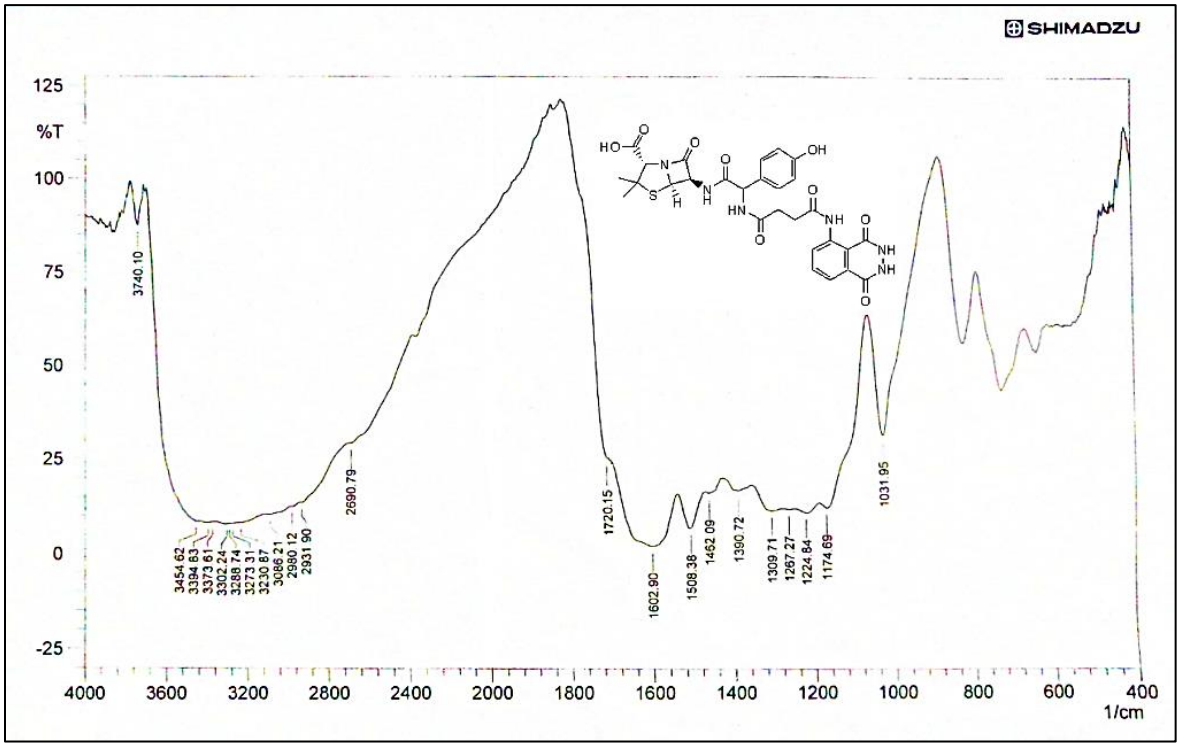

Figure 77: FT-IR spectrum for TH14

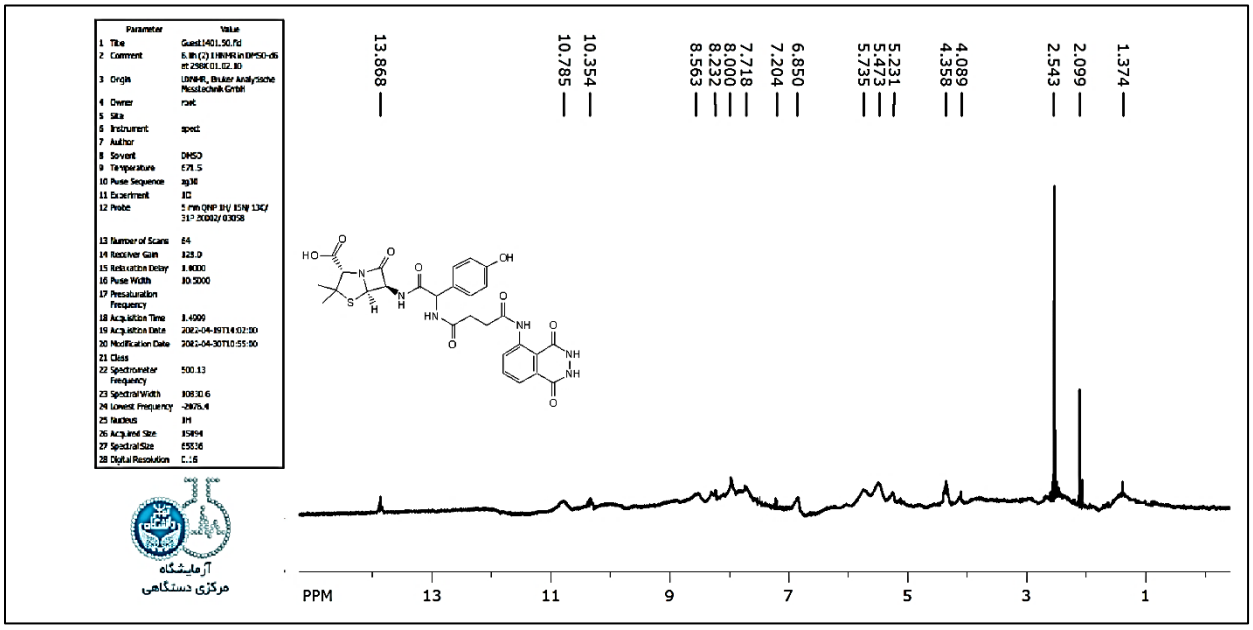

Figure 78: ^{1}H-NMR spectrum for TH14.

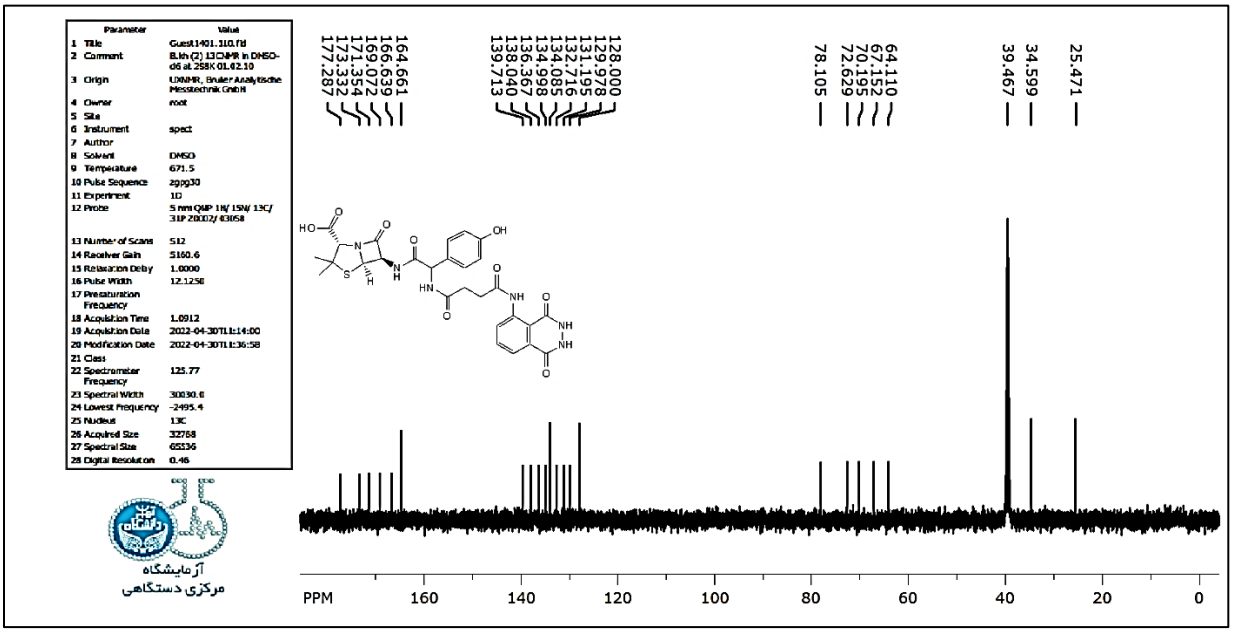

Figure 79: ^{13}C-NMR spectrum for TH14.

Ampicillin was reacted with LS to produce TH15 , the equation 28 shows how the preparation reaction occurs.

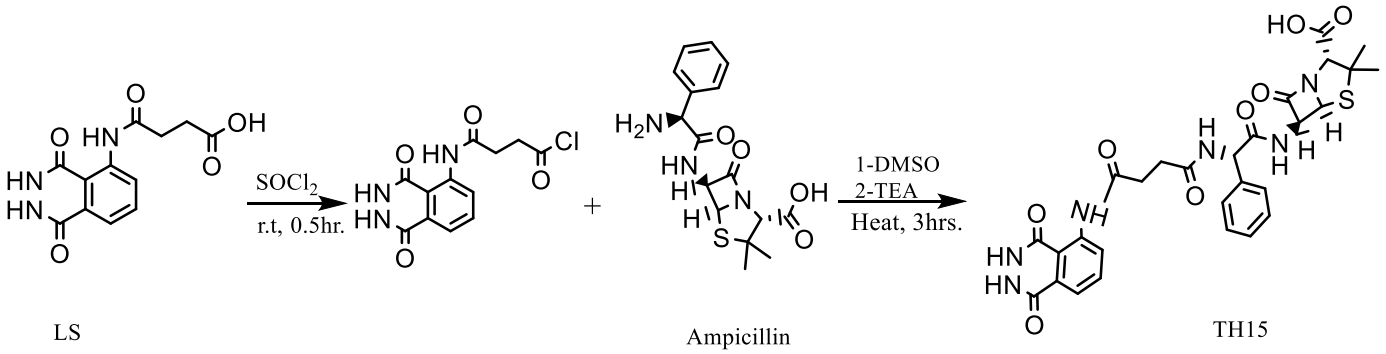

The equation 28: Synthesis for TH15 .

FTIR spectrum for **TH15[(2R,5S,6S)-6-((S)-2-(4-((1,4-dioxo-1,2,3,4-tetrahydrophthalazin-5-yl)amino)-4-oxobutanamido)-2-phenylacetamido)-3,3-dimethyl-7-oxo-4-thia-1-azabicyclo[3.2.0]heptane-2-carboxylic acid]** showed the following values (V max., cm-1): 3269;3207 (OH groups, NH groups str.) overlap, 3070 (CH str. Ar.), 2966 (CH str. alkane), 2557 (S-H str. mercaptans), 1776(C = O str. β-lactam ring), 1718 (C=O str. carboxyl), 1645 (C = O str. amide), 1602 (C = C str. Ar.) , 1516 (C = N str.), 1392 (C-N str. aryl), 1224 (C-O str. carboxyl) , 1045 (C-N str. alkyl) Figure 80. ^{1}H NMR (500 MH, δ ppm):11.87 (OH ,carboxylic acid) , 9.96 ;8.27;8.12 ;8.04 (NH, sec. amide), 7.98-6.85 (CH, benzene), 5.49 (CH ,methine) , 5.11 ;4.52 **(**H, propiolactam) , 3.48, 3.14 (CH_2, methylene) , 2.58 (DMSO), 2.21 ;2.11 (CH, methyl) Figure 81. ^{13}CNMR (125 MH, δ ppm): 175.02 (C=O ,carboxyl) , 172.0 ;165.16 (C=O amide) , 140.21 ;125.11 (CH-benzene), 78.82 – 67.55 (CH, aliphatic) , 39.58 (DMSO), 32.74 (CH_2, aliphatic), 26.10 (CH_3). This spectrum is presented in Figure 82 .

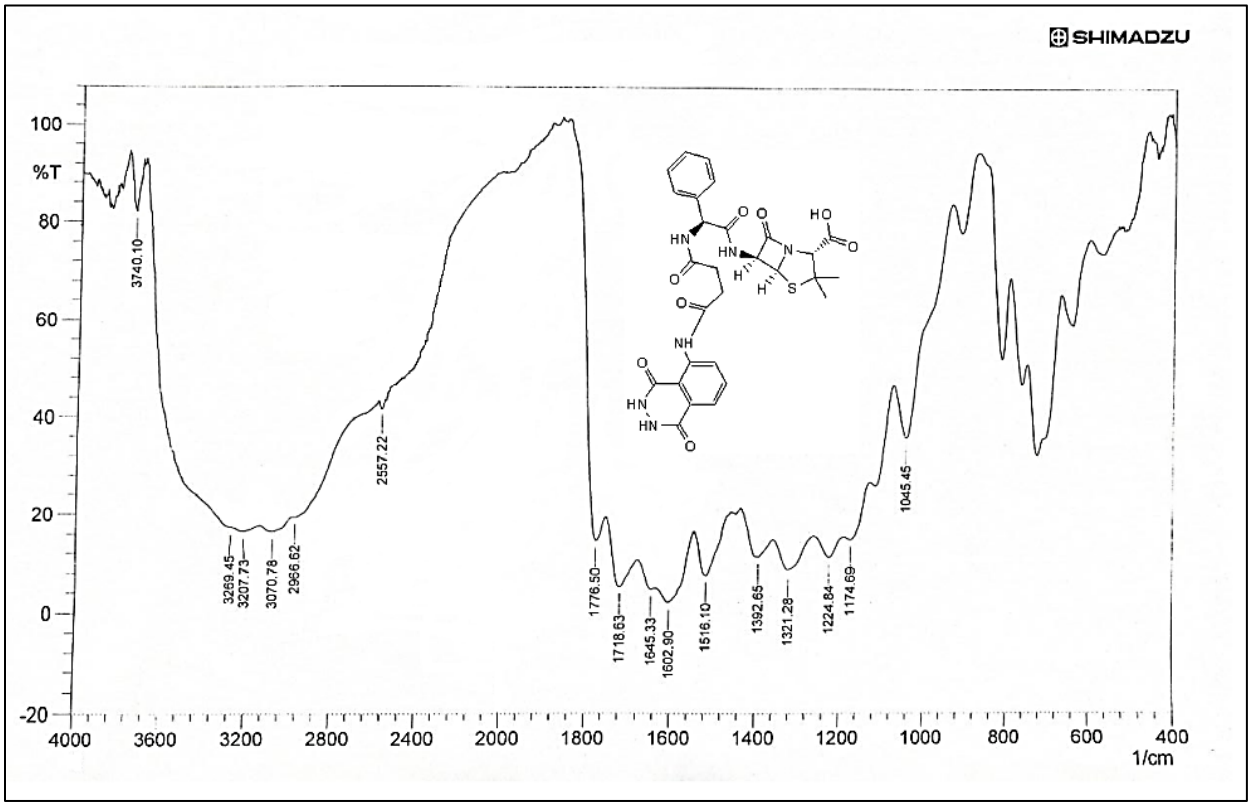

Figure 80: FT-IR spectrum for TH15

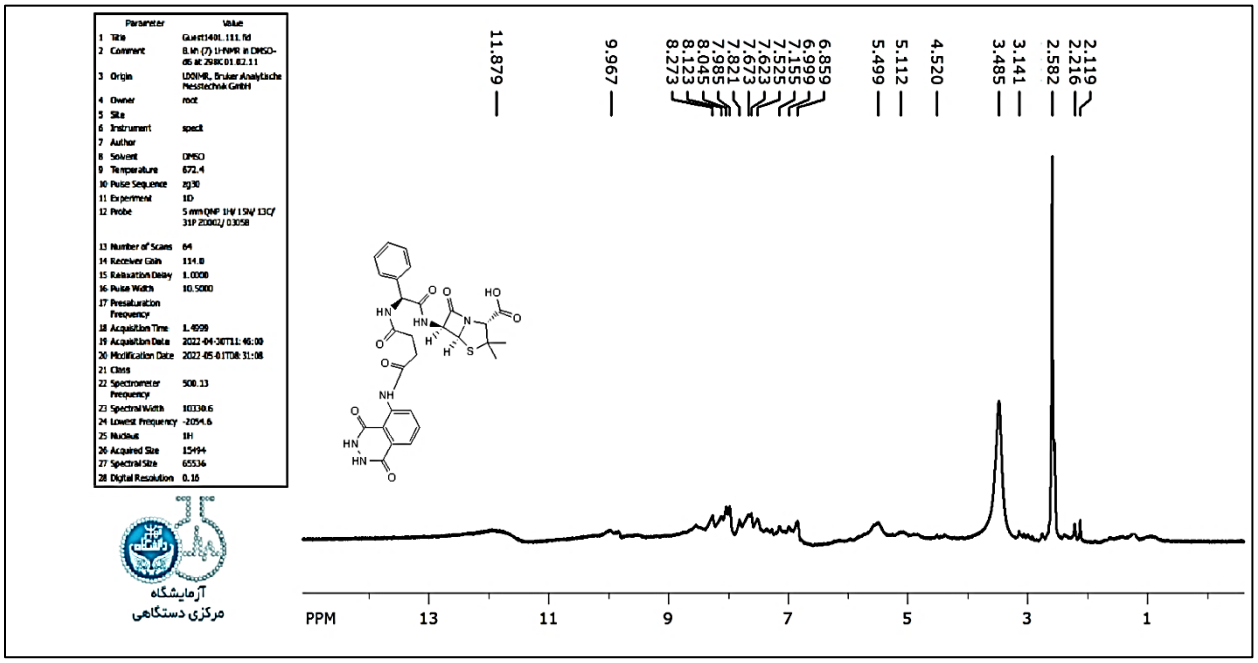

Figure 81: ^{1}H-NMR spectrum for TH15

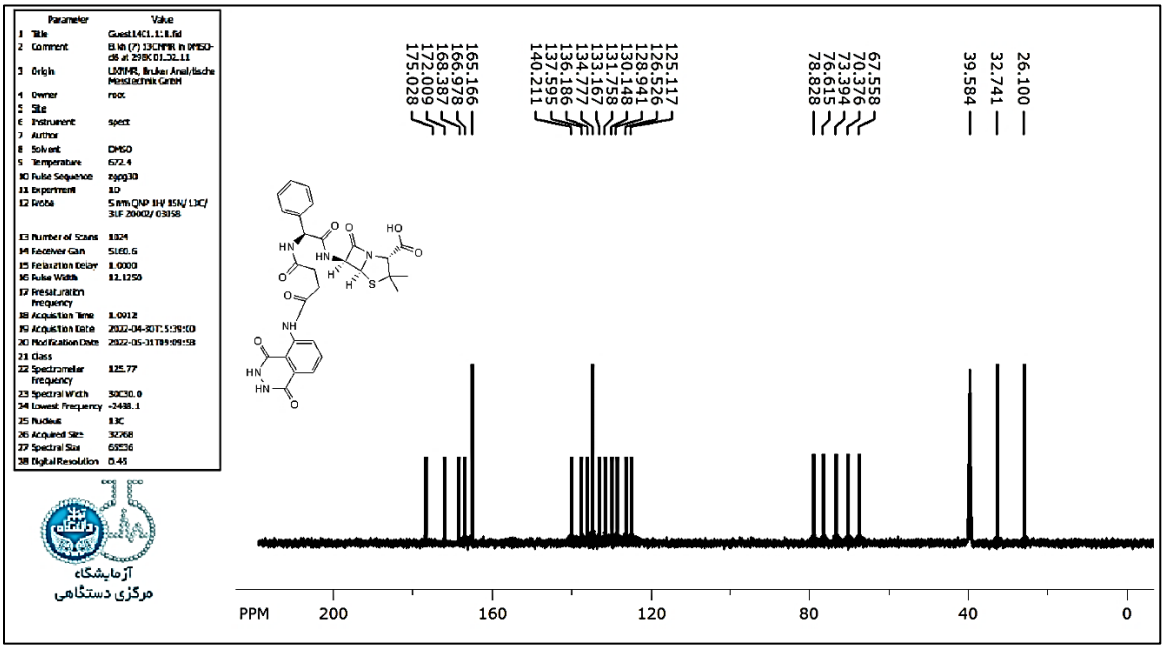

Figure 82 : ^{13}C-NMR spectrum for TH15.

Table 2: C.H.N.S Elementary analysis for the synthesized derivatives .

COMP. SYM.	Calculated %				Found values %			
	C	H	N	S	C	H	N	S
TH1	67.86	4.92	10.79		65.44	4.60	9.85	
TH2	69.02	6.34	11.50		68.10	6.11	10.12	
TH3	58.04	3.54	12.31		56.50	3.33	11.1	
TH4	56.91	4.38	16.59	6.33	55.57	4.21	15.65	5.87
TH5	61.22	4.73	17.13		60.90	4.54	16.90	
TH6	68.99	5.03	13.99		67.66	4.88	13.77	
TH7	43.75	3.25	21.59	13.48	41.22	3.11	20.53	11.78
TH8	56.68	4.76	16.53	6.30	56.15	4.44	15.62	6.13
TH9	46.90	3.61	18.23	10.43	45.93	3.48	17.98	10.20
TH10	56.12	4.55	13.54	5.17	55.77	4.22	12.95	4.98
TH11	64.79	4.83	11.19		64.14	4.59	10.84	
TH12	58.54	4.42	13.65		57.78	4.11	12.81	
TH13	51.94	3.90	22.31		51.66	3.79	22.10	
TH14	53.84	4.52	13.45	5.13	53.34	4.44	13.11	4.87
TH15	55.26	4.64	13.81	5.27	54.75	4.49	13.26	5.12

3.4. The solubility of the synthesized:

The solubility for synthesized compounds was studied by using different polarity solvents, all prepared compounds are partially soluble in water due to relatively high molecular weight and they are completely soluble in each of DMSO, and DMF. All synthesized compounds are insoluble in each hexane and petroleum ether, and because the polarity for prepared compounds is higher than the polarity of these solvents.

Table 3: Solubility of prepared derivatives in different solvents.

Sol. / Comp.	DMSO	DMF	DCM	Petroleum ether	Ethyl acetate	Acetone	Di ethyl ether	Water	Hexane	Ethanol
TH1	+	+	-	-	Partial	-	-	Partial	-	+
TH2	+	+	+	-	-	-	-	Partial	-	Partial
TH3	+	+	-	-	-	-	-	Partial	-	+
TH4	+	+	-	-	-	-	-	Partial	-	Partial
TH5	+	+	-	-	-	+	-	Partial	-	Partial
TH6	+	+	Partial	-	Partial	Partial	Partial	Partial	-	Partial
TH7	+	+	-	-	-	Partial	-	Partial	-	-
TH8	+	+	Partial	-	Partial	Partial	-	Partial	-	Partial
TH9	+	+	Partial	-	-	-	Partial	Partial	-	-
TH10	+	+	Partial	-	Partial	Partial	-	Partial	-	Partial
TH11	+	+	Partial	-	partial	+	Partial	Partial	-	-
TH12	+	+	-	-	-	-	-	Partial	-	-
TH13	+	+	Partial	-	-	+	Partial	Partial	-	-
TH14	+	+	Partial	-	-	-	-	Partial	-	+
TH15	+	+	-	-	-	Partial	-	Partial	-	Partial

3.5. Antibacterial activity:

The results of the antibacterial activity test for new derivatives (TH1-TH15) were recorded in the Table 4 , these derivatives have the ability to prevent the diffusion of bacteria more than LUMINOL and the other medicines that are utilized in the synthesis of these new derivatives (TH1-TH15). Dimethylsulfoxide was used to dissolve compounds. agar disc- diffusion method was used to determine the biological activity for prepared compounds versus two classes of bacteria; *Staphylococcus aureus* (Staph. aureus) (gram +ve), and *Escherichia* (E. coli) (gram -ve) .

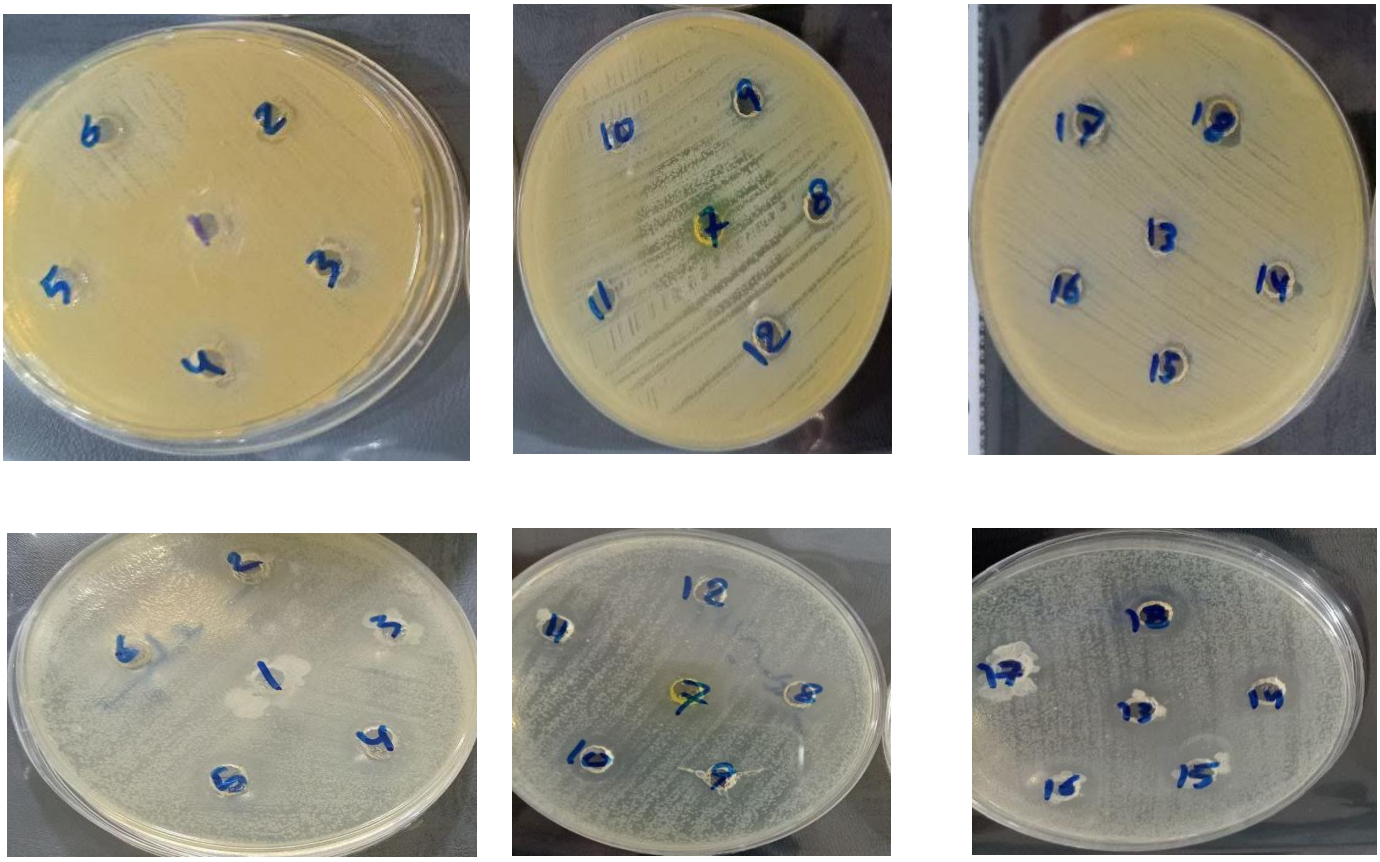

Figure 83: Inhibition zones in Petri dishes used in study of anti-bacterial activity

Table 4: anti-bacterial activity for prepared compounds and other drugs that are used in preparations at 1mg/mL concentration.

Comp.s	Gram +ve (Staphylococcus aureus)(mm)	Gram –ve (E-coli) (mm)	Pure drug	Gram +ve (Staphylococcus aureus)	Gram -ve (E- coli)
TH1	0	15	Ibuprofen	6	14
TH2	0	0	Diclofenac sodium	6	0
TH3	0	20	Mefenamic acid	0	8
TH4	30	20	Ampicillin	35	26
TH5	30	16	Naproxen	32	30
TH6	0	15	Cephalexin	30	15
TH7	0	15	Ciprofloxacin	30	22
TH8	10	15	Ceftriaxone	12	33
TH9	0	15	Cefotaxime	20	35
TH10	0	15	Cephalexin	30	15
TH11	0	15	Mefenamic	0	8
TH12	0	15	Paracetamol	13	4
TH13	0	20	Theophylline	0	10
TH14	0	15	Amoxicillin	9	10
TH15	0	15	Ampicillin	35	26
LUMINOL	0	10			
DMSO	0	0			

3.6. X-rays Patterns for CoO

3.6.1. X-rays Analysis of CoO.

X-ray diffraction technique was used to study the crystallization state and determine the particles size of the used cobalt oxide . From the analysis of X-rays diffraction patterns the average particle size (D) was estimated by applying Scherer equation. These patterns are shown in Figure 84. From these patterns it can be seen that, main peaks of CoO were appeared at 2θ= 18, 33, 37, 39, 43, 45, 56, 59, 62, 65, 74, 78, 79 [124]. These diffraction peaks are assigned to this oxide and its average particle size can be calculated

using Scherer equation:

$D = kx\lambda / Bx\cos\theta$

From this equation, the particle size for cobalt oxide was around 10 nm.

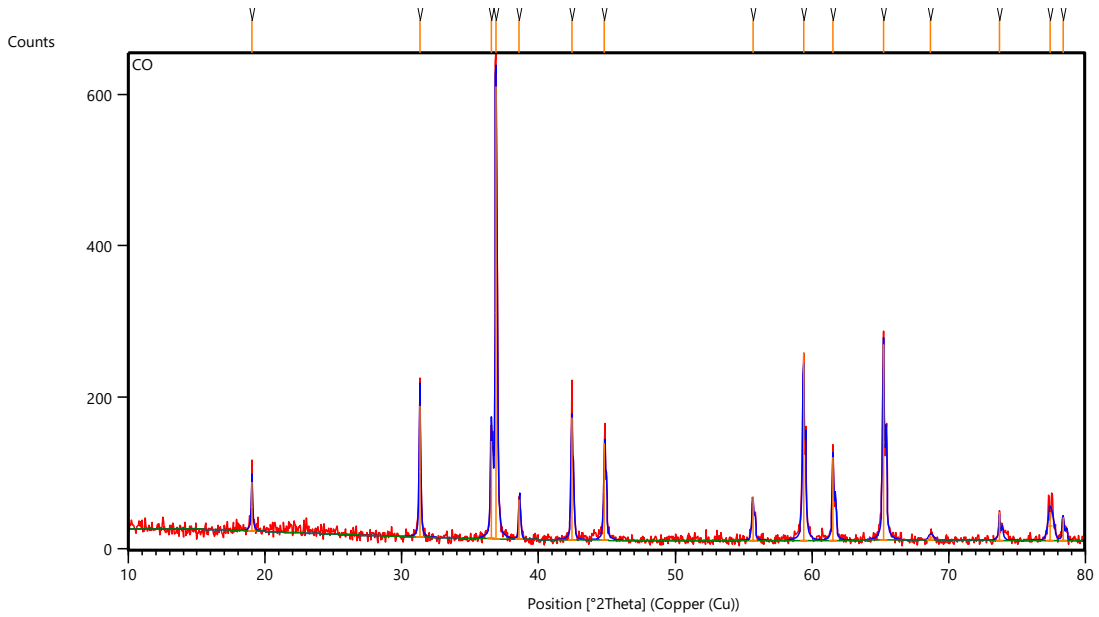

Figure 84: XRD patterns for cobalt oxide NPs

3.6.2. Scanning Electron Microscopy for CoO (SEM)

This technique is used to investigate Morphology of the solid surface. The obtained results are presented in Figure 85. From these images, it can be seen that, surface of CoO shows a relative homogeneity of this material with some aggregation, this aggregation can be related to different attraction forces that may occur among CoO particles and the average particle size from SEM images was around 27 nm. This result is reasonable In comparison with that obtained from XRD patterns applying Scherer equation.

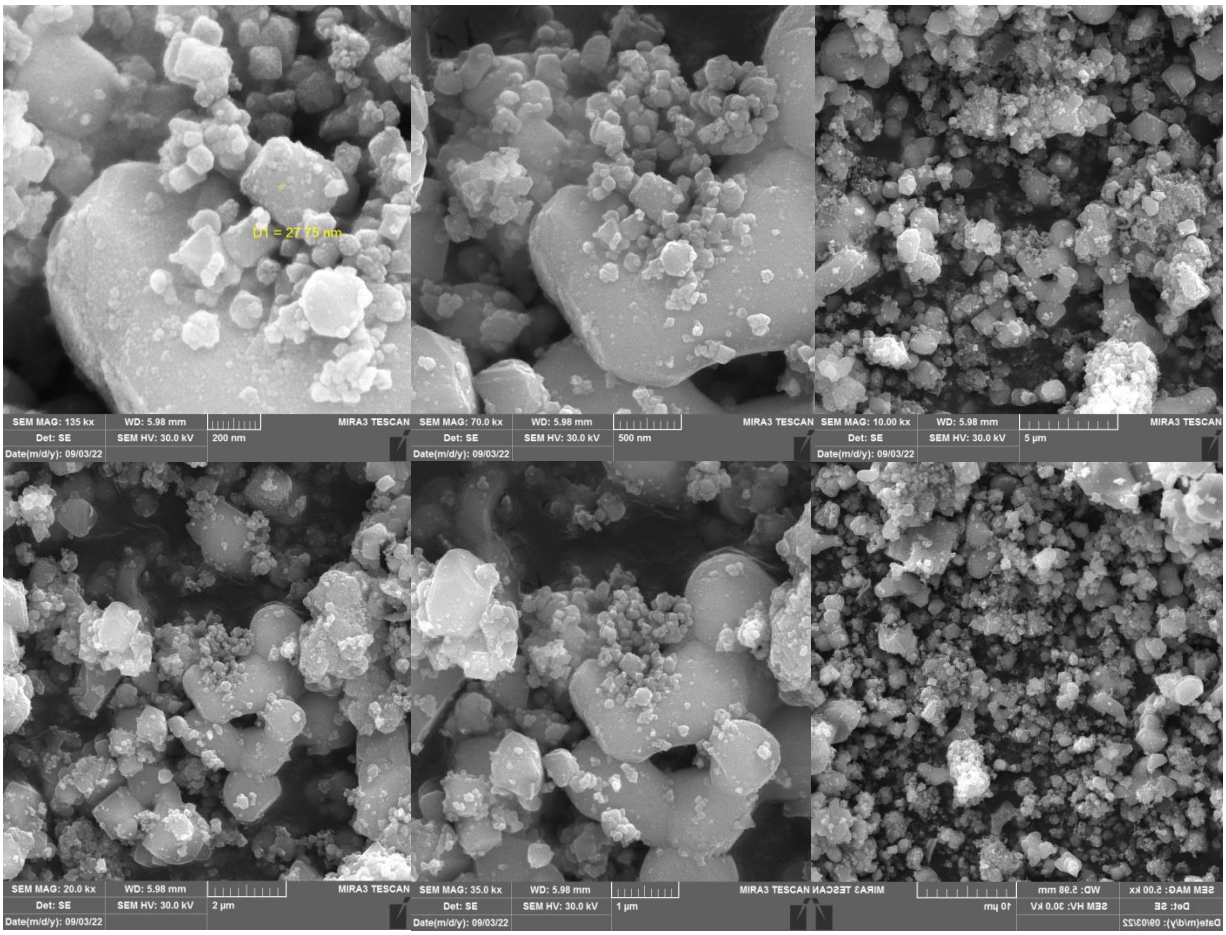

Figure 85 : FE-SEM images of CoO

3.7. Photolysis and photocatalytic reactions

3.7.1. Effect of temperature on photolysis of the compounds TH2 and TH11 compounds

In order to screen photolysis of TH2 and TH11 under illumination with UV light. A series of experiments were performed using solutions with a concentration of 80 ppm from compounds TH2 and TH11 with illumination with UV radiation from Xenon lamp. At First at a temperature of 25 ℃ , 30 ℃ and at 35 ℃ , the photolysis of molecules of these compounds was followed by withdrawing samples of irradiated system at interval times with measuring the absorbance's at wavelength of 356 nm. The obtained results are presented as C_t/C_o against irradiation time in minute. These results are presented in Table 5 . From obtained results of the effect of temperature on photolysis process, it was found that, the photolysis activity for these compounds was decreased with increasing temperature. The best photolysis result was recorded at 25 °C. The reason for this is probably due to the increase in the mobility of molecules inside the solution with increasing temperature which leads to increase scattering of the incident photons, This observation can lead to decreases the efficiency of photolysis process with the increase in reaction temperature.

Table 5: Photolysis of TH2 (80 ppm) under illumination with UV radiation only at 25℃ ,30℃ and 35℃ .

Time	Abs. at 25℃	Abs. at 30℃	Abs. at 35℃
0	3.175	2.723	2.483
30	2.805	2.659	2.312
60	2.063	2.474	2.169
90	1.752	2.334	1.882
120	1.546	2.281	1.798
150	1.308	2.175	1.632
180	1.268	2.066	1.576
210	1.172	1.984	1.511

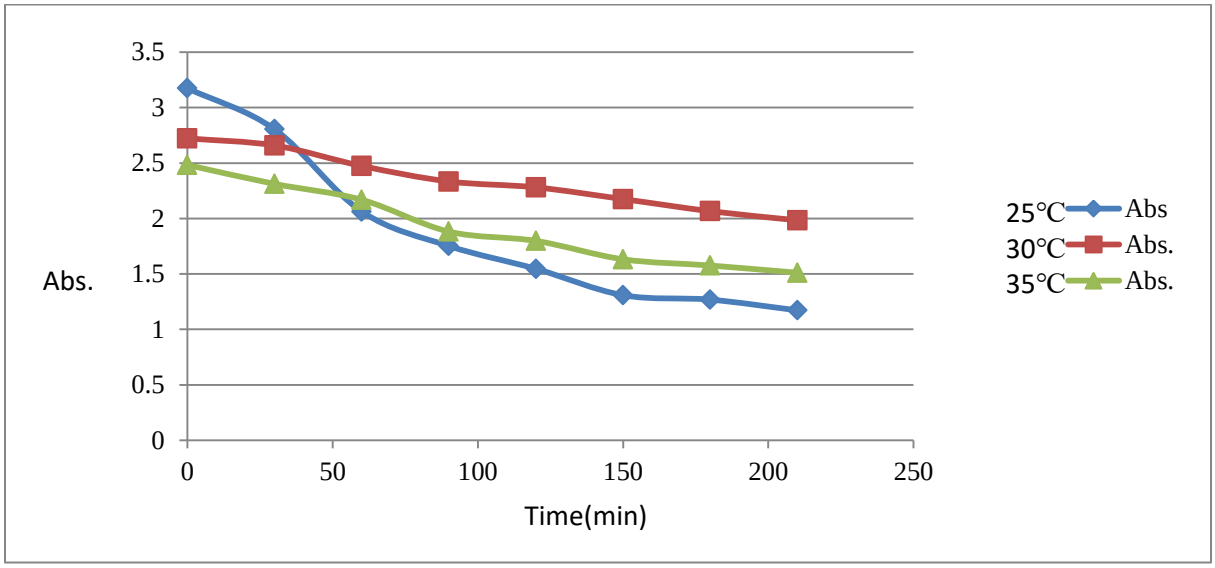

Figure 86: Photolysis of TH2 (80 ppm) under illumination with UV radiation only at 25℃ , 30℃ and 35℃ .

Table 6: Photolysis of TH2 (80 ppm) under illumination with UV radiation at 25℃,30℃ and 35℃ are presented as Ct\C$_o$ against time irradiation in minute.

Time (min)	C_t/C_o		
	25℃	30℃	35℃
0	1	1	1
30	0.88346	0.9765	0.93113
60	0.64976	0.90856	0.87354
90	0.55181	0.85714	0.75795
120	0.48693	0.83768	0.72412
150	0.41197	0.79875	0.65727
180	0.39937	0.75872	0.63472
210	0.36913	0.72861	0.60854

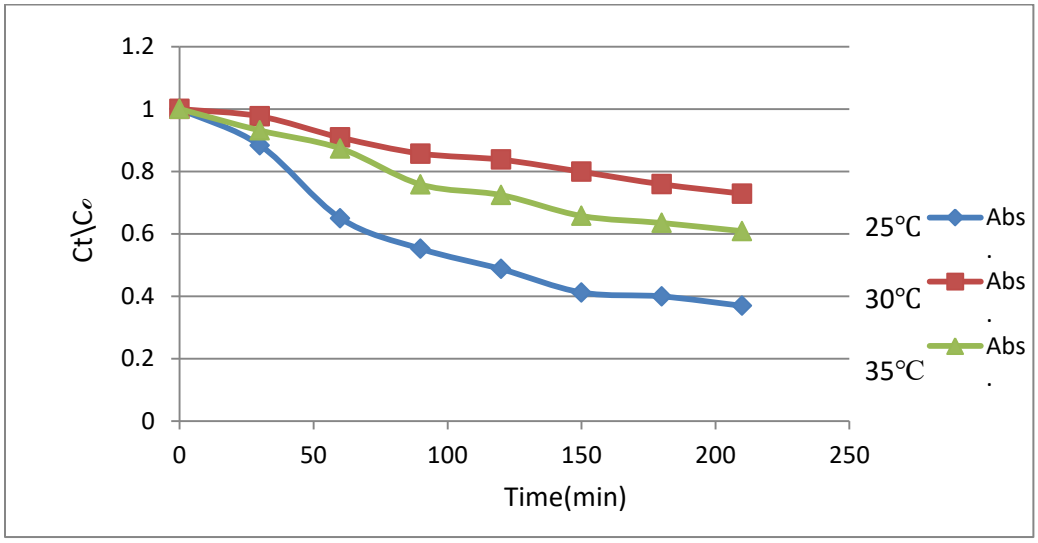

Figure 87:Photolysis of TH2 (80 ppm) under illumination with UV radiation at 25℃ ,30℃ and 35 ℃ are presented as C_t/C_o against time of irradiation in minute.

From above results, there was a decrease in the efficiency of photolysis upon the increase in temperature from 25 ℃_30 ℃ , then a slight improvement occurs in the photolysis of this compound upon increase reaction temperature from 30 ℃ to 35 ℃ under these conditions. The reason for that can be argued to scattering of photons if the incident light in the solution and then when a relatively high temperature is reached 35 ℃ we find that there is a relative improvement in photolysis at this degree compared to the temperature of 30 ℃ and this may be caused by a decrease in the viscosity of the solution with the increase in temperature and this factor leads to a decrease in scattering of photons of light as well as the possibility of their penetration and access to all parts of the solution and thus the largest possible number of molecules of the compound TH2 exposed to collision with the photons. This can lead to degrade and break down more number of molecules of this compound [125,126]. The obtained results are presented in Figure 86 and Table 5. The same arrangements were followed in case of photolysis of the compound TH11 and the obtained results are shown in Table 7 and Figure 88. Same observations exactly were found in this case, these can be argued as it was mentioned above in concern with photolysis of compound TH2.

Table 7 : Photolysis of TH11 (80 ppm) under illumination with UV radiation only at 25 ℃ .

Time	Abs.
0	2.246
30	1.99
60	1.618
90	1.301
120	1.249
150	1.14
180	1.033
210	0.853

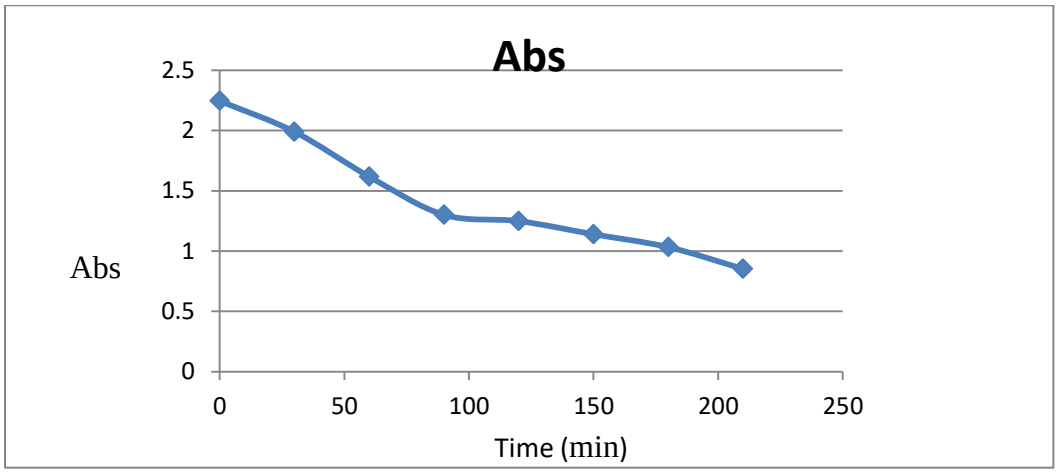

Figure 88 : Photolysis of TH11 (80 ppm) under illumination with UV radiation only at 25℃ .

Table 8 : Photolysis of TH11 (80 ppm) under illumination with UV radiation at 25℃ are presented as $\mathbf{C_t/C_o}$ against time irradiation in minute.

Time	Abs.
0	1.00000
30	0.88602

60	0.720392
90	0.579252
120	0.5561
150	0.507569
180	0.459929
210	0.379786

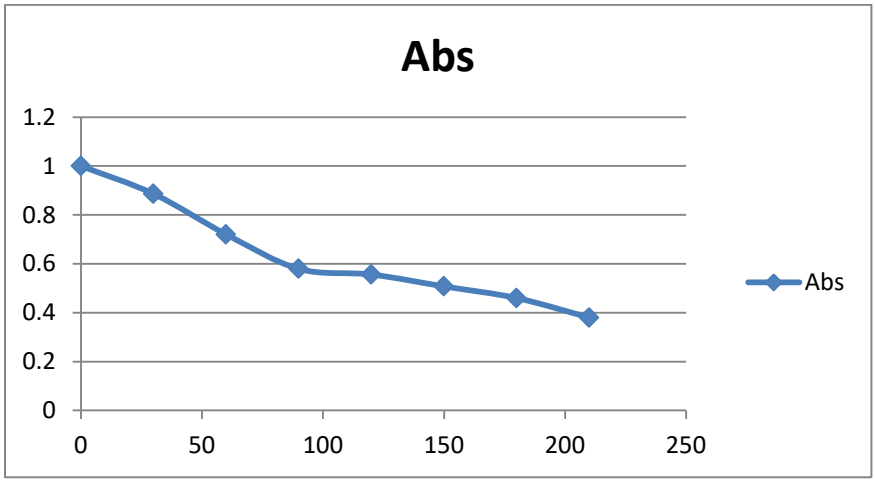

Figure 89: Photolysis of TH11 (80 ppm) under illumination with UV radiation at 25℃ are presented as $\mathbf{C_t/C_o}$ against time of irradiation in minute.

Table 9: Photolysis of TH11 (80 ppm) under illumination with UV radiation at 25℃ was presented as $\mathbf{C_t/C_o}$ against time irradiation in minute.

Time	25 ℃
	Abs.
0	1.0000
30	0.88602
60	0.720392
90	0.579252
120	0.5561
150	0.507569
180	0.459929
210	0.379786

From the results included in the table and drawn in the figure related to TH11 photolysis at a temperature of 25℃ by ultraviolet irradiation, we find that there is a direct relationship regarding the efficiency of the photolysis of the compound with the progression of the reaction time and this is consistent with the first law of photochemistry, which states that the occurrence of chemical change The photosynthesis of the reactive species requires that they be absorbed by a photon of an appropriate energy. Therefore, the progression of the reaction time gives a greater chance for a large number of molecules to absorb a large number of molecules of the TH11 compound for the photons, and therefore we find that there is an improvement in the efficiency of the photolysis of the dye with the progression of time.

3.7.2. Photo catalytic degradation of the compounds TH2 and TH11 over CoO

Photocatalytic degradation of compounds TH2 and TH11 was investigated over a suspension of cobalt oxide under illumination with UV radiation for a period of 210 minute. In this case irradiation of CoO particles with light of energy that is comparable to its band gap energy (Eg) generates valence band holes and conduction band electrons. These species would involve in generation of some reactive species such as $OH^{\cdot}$ radical and $O^{2-\cdot}$, these redox species would participate in redox reactions for the adsorbed species at the surface of the photocatalyst, these reactive species react with adsorbed molecules of compound TH2 and leads to breakdown some of these molecules which leads to fragmentation or formation of new smaller molecules. From the obtained results, it can be seen that, the efficiency of photoctalytic degradation of these compounds was enhanced with elevation in reaction temperature from 25 ℃ to 30 C^{o} and then it was reduced at 35 °C. These observations can be related to the effect of temperature on other processes that are accompanied with photocatalytic processes such as diffusion of reacting species from bulk on to the surface of the photocatalyst and reduction in the viscosity of the solution. At high temperature (more than 25 °C), there was reduction in the efficiency of photocatalytic degradation of compound TH2, this is due to the increase in kinetic energy of adsorbed molecules and these then diffuse away from active sites to the bulk of solution[127,128].

3.7.2.1. The effect of weight of the used CoO on photocatalytic degradation of the compound TH2

In photocatalytic reactions, the main effect is the concentration of redox species (valence band hole and conduction band electron) , these species are produced upon irradiation of photocatalyst particles with radiation with proper energy. So that variation in the mass of the used catalyst leads to variation in concentration of the redox species directly. In this manner increase weight of the used photocatalyst leads to produce more redox species which leads to formation of more reactive hydroxyl and superoxide radicals. These radicals lead to breakdown adsorbed molecules of TH2 compound. To investigate this parameter a series of experiments were conducted under fixed reaction conditions with change only on the mass of the used CoO , 0.1 g., 0.15 g., and 0.20 g.. Photocatalytic activity was investigated by measuring the absorbance for the reacted samples at interval reaction period. The obtained results are presented in Table 10 and Figure 90 . From these results it was found that, there was improvement in the efficiency of the photocatalytic degradation of molecules of compound TH2 when increasing weight of the used CoO from 0.1 to 0.15 g., this can be attributed to increasing absorbing particles of CoO to the incident photons which leads to increase concentration of redox species. On the other hand, when increasing the weight from 0.15 to 0.20 g., of the used CoO, there was decline in the efficiency of the photocatalytic degradation, this probably due to formation of aggregation and/or inner filter of CoO particles in the bulk solution. These filters or aggregations can prevent photons to pass to another parts of the reacting mixture which leads to reduce in concentration of redox species[129-131].

Table 10: The effect of weight of CoO on the efficiency of photocatalytic degradation of TH2 compounds.

Time(min).	Abs.		
	0.1g	0.15g	0.20g
0	3.202	3.024	2.874
15	3.19	3.014	2.856
30	3.135	2.985	2.8
60	3.087	2.922	2.786

90	2.686	2.874	2.661
120	2.573	2.805	2.615

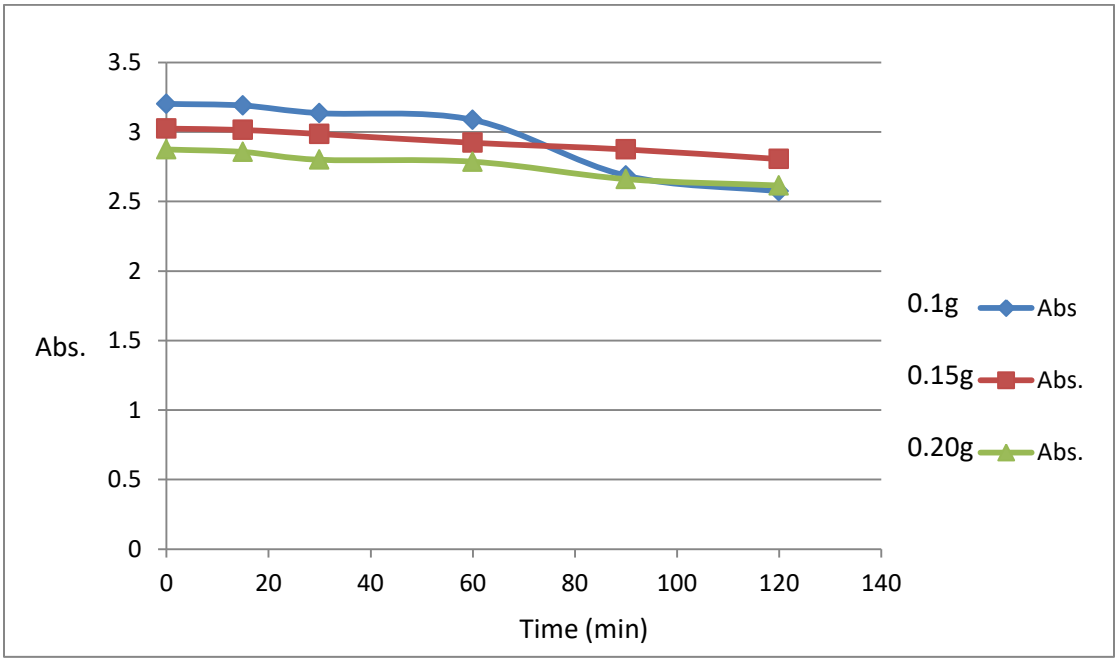

Figure 90 : The effect of weight of CoO on the efficiency of photocatalytic degradation of TH2(80 ppm) over CoO.

Table 11: Photocatalytic degradation of TH2 (80 ppm) under illumination with UV radiation at different weights of CoO.

Time(min)	C_t/C_o		
	0.1 g	0.15 g	0.20 g
0	1	1	1
15	0.996252	0.996693	0.993737
30	0.979076	0.987103	0.974252
60	0.964085	0.96627	0.969381
90	0.838851	0.950397	0.925887
120	0.80356	0.927579	0.909882

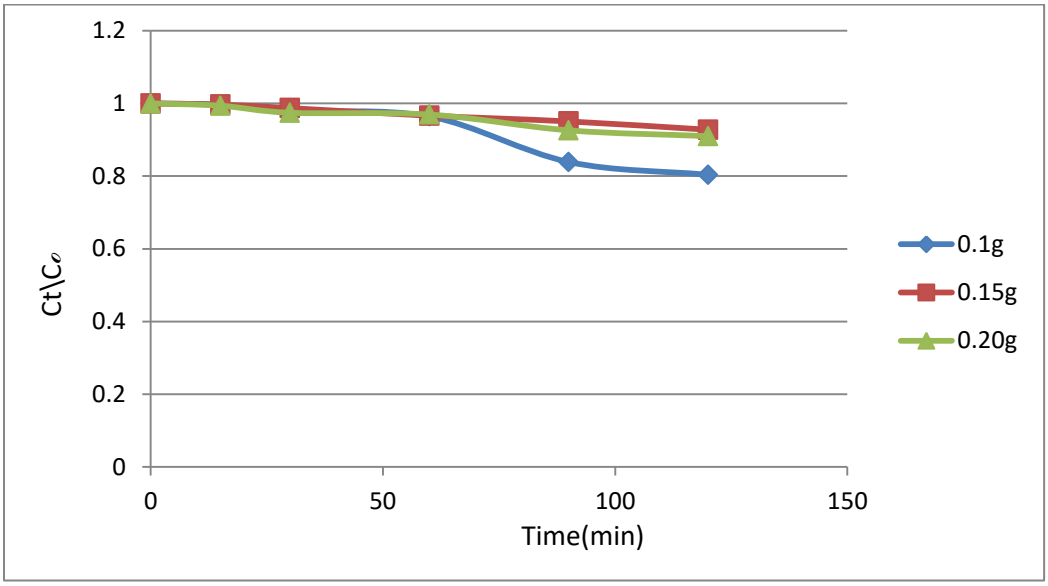

Figure 91 :Photocatalytic degradation of TH2 (80 ppm) under illumination with UV radiation at different weights of CoO.

The same arrangements were conducted for photocatalytic degradation of compounds TH11 over a suspension of CoO as a photocatalyst using different weights of CoO 0.10 g , 0.15 g ,and 0.20 g .

The obtained results are presented in Table 12 and Figure 92 .These results show same finding that are regarding to the compound TH2 and same observations were found for this case exactly and same arguments can be considered.

Table 12 : Photocatalytic degradation of TH11 (80 ppm) under illumination with UV radiation at different weights of CoO

Time(min)	Abs.		
	0.1g	0.15g	0.20g
0	2.26	2.069	2.107
15	2.142	2.039	2.088
30	1.962	1.979	1.982
60	1.732	1.924	1.957
90	1.59	1.75	1.92
120	1.332	1.62	1.852

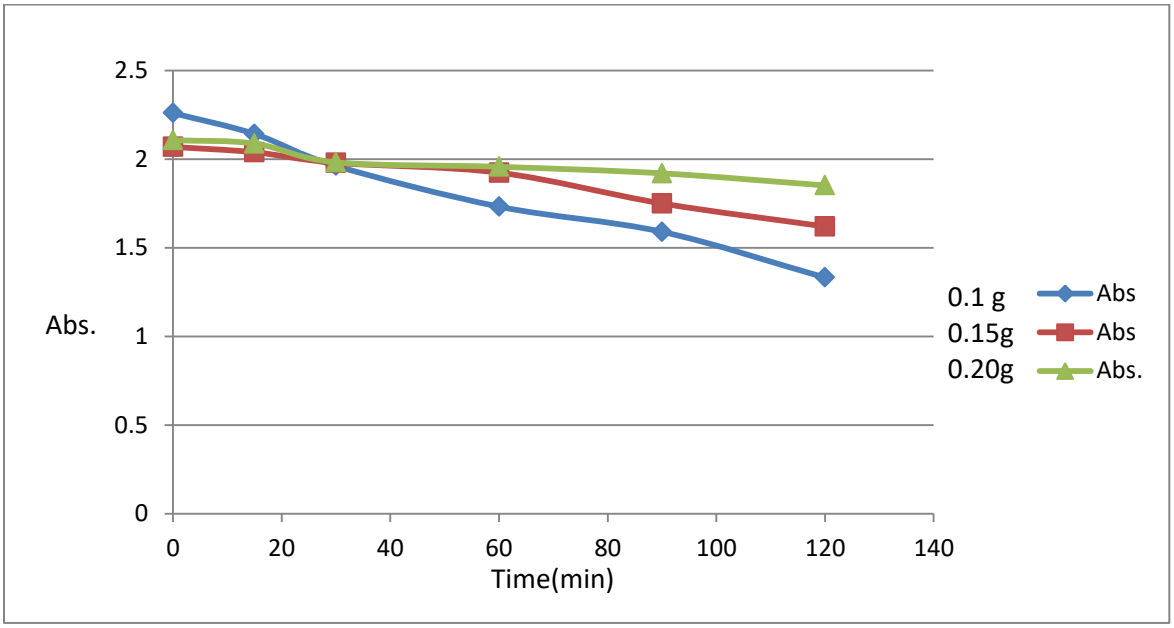

Figure 92 : The effect of weight of CoO on the efficiency of photocatalytic degradation of TH11 over CoO.

Table 13 : Relation of C_t/C_o against time in minute, the effect of the weight of CoO on the efficiency of photocatalytic degradation of TH11 over CoO.

Time(min)	C_t/C_o		
	0.1g	0.15g	0.20g
0	1	1	1
15	0.947788	0.9855	0.990982
30	0.868142	0.956501	0.940674
60	0.766372	0.929918	0.928809
90	0.70354	0.845819	0.911248
120	0.589381	0.782987	0.878975

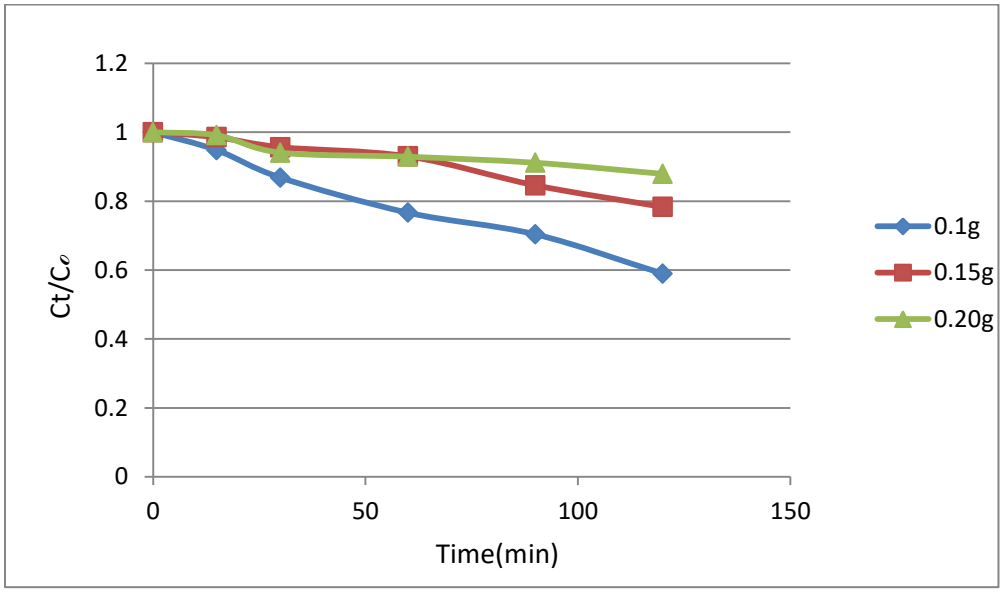

Figure 93: Relation of $\mathbf{C_t/C_o}$ against time in minute, the effect of the weight of CoO on the efficiency of photocatalytic degradation of TH11 over CoO.

3.7.2.2. The effect of reaction temperature on the efficiency of photocatalytic degradation.

In order to investigate effect of temperature of reaction mixture on the efficiency of photocatalytic degradation of compound TH2 over a suspension of CoO under irradiation with UV light. A series of experiments were conducted under a fixed reaction conditions exactly with change reaction temperature only. In this case, three reaction temperature were carried out, 25 ℃ , 30 ℃ and 35 ℃ .Reaction progress was followed via measuring absorbance of samples of supernatant liquids of reaction mixture at periodically interval time by measuring absorbance at 365nm. The obtained results are presented in Table 14 and Figure 94. From these results it can be seen that, there was enhancement in the activity of photocatalytic degradation of compound TH2 with elevation of reaction temperature from 25 ℃ , 30 ℃ and 35 °C. This improvement in efficiency of photoctalytic degradation of compound TH2 with increase of temperature is due to role of temperature elevation in increasing mobility of molecules with reduction in viscosity of the reaction mixture[132,133].

Table 14 : The effect of temperature 25 ℃ , 30 ℃ ,35 ℃ of on the efficiency of photocatalytic degradation of TH2 compounds over CoO.

Time	Abs.		
	25 ℃	30 ℃	35 ℃
0	3.202	2.856	2.819
30	3.135	2.819	2.713
60	3.087	2.729	2.593
90	2.686	2.49	2.34
120	2.573	2.37	2.117

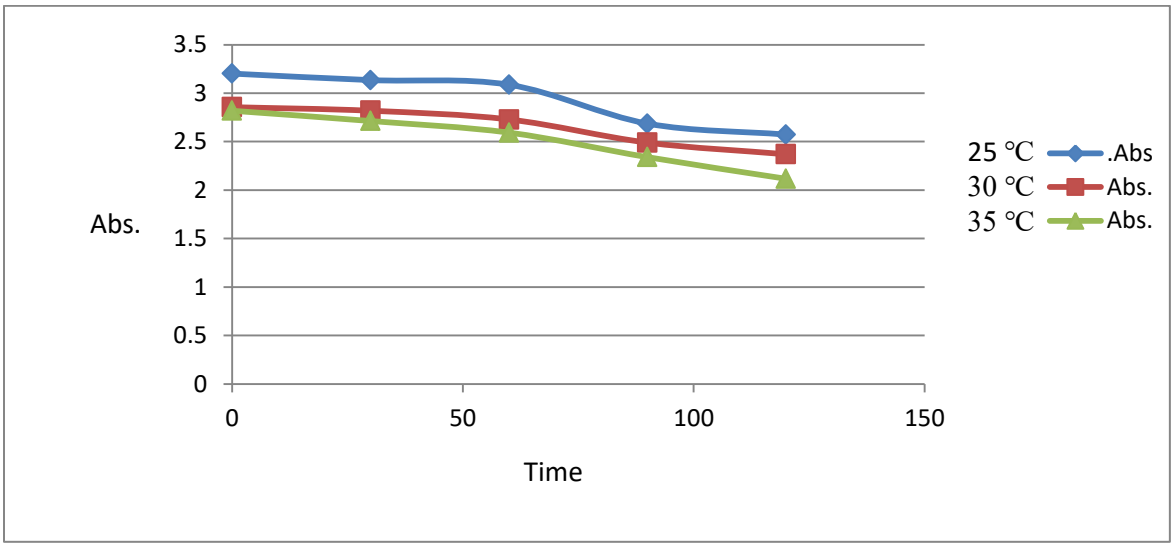

Figure 94 :The effect of temperature 25 ℃ , 30 ℃ ,35 ℃ of on the efficiency of photocatalytic degradation of TH2 compounds over CoO.

Table 15: Relation of C_t/C_o against time in minute, the effect of different temperature on the efficiency of photocatalytic degradation of TH2 over CoO.

Time	Abs.		
	25 ℃	30 ℃	35 ℃
0	1	1	1
30	0.979076	0.987045	0.962398
60	0.964085	0.955532	0.91983
90	0.838851	0.871849	0.830082
120	0.80356	0.829832	0.750976

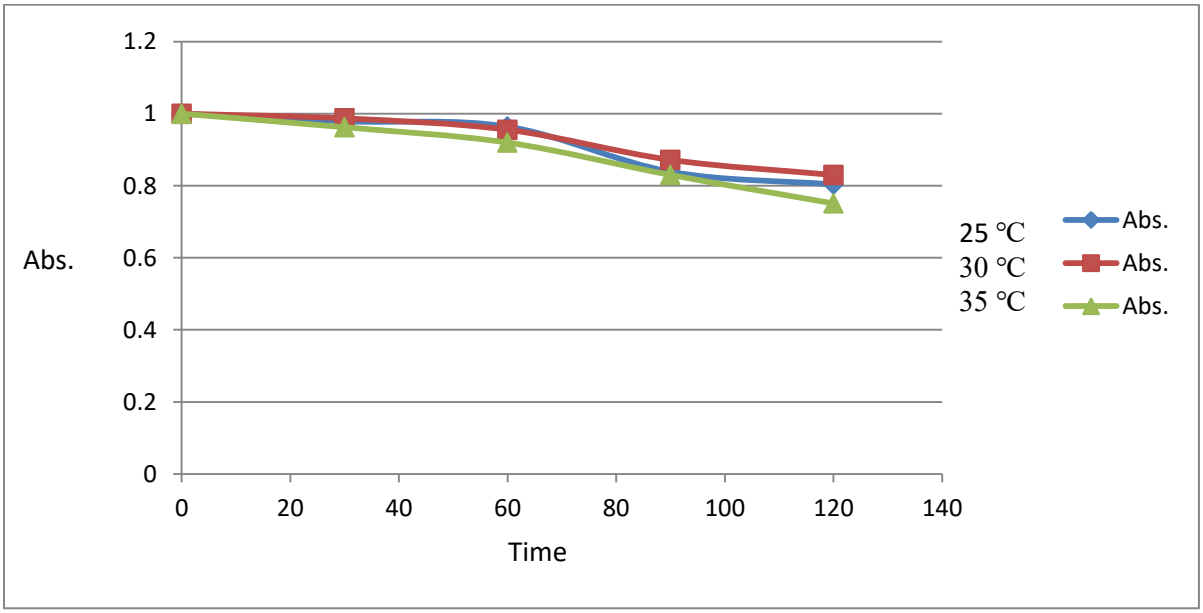

Figure 95: Relation of C_t/C_o against time in minute, the effect of different temperature on the efficiency of photocatalytic degradation of TH2 over CoO.

Conclusions:

- T1-T9 and TH1-TH15 compounds were successfully synthesized based on Luminol with amino and carboxylic drugs.
- The structures of the synthesized targeted molecules were confirmed and characterized by FT-IR , ^{1}H-NMR, ^{13}C-NMR spectra and CHNS .
- TLC and M.P. were used in confirmation of the synthesized derivatives.
- Most of the synthesized derivatives showed a good anti-bacterial activity toward staphylococcus and E-coli bacteria more than Luminol and some of pure drugs .
- From photo experiments, it can be reported that, the compound TH2 showed photolysis degradation behavior more than that in case of photocatalytic degradation over cobalt oxide under the same reaction conditions.
- Photolysis effect was increased with increase of irradiation period.
- In case of photocatalytic degradation experiments, it was found that increasing mass of the used cobalt oxide does not lead to increase efficiency of the photocatalytic process under the applied reaction conditions,
- In photocatalytic reactions there was enhancement in efficiency of photocatalytic degradation of compound TH2 with elevation in reaction temperature.
- In general the investigated TH2 and TH11 compounds showed a good resistance against both photolysis and photocatalytic behavior, this a good property as these derivatives can be used in synthesis of some pharmaceutical materials.

Recommendations and future works :

Due to the significance of Luminol derivatives in numerous industries, including the medical, pharmaceutical, and industrial, we advised:

- Researching the therapeutic applications of the produced chemicals.
- Researching the mechanism of the prepared food's bacterial inhibition compounds.
- Making pharmaceutical compounds from the processed
  As a starting point, compounds.

References:

1- Albrecht, Herbert Otto. "Über die chemiluminescenz des aminophthalsäurehydrazids." Zeitschrift für Physikalische Chemie 136, no. 1 (1928): 321-330.

2- Luo, Yun, Yi Li, Baoqiang Lv, Zaide Zhou, Dan Xiao, and Martin MF Choi. "A new luminol derivative as a fluorescent probe for trace analysis of copper (II)." Microchimica Acta 164, no. 3 (2009): 411-417.

3- Ferreira, Ernesto Correa, and Adriana Vitorino Rossi. "Chemiluminescence as an analytical tool: from the mechanism to applications of the reaction of luminol in kinetic based methods." Quimica Nova 25 (2002): 1003-1011.

4- Yang, Chunyan, Zhujun Zhang, and Jinli Wang. "A new luminol chemiluminescence reaction using a tetravalent nickel-periodate complex as the oxidant." Microchimica Acta 167, no. 1 (2009): 91-96.

5- The Merck Index: An Encyclopedia of Chemicals, Drugs, and Biologicals, 11th Edition, Centennial Edition (1989) : 5470

6- Moxley, Khan P. Idrees D. "Corbett JA Ahmad F. Figura G. Sly WS Waheed A. Hassan MI Luminol Based Chemiluminescent Signals: Clinical and Non-Clinical Application and Future Uses." Appl. Biochem. Biotechnol 173, no. 2 (2014): 333-355.

7- Wiedemann, Eilhard. "Ueber fluorescenz und phosphorescenz i. abhandlung." Annalen der Physik 270, no. 7 (1888): 446-463.

8- Garcia-Campana, A. M., W. R. G. Baeyens, L. Cuadros-Rodriguez, F. Barrero, J. M. Bosque-Sendra, and L. Gamiz-Gracia. "Potential of chemiluminescence and bioluminescence in organic analysis." Current Organic Chemistry 6, no. 1 (2002): 1-20.

9- Hastings, J. Woodland, and Carl Hirschie Johnson. "[3] Bioluminescence and chemiluminescence." In Methods in enzymology, vol. 360, pp. 75-104. Academic press, (2003).

10- Roda, Aldo, Massimo Guardigli, Elisa Michelini, Mara Mirasoli, and Patrizia Pasini. "Peer reviewed: analytical bioluminescence and chemiluminescence." (2003): 462-A.

11- Barnett, Neil, and Paul Francis. "Chemiluminescence: liquid-phase." Encyclopedia of analytical science (2nd ed.) 1 (2005): 511-521.
12- White, E. H., McElroy, W. D., Glass, B., Eds.; Light and Life, John Hopkins Press: Baltimore, (1961): pp 183-195.

13- White, E. H.; Bursey, M. M. J. Am. Chem. Soc. (1964): 86, 941.
14- White, E. H.; Zafiriou, O.; Kagi, H. H.; Hill, J. H. M. J. Am. Chem. Soc. (1964): 86, 940.
15- Gundermann, Karl-Dietrich, and Frank McCapra. "Chemiluminescence in the Future." In Chemiluminescence in Organic Chemistry, pp. 203-203. Springer, Berlin, Heidelberg, (1987).
16- Gundermann, K-D. "Chemiluminescence in organic compounds." Angewandte Chemie International Edition in English 4, no. 7 (1965): 566-573.
17- Schneider, H. W. "A new, long-lasting luminol chemiluminescent cold light." Journal of Chemical Education 47, no. 7 (1970): 519.
18- Roswell, David F., and Emil H. White. "[36] The chemiluminescence of luminol and related hydrazides." In Methods in enzymology, vol. 57, pp. 409-423. Academic Press, (1978).

19- B.Z. Shakhashiri, Oxidations of Luminol, Chemical Demonstrations, vol.1, University of Wisconsin Press, Madison, (1983): pp. 156–167.

20- M.M. Rauhut, in: M. Grayson (Ed.), Kirk-Othmer Concise Encyclopedia of Chemical Technology, third ed., John Wiley and Sons Inc., New York,1985, pp. 247–248.

21- King, Richard, and Gordon M. Miskelly. "The inhibition by amines and amino acids of bleach-induced luminol chemiluminescence during forensic screening for blood." Talanta 67, no. 2 (2005): 345-353.

22- Larena, A., M. Valero, and E. Bernabeu. "Some chemiluminescence reactions in the presence of different metal ions." Optica Pura Y Aplicada 16 (1983): 91-96.

23- Albertin, Ricardo, Marco AG Arribas, Erick L. Bastos, Sascha Röpke, Patricia N. Sakai, Adrey MM Sanches, Cassius V. Stevani, Ilka S. Umezu, Joana Yu, and Wilhelm J. Baader. "Quimiluminescência orgânica: alguns experimentos de demonstração para a sala de aula." Química Nova 21 (1998): 772-779.

24- PETRE, Răzvan, and Gheorghe HUBCĂ. "A performing synthesis strategy of luminol, a standard chemiluminescent substance." UPB Sci. Bull. Ser. B Chem. Mater. Sci 75 (2013): 23-34.

25- Díaz, A. Navas, J. A. Gonzalez Garcia, and J. Lovillo. "Enhancer effect of fluorescein on the luminol–H2O2–horseradish peroxidase chemiluminescence: energy transfer process." Journal of bioluminescence and chemiluminescence 12, no. 4 (1997): 199-205.

26- Li, S. F., H. Y. Wang, X. Min, L. Zhang, J. Wang, J. Du, J. Q. Zhang et al. "Chemiluminescence behavior of luminol-KIO 4-Ag nanoparticles system and its analytical applications." Journal of Biomedical Science and Engineering 7, no. 06 (2014): 307.

27- Khajvand, Tahereh, Reza Akhoondi, Mohammad Javad Chaichi, Ehsan Rezaee, and Hamid Golchoubian. "Two new dinuclear copper (II) complexes as efficient catalysts of luminol chemiluminescence." Journal of Photochemistry and Photobiology A: Chemistry 282 (2014): 9-15.

28- Aiube, Zakaria H., and Zainab A. Jabarah. "Design–Syntheses, Characterization and Evaluation Antimicrobial Activity for Some azobenzen-p, p'-disubstituted with (3, O),(3, N-) substitute,(3, H)-quinazolin-4-one-2yl and 4-substituted quinazolin-2yl moieties." , (2017).

30- Jabarah, Zainab, Inas Salim Mahdi, and Wurood Jaafer. "Lumonil Compounds in Criminal Chemistry (A Review)." Egyptian Journal of Chemistry 62, no. 10 (2019): 1907-1916.

31- Abd, Abeer Kadhim, and Lamia Abdultef Risan Al-Iessa. "Synthesis and Spectral Properties of some new derivatives of Luminol azo dyes." Journal of Kufa for Chemical Science Vol 2, no. 6 (2020).

32- Pantelia, Anna, Ira Daskalaki, M. Consuelo Cuquerella, Georgios Rotas, Miguel A. Miranda, and Georgios C. Vougioukalakis. "Synthesis and chemiluminescent properties of amino-acylated luminol derivatives bearing phosphonium cations." Molecules 24, no. 21 (2019): 3957.

33- Jiao, Tifeng, Béatrice D. Leca-Bouvier, Paul Boullanger, Loïc J. Blum, and Agnes P. Girard-Egrot. "Phase behavior and optical investigation of two synthetic luminol derivatives and glycolipid mixed monolayers at the air–water interface."

Colloids and Surfaces A: Physicochemical and Engineering Aspects 321, no. 1-3 (2008): 137-142.

34- Jiao, Ti Feng, Yuan Yuan Xing, Jing Xin Zhou, and Wei Wang. "Synthesis and characterization of some functional luminol derivatives with aromatic substituted groups." In Advanced Materials Research, vol. 197, pp. 606-609. Trans Tech Publications Ltd, (2011).

35- Jiao, Ti Feng, Yuan Yuan Xing, and Jing Xin Zhou. "Synthesis and characterization of functional cholesteryl substituted luminol derivative." In Materials Science Forum, vol. 694, pp. 565-569. Trans Tech Publications Ltd, (2011).

36- Simon, Deepa, Sabbasani Rajasekhara Reddy, and Kannapiran Rajendrakumar. "Green Chemiluminescence of Highly Fluorescent Symmetrical Azo-based Luminol derivative." Oriental Journal of Chemistry 34, no. 2 (2018): 894.

37- Jiao, Tifeng, Qinqin Huang, Qingrui Zhang, Debao Xiao, Jingxin Zhou, and Faming Gao. "Self-assembly of organogels via new luminol imide derivatives: diverse nanostructures and substituent chain effect." Nanoscale Research Letters 8, no. 1 (2013): 1-8.

38- White, Emil Henry, and Kohtaro Matsuo. "Synthesis and chemiluminescence of an amino derivative and sulfur analog of luminol." The Journal of Organic Chemistry 32, no. 6 (1967): 1921-1926.

39- Sato, Shinichi, Kosuke Nakamura, and Hiroyuki Nakamura. "Tyrosine-specific chemical modification with in situ hemin-activated luminol derivatives." ACS Chemical Biology 10, no. 11 (2015): 2633-2640.

40- Shibata, Takayuki, Hiroki Yoshimura, Asako Yamayoshi, Nobuaki Tsuda, and Shpend Dragusha. "Hydrazide derivatives of luminol for chemiluminescence-labelling of macromolecules." Chemical and Pharmaceutical Bulletin 67, no. 8 (2019): 772-774.

41- Ewies, Ewies, Naglaa Fathy El-Sayed, Marwa El-Hussieny, and Mohamed Abdelaziz. "Synthesis and antimicrobial evaluation of new 5-amino-2, 3-dihydrophthalazine-1, 4-dione derivatives." Egyptian Journal of Chemistry 64, no. 12 (2021): 7165-7173.

42- Al AlBaheley, Noor, T. A. Fahad, and Asaad A. Ali. "Synthesis, spectroscopic, and thermal studies of azo compounds from luminol and procaine

with acetylacetone and their complexes." In *Journal of Physics: Conference Series*, vol. 2063, no. 1, p. 012016. IOP Publishing, (2021).

43- Ali, Asaad A., Tarek A. Fahad, and Alaa A. Al-muhsin. "Preparation and Spectroanalytical Studies of Two New Azo Dyes Based on Luminol." In IOP Conference Series: Materials Science and Engineering, vol. 928, no. 5, p. 052007. IOP Publishing, (2020).

44- Barni, Filippo, Simon W. Lewis, Andrea Berti, Gordon M. Miskelly, and Giampietro Lago. "Forensic application of the luminol reaction as a presumptive test for latent blood detection." Talanta 72, no. 3 (2007): 896-913.

45- Laux DL, James S, Kish PE, Sutton TP. Boca Raton: CRC Press. (2005):369–389.

46- Frégeau, Chantal J., Olivier Germain, and Ron M. Fourney. "Fingerprint enhancement revisited and the effects of blood enhancement chemicals on subsequent Profiler Plus™ fluorescent short tandem repeat DNA analysis of fresh and aged bloody fingerprints." Journal of Forensic Science 45, no. 2 (2000): 354-380.

47- Lytle, L. T., and D. G. Hedgecock. "Chemiluminescence in the visualization of forensic bloodstains." Journal of Forensic Science 23, no. 3 (1978): 550-562.

48- Pex OJ. International Association. Bloodstain Pattern Analysis. Newslett. (2005):11–15.

49- Motsenbocker, M., T. Sugawara, M. Shintani, H. Masuya, Y. Ichimori, and K. Kondo. "Establishment of the optically pumped chemiluminescence technique for diagnostics." Analytical Chemistry 65, no. 4 (1993): 403-408.

50- Kikuchi, Kazuya, Tetsuo Nagano, Hiroshi Hayakawa, Yasunobu Hirata, and Masaaki Hirobe. "Detection of nitric oxide production from a perfused organ by a luminol-hydrogen peroxide system." Analytical chemistry 65, no. 13 (1993): 1794-1799.

51- Whitehead, T. P., G. H. G. Thorpe, and S. R. J. Maxwell. "Enhanced chemiluminescent assay for antioxidant capacity in biological fluids." Analytica Chimica Acta 266, no. 2 (1992): 265-277.

52- Yamaguchi, Masatoshi, Hideyuki Yoshida, and Hitoshi Nohta. "Luminol-type chemiluminescence derivatization reagents for liquid chromatography and capillary electrophoresis." Journal of Chromatography A 950, no. 1-2 (2002): 1-19.

53- Zhu, Ruohua, and Wim Th Kok. "Post-column derivatization for fluorescence and chemiluminescence detection in capillary electrophoresis." Journal of pharmaceutical and biomedical analysis 17, no. 6-7 (1998): 985-999.
54- Fletcher, Philip, Kevin N. Andrew, Anthony C. Calokerinos, Stuart Forbes, and Paul J. Worsfold. "Analytical applications of flow injection with chemiluminescence detection—a review." Luminescence: The journal of biological and chemical luminescence 16, no. 1 (2001): 1-23.
55- Felmlee TA, Mitchell PS, Ulfelder KJ, Persing DH, Landers JP. Journal. Capital. Electron. 1995;2:125–130. Miyazawa, T., Suzuki, T., Fujimoto, K., & Kinoshita, M. (1996). Mechanisms of Ageing and Development, 86(3), 145–150.
56- Lin, Zongtao, Hong Wang, Ying Xu, Jing Dong, Yuki Hashi, and Shizhong Chen. "Identification of antioxidants in Fructus aurantii and its quality evaluation using a new on-line combination of analytical techniques." Food chemistry 134, no. 2 (2012): 1181-1191.
57- Fall, Barbara I., Bernadette Eberlein-König, Heidrun Behrendt, Reinhard Niessner, Johannes Ring, and Michael G. Weller. "Microarrays for the screening of allergen-specific IgE in human serum." Analytical chemistry 75, no. 3 (2003): 556-562.
58- Kricka, Larry J. "Stains, labels and detection strategies for nucleic acids assays." Annals of Clinical Biochemistry 39, no. 2 (2002): 114-129.
59- Cheek, Brady J., Adam B. Steel, Matthew P. Torres, Yong-Yi Yu, and Hongjun Yang. "Chemiluminescence detection for hybridization assays on the flow-thru chip, a three-dimensional microchannel biochip." Analytical Chemistry 73, no. 24 (2001): 5777-5783.
60- Huang, Ruo-Pan. "Detection of multiple proteins in an antibody-based protein microarray system." Journal of immunological methods 255, no. 1-2 (2001): 1-13.
61- Roda, A., M. Guardigli, C. Russo, P. Pasini, and M. Baraldini. "Protein microdeposition using a conventional ink-jet printer." Biotechniques 28, no. 3 (2000): 492-496.
62- Huang, Ruo-Pan, Ruochun Huang, Yan Fan, and Ying Lin. "Simultaneous detection of multiple cytokines from conditioned media and patient's sera by an antibody-based protein array system." Analytical biochemistry 294, no. 1 (2001): 55-62.

63- Beck, Michael T., Lori Holle, and Wen Y. Chen. "Combination of PCR subtraction and cDNA microarray for differential gene expression profiling." Biotechniques 31, no. 4 (2001): 782-786.

64- Créton, Robbert, and Lionel F. Jaffe. "Chemiluminescence microscopy as a tool in biomedical research." Biotechniques 31, no. 5 (2001): 1098-1105.

65- Pasini, Patrizia, Monica Musiani, Carmela Russo, Piero Valenti, Giorgio Aicardi, Jean E. Crabtree, Mario Baraldini, and Aldo Roda. "Chemiluminescence imaging in bioanalysis." Journal of pharmaceutical and biomedical analysis 18, no. 4-5 (1998): 555-564.

66- Bronstein, Irena, John Fortin, Philip E. Stanley, Gordon SAB Stewart, and Larry J. Kricka. "Chemiluminescent and bioluminescent reporter gene assays." Analytical biochemistry 219, no. 2 (1994): 169-181.

67- Bronstein, Irena, Chris S. Martin, J. J. Fortin, C. E. Olesen, and J. C. Voyta. "Chemiluminescence: sensitive detection technology for reporter gene assays." Clinical Chemistry 42, no. 9 (1996): 1542-1546.

68- Chai, Ying, Dayong Tian, Wei Wang, and Hua Cui. "A novel electrochemiluminescence strategy for ultrasensitive DNA assay using luminol functionalized gold nanoparticles multi-labeling and amplification of gold nanoparticles and biotin–streptavidin system." Chemical communications 46, no. 40 (2010): 7560-7562.

69- Zhang, Lijuan, Biqi Lu, and Chao Lu. "Chemiluminescence sensing of aminothiols in biological fluids using peroxymonocarbonate-prepared networked gold nanoparticles." Analyst 138, no. 3 (2013): 850-855.

70- Yu, Xijuan, Xiangnan Liu, Chuanqin Mou, and Zhiguang Wang. "DNA-based chemiluminescent nanoprobes for highly sensitive and selective detection of mercury (II) ion." Luminescence 28, no. 6 (2013): 847-852.

71- Alam, Al-Mahmnur, Mohammad Kamruzzaman, Trung-Dung Dang, Sang Hak Lee, Young Ho Kim, and Gyu-Man Kim. "Enzymeless determination of total sugar by luminol–tetrachloroaurate chemiluminescence on chip to analyze food samples." Analytical and bioanalytical chemistry 404, no. 10 (2012): 3165-3173.

72- N.J. Turo, Modern molecular photochemistry, Benjamin Cummings Publication Co., California, (1978): p: 4.

73- C. Benson, Physical Chemistry, Global Media, (2009), India, pp: 232-233.

74- P. Alistair, and J. Lees, Springer- Verlag, Brlin Heidelberg. " Photophysics of Organometallics", (2010), p:1

75- Itoh, Susumu, and Shoju Onishi. "Kinetic study of the photochemical changes of (ZZ)-bilirubin IX α bound to human serum albumin. Demonstration of (EZ)-bilirubin IX α as an intermediate in photochemical changes from (ZZ)-bilirubin IX α to (EZ)-cyclobilirubin IX α." Biochemical Journal 226, no. 1 (1985): 251-258.

76- Toltl, Nicholas P., William J. Leigh, Gerlinde M. Kollegger, William G. Stibbs, and Kim M. Baines. "Nanosecond Laser Flash Photolysis Studies of the Photochemistry of Dimesitylgermylene Precursors." Organometallics 15, no. 17 (1996): 3732-3736.

77- Coyle, Emma. "Green Photochemistry: The synthesis of fine chemicals with sunlight." PhD diss., Dublin City University, 2010.

78- Bunce, N. J. "h CRC Handbook of organic photochemistry. Vol. I. Edited by JC Scaiano." (1989): 241.

79- Oelgemöller, Michael, and Oksana Shvydkiv. "Recent advances in microflow photochemistry." Molecules 16, no. 9 (2011): 7522-7550.

80- Icli, S., H. Icil, and I. Gürol. "High Rates of Fluorescence Quenching Between Perylene Dodecyldiimide and Certain\pi-Electron Donors." Turkish Journal of Chemistry 21, no. 4 (1997): 363-368.

81- Boreen, Anne L., William A. Arnold, and Kristopher McNeill. "Photochemical fate of sulfa drugs in the aquatic environment: sulfa drugs containing five-membered heterocyclic groups." Environmental Science & Technology 38, no. 14 (2004): 3933-3940.

82- Alam G. Trovo´, Raquel F.P. Nogueiraa, Ana Agu¨ erab, , Amadeo R. Fernandez-Albab,Carla Sirtorib, , and Sixto Malato, "Degradation of

sulfamethoxazole in water by solarphoto-Fenton. Chemical and toxicological evaluation", Water Research,43, (2009), 3922–3931.

83- Chiang, Mao-Yuan, and Heh-Nan Lin. "Enhanced photocatalysis of ZnO nanowires co-modified with cuprous oxide and silver nanoparticles." Materials Letters 160 (2015): 440-443.

84- Sun, Guanhua, Chaosheng Zhu, Jingtang Zheng, Bo Jiang, Huacheng Yin, Han Wang, Shi Qiu et al. "Preparation of spherical and dendritic CdS@ TiO2 hollow double-shelled nanoparticles for photocatalysis." Materials Letters 166 (2016): 113-115.

85- Ming, Tingzhen, Philip Davies, Wei Liu, and Sylvain Caillol. "Removal of non-CO2 greenhouse gases by large-scale atmospheric solar photocatalysis." Progress in Energy and Combustion Science 60 (2017): 68-96.

86- Khan, I., K. Saeed, and I. Khan. "Nanoparticles: properties, applications and toxicities. Arab J Chem 12: 908." (2017).

87- Andrade, George RS, Cristiane C. Nascimento, Zenon M. Lima, Erico Teixeira-Neto, Luiz P. Costa, and Iara F. Gimenez. "Star-shaped ZnO/Ag hybrid nanostructures for enhanced photocatalysis and antibacterial activity." Applied Surface Science 399 (2017): 573-582.

88- Liu, Yuan, Changsheng Xie, Huayao Li, Hao Chen, Tao Zou, and Dawen Zeng. "Improvement of gaseous pollutant photocatalysis with WO3/TiO2 heterojunctional-electrical layered system." Journal of Hazardous Materials 196 (2011): 52-58.

89- Zhang, Xiaojing, Shan Yu, Yang Liu, Qian Zhang, and Ying Zhou. "Photoreduction of non-noble metal Bi on the surface of Bi2WO6 for enhanced visible light photocatalysis." Applied Surface Science 396 (2017): 652-658.

90- Khataee, Alireza, Samira Arefi-Oskoui, Mehrangiz Fathinia, Arezoo Fazli, Ali Shahedi Hojaghan, Younes Hanifehpour, and Sang Woo Joo. "Photocatalysis of sulfasalazine using Gd-doped PbSe nanoparticles under visible light irradiation: kinetics, intermediate identification and phyto-toxicological studies." Journal of Industrial and Engineering Chemistry 30 (2015): 134-146.

91- Samu, Gergely F., Ágnes Veres, Balázs Endrődi, Erika Varga, Krishnan Rajeshwar, and Csaba Janáky. "Bandgap-engineered quaternary MxBi2− xTi2O7 (M: Fe, Mn) semiconductor nanoparticles: Solution combustion synthesis, characterization, and photocatalysis." Applied Catalysis B: Environmental 208 (2017): 148-160.

92- Liu, Min, De-Xiang Zhang, Shumei Chen, and Tian Wen. "Loading Ag nanoparticles on Cd (II) boron imidazolate framework for photocatalysis." Journal of Solid State Chemistry 237 (2016): 32-35.

93- Asapu, Ramesh, Nathalie Claes, Sara Bals, Siegfried Denys, Christophe Detavernier, Silvia Lenaerts, and Sammy W. Verbruggen. "Silver-polymer core-shell nanoparticles for ultrastable plasmon-enhanced photocatalysis." Applied Catalysis B: Environmental 200 (2017): 31-38.

94- Aleksandrzak, Malgorzata, Wojciech Kukulka, and Ewa Mijowska. "Graphitic carbon nitride/graphene oxide/reduced graphene oxide nanocomposites for photoluminescence and photocatalysis." Applied Surface Science 398 (2017): 56-62.

95- Zhang, Li, Qinghong Zhang, Hongyong Xie, Jiang Guo, Hailong Lyu, Yaogang Li, Zhiguo Sun, Hongzhi Wang, and Zhanhu Guo. "Electrospun titania nanofibers segregated by graphene oxide for improved visible light photocatalysis." Applied Catalysis B: Environmental 201 (2017): 470-478.

96- Blum, Jochanan, Ayelet Rosenfeld, Faina Gelman, Herbert Schumann, and David Avnir. "Hydrogenation and dehalogenation of aryl chlorides and fluorides by the sol–gel entrapped RhCl3–Aliquat 336 ion pair catalyst." Journal of Molecular Catalysis A: Chemical 146, no. 1-2 (1999): 117-122.

97- Liu, S. X., X. Y. Chen, and X. Chen. "A TiO2/AC composite photocatalyst with high activity and easy separation prepared by a hydrothermal method." Journal of hazardous materials 143, no. 1-2 (2007): 257-263.

98- Cordero, Tulynan, Jean-Marc Chovelon, Christian Duchamp, Corinne Ferronato, and Juan Matos. "Surface nano-aggregation and photocatalytic activity of TiO2 on H-type activated carbons." Applied Catalysis B: Environmental 73, no. 3-4 (2007): 227-235.

99- Liu, Shouxin, and Xiaoyun Chen. "Preparation and characterization of a novel activated carbon-supported N-doped visible light response photocatalyst (TiO2− xNy/AC)." Journal of Chemical Technology & Biotechnology: International Research in Process, Environmental & Clean Technology 82, no. 5 (2007): 453-459.

101- Ou, Yan, Jing-Dong Lin, Hong-Mei Zou, and Dai-Wei Liao. "Effects of surface modification of TiO2 with ascorbic acid on photocatalytic decolorization of an azo dye reactions and mechanisms." Journal of Molecular Catalysis A: Chemical 241, no. 1-2 (2005): 59-64.

102- Yi, Zhiguo, Jinhua Ye, Naoki Kikugawa, Tetsuya Kako, Shuxin Ouyang, Hilary Stuart-Williams, Hui Yang et al. "An orthophosphate semiconductor with photooxidation properties under visible-light irradiation." Nature materials 9, no. 7 (2010): 559-564.

103- Ma, Xinguo, Bin Lu, Di Li, Rui Shi, Chenshi Pan, and Yongfa Zhu. "Origin of photocatalytic activation of silver orthophosphate from first-principles." The Journal of Physical Chemistry C 115, no. 11 (2011): 4680-4687.

104- Zhang, Liwu, Yi Man, and Yongfa Zhu. "Effects of Mo replacement on the structure and visible-light-induced photocatalytic performances of Bi2WO6 photocatalyst." Acs Catalysis 1, no. 8 (2011): 841-848.

105- Liu, Yongping, Liang Fang, Huidan Lu, Laijun Liu, Hai Wang, and Changzheng Hu. "Highly efficient and stable Ag/Ag3PO4 plasmonic photocatalyst in visible light." Catalysis Communications 17 (2012): 200-204.

106- Asahi, R., T. Morikawa, T. Ohwaki, K. Aoki, and Y. Taga. "Photocatalysts sensitive to visible light-response." Science 295, no. 5555 (2002): 627-627.

107- Wu, Guosheng, Jiali Wen, Samantha Nigro, and Aicheng Chen. "One-step synthesis of N-and F-codoped mesoporous TiO2 photocatalysts with high visible light activity." Nanotechnology 21, no. 8 (2010): 085701.

108- Tian, Yong, Gui-Fang Huang, Li-Juan Tang, Ming-Gang Xia, Wei-Qing Huang, and Zhi-Li Ma. "Size-controllable synthesis and enhanced photocatalytic activity of porous ZnS nanospheres." Materials Letters 83 (2012): 104-107.

109- Chen, Yuan, Gui-Fang Huang, Wei-Qing Huang, B. S. Zou, and Anlian Pan. "Enhanced visible-light photoactivity of La-doped ZnS thin films." Applied Physics A 108, no. 4 (2012): 895-900.

110- Etacheri, Vinodkumar, Michael K. Seery, Steven J. Hinder, and Suresh C. Pillai. "Highly visible light active TiO2− x N x heterojunction photocatalysts." Chemistry of Materials 22, no. 13 (2010): 3843-3853.

111- Feng, Lu, Ke Feng He, and Wan Ping Chen. "Study on stability of AgI/TiO2 visible light photocatalysts in solutions of various pH values." In Advanced Materials Research, vol. 399, pp. 1272-1275. Trans Tech Publications Ltd, 2012.

112- Feng, X. Y., C. Shen, Y. Yu, S. Q. Wei, and C. H. Chen. "Synthesis and electrochemical properties of sticktight-like and nanosheet Co3O4 particles." Journal of power sources 230 (2013): 59-65.

113- Ma, Jianmin, and Arumugam Manthiram. "Precursor-directed formation of hollow Co 3 O 4 nanospheres exhibiting superior lithium storage properties." Rsc Advances 2, no. 8 (2012): 3187-3189.
114- Saeed, Muhammad, Majid Muneer, Nida Mumtaz, Mohsin Siddique, Nadia Akram, and Muhammad Hamayun. "Ag-Co3O4: Synthesis, characterization and evaluation of its photo-catalytic activity towards degradation of rhodamine B dye in aqueous medium." Chinese journal of chemical engineering 26, no. 6 (2018): 1264-1269.
115- Sahoo, Nanda Gopal, Sravendra Rana, Jae Whan Cho, Lin Li, and Siew Hwa Chan. "Polymer nanocomposites based on functionalized carbon nanotubes." Progress in polymer science 35, no. 7 (2010): 837-867.
116- Faucon, Michel-Pierre, Olivier Pourret, and Bastien Lange. "Element Case Studies: Cobalt." In Agromining: Farming for Metals, pp. 385-391. Springer, Cham, 2021.
117- Iravani, Siavash, and Rajender S. Varma. "Sustainable synthesis of cobalt and cobalt oxide nanoparticles and their catalytic and biomedical applications." Green Chemistry 22, no. 9 (2020): 2643-2661.
118- Anyaegbunam, F. N. C., and C. Augustine. "A study of optical band gap and associated urbach energy tail of chemically deposited metal oxides binary thin films." Dig J Nanomater Biostruct 3, no. 3 (2018): 847-56.
119- Stella, C., N. Soundararajan, and K. J. A. A. Ramachandran. "Structural, optical, and magnetic properties of Mn and Fe-doped Co3O4 nanoparticles." AIP Advances 5, no. 8 (2015): 087104.
120- Kumar, Rajesh, Hyun-Jun Kim, Sungjin Park, Anchal Srivastava, and Il-Kwon Oh. "Graphene-wrapped and cobalt oxide-intercalated hybrid for extremely durable super-capacitor with ultrahigh energy and power densities." Carbon 79 (2014): 192-202.
121- Hagelin-Weaver, Helena AE, Gar B. Hoflund, David M. Minahan, and Ghaleb N. Salaita. "Electron energy loss spectroscopic investigation of Co metal, CoO, and Co3O4 before and after Ar+ bombardment." Applied Surface Science 235, no. 4 (2004): 420-448.
122- Hardee, David J., Lyudmila Kovalchuke, and Tristan H. Lambert. "Nucleophilic acyl substitution via aromatic cation activation of carboxylic acids: rapid generation of acid chlorides under mild conditions." Journal of the American Chemical Society 132, no. 14 (2010): 5002-5003.

123- Bousfield, Thomas W., Katharine PR Pearce, Simbarashe B. Nyamini, Athanasios Angelis-Dimakis, and Jason E. Camp. "Synthesis of amides from acid chlorides and amines in the bio-based solvent Cyrene™." Green Chemistry 21, no. 13 (2019): 3675-3681.
Hiran, B. L., R. Boriwal, S. Bapana, and S. N. Paliwal. "Synthesis and Characterization of Polymers, of Substituted Maleimide Derivative." Journal of the University of Chemical Technology and Metallurgy 45, no. 2 (2010): 127-132.

124- Rajan Lakraa Rahul Kumarb Dhirendra Nath Thatoia Prasanta Kumar Sahooa Ankur Soam, "Synthesis and characterization of cobalt oxide (Co_3O_4) nanoparticles" , Materials Today, Volume 41, Part 2, (2021): 269-271.
125- Kaczmarek H, Kaminska A, Swiatek M, Sanyal S: Photoinition degradation of PS in the presence of low molecular organic compounds. European polymer Journal 1999, 36: 1167-1173.
126- Feldman, D. "Polymer weathering: photo-oxidation." Journal of Polymers and the Environment 10, no. 4 (2002): 163-173.
127- Chen, Yu-Wen, and Yu-Hsuan Hsu. "Effects of reaction temperature on the photocatalytic activity of TiO2 with Pd and Cu cocatalysts." Catalysts 11, no. 8 (2021): 966.
128- Moongraksathum, Benjawan, Pei-Ting Hsu, and Yu-Wen Chen. "Photocatalytic activity of ascorbic acid-modified TiO2 sol prepared by the peroxo sol–gel method." Journal of Sol-Gel Science and Technology 78, no. 3 (2016): 647-659.
129- Kumar, Ankit, and G. Pandey. "A review on the factors affecting the photocatalytic degradation of hazardous materials." Mater. Sci. Eng. Int. J 1, no. 3 (2017): 1-10.
130- Azad, Kumar, and Pandey Gajanan. "Photocatalytic degradation of Eriochrome Black-T by the Ni: TiO2 nanocomposites." Desalination and Water Treatment 71 (2017): 406-419.
131- KUMAR, AZAD, and GAJANAN PANDEY. "Photocatalytic activity of Co: TiO2 nanocomposites and their application in photodegradation of acetic acid." Chemical Science 6, no. 3 (2017): 385-392.
132- Salimi, Anis, and Aliakbar Roosta. "Experimental solubility and thermodynamic aspects of methylene blue in different solvents." Thermochimica Acta 675 (2019): 134-139.

133- Kumar, Ankit, and G. Pandey. "A review on the factors affecting the photocatalytic degradation of hazardous materials." Mater. Sci. Eng. Int. J 1, no. 3 (2017): 1-10.

الخلاصة :

تصف الدراسة الحالية تخليق بعض مشتقات اللومينول الجديدة. تم تخليق هذه المركبات الوظيفية الجديدة بناءً على مشتقات اللومينول . يتضمن هذا العمل مسارين :

المسار الأول: يتضمن تفاعل مركب اللومينول مع أدوية تحتوي مجموعة كاربوكسيل مختلفة مثل نابروكسين ، حمض الميفيناميك ، ايبوبروفين ، حمض ديكلوفيناك ، أمبيسيلين ، سيبروفلكسين ، سيفوتاكسيم ، سيفترياكسون ، سيفالكسين). أجريت عمليات التخليق عن طريق تحويل مجموعة الكربوكسيل في الأدوية إلى مشتقة كلوريد الحامض بالتفاعل مع $SOCl_2$ ، ثم تم تفاعل مشتقات الكلوريد المركب (T1-T9) مع اللومينول في وجود DMSO و TEA لإنتاج الجزيئات المستهدفة النهائية (TH1-TH9).

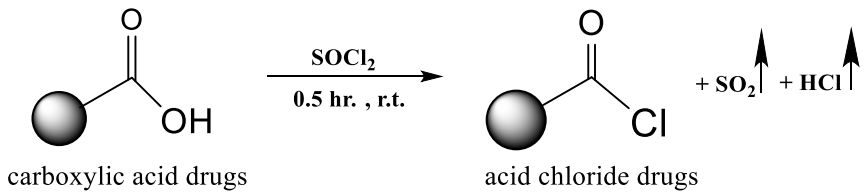

المعادلة (1): المعادلة العامة لتخليق كلوريد الحامض للأدوية (T1-T9).

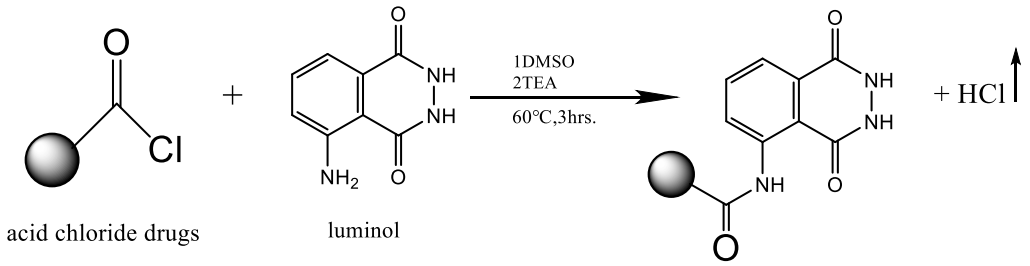

المعادلة (2): المعادلة العامة لتخليق المشتقات (TH1-TH9).

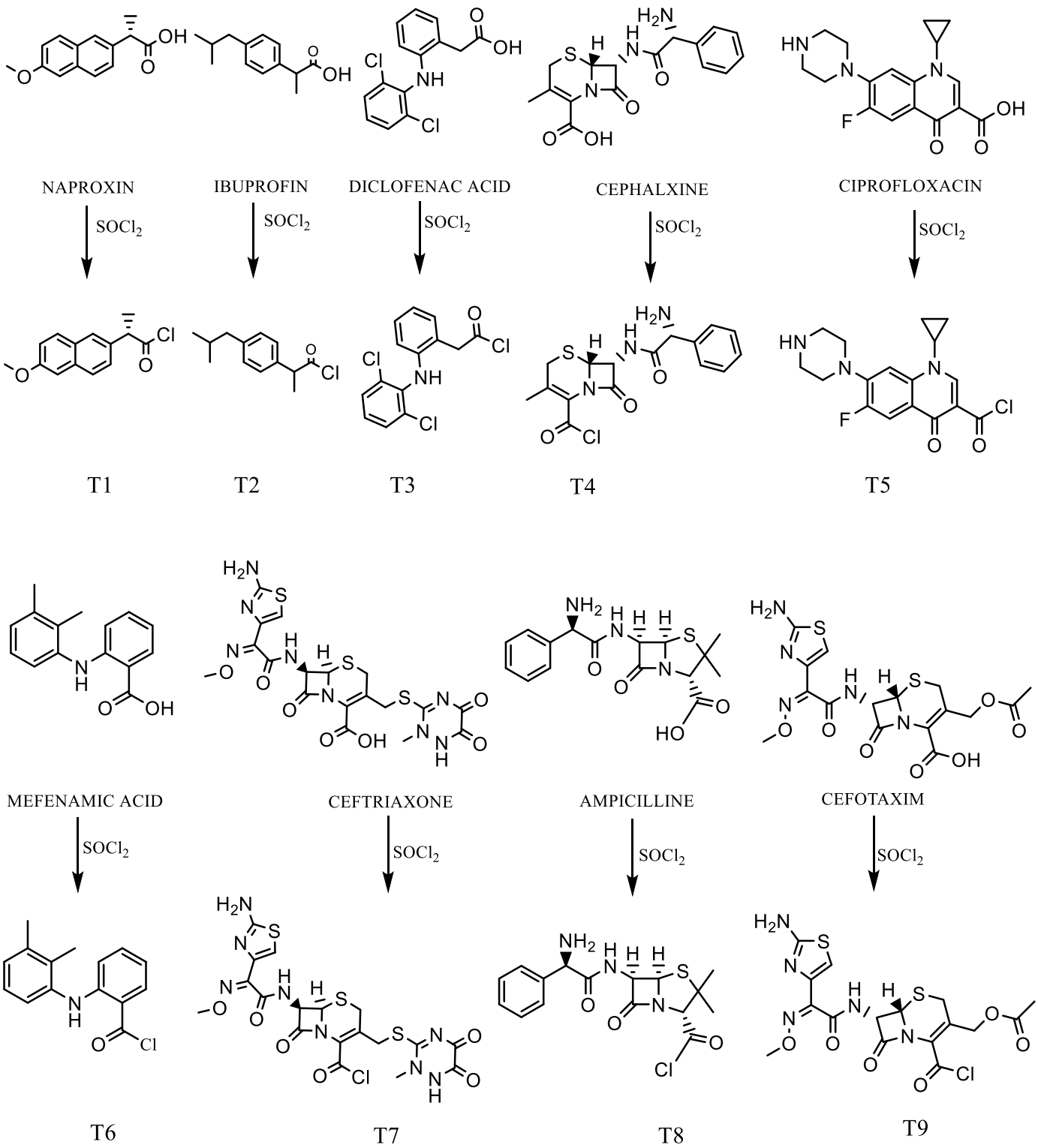

مخطط (1): وصف تخطيطي لتخليق المشتقات (T1-T9).

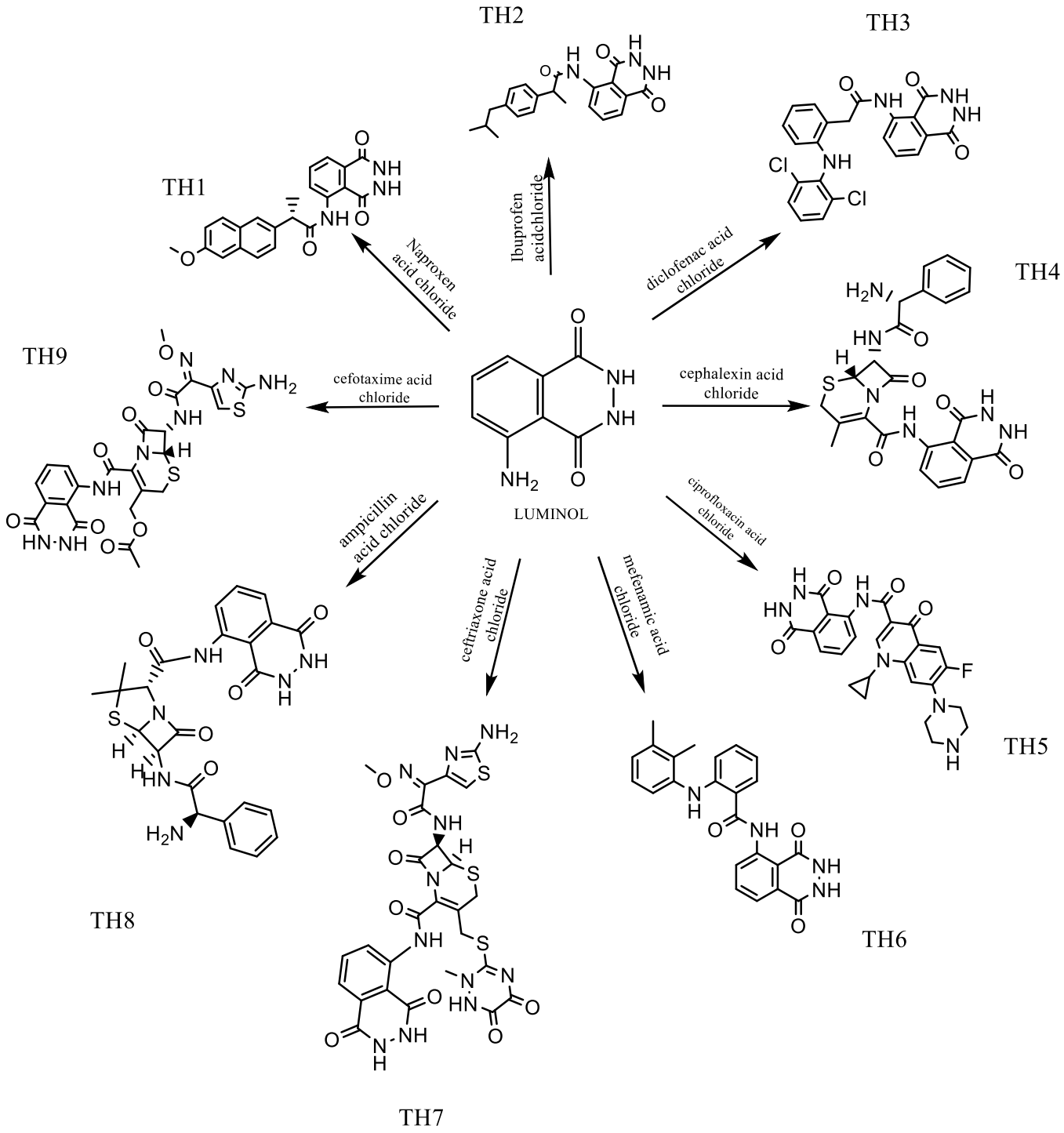

مخطط (2): وصف تخطيطي لتخليق المشتقات (TH1-TH9).

المسارالثاني: يتضمن تفاعل اللومينول مع سكسنيك أنهيدريد عن طريق إضافة DMSO ثم تحويل المخاليط التي تم الحصول عليها إلى كلوريد حامض بواسطة $SOCl_2$ بعد إضافة DMSO للخليط وإضافة الأدوية الأمينية للتفاعل في وجود TEA لإنتاج الجزيئات المستهدفة النهائية (TH10-TH15).

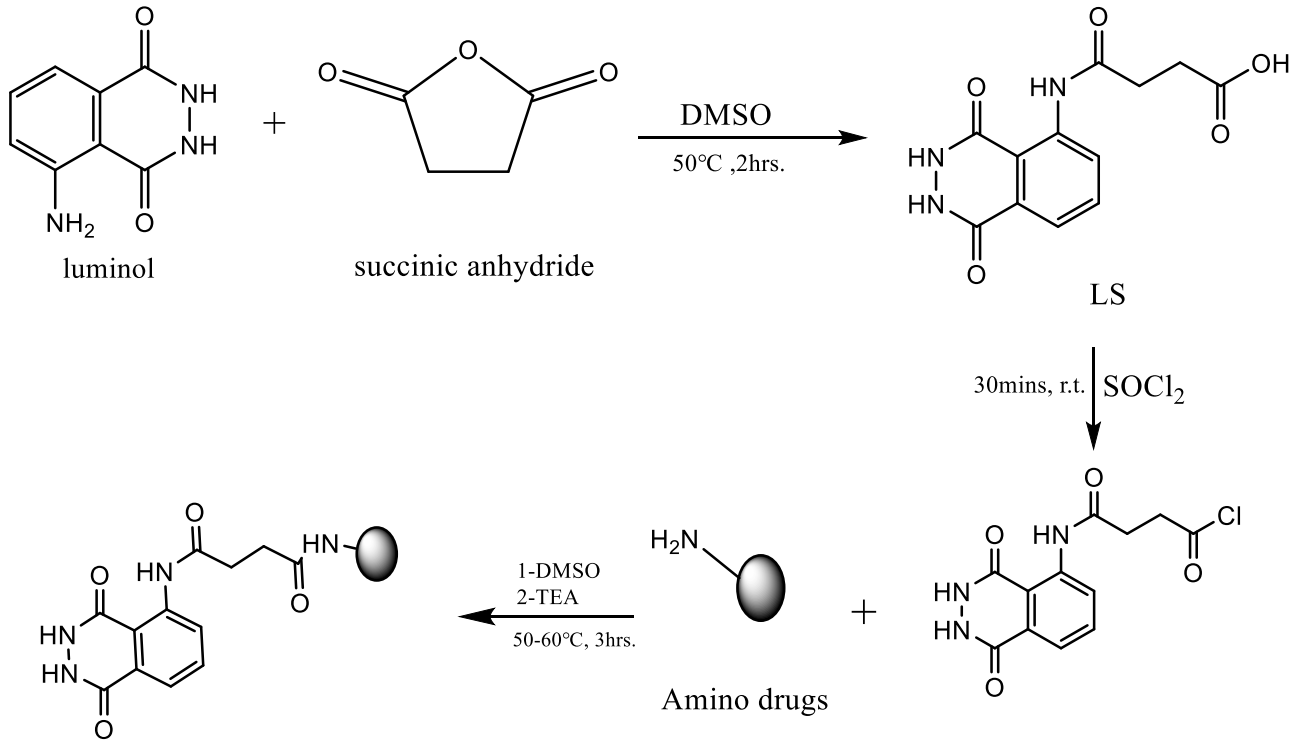

مخطط (3): وصف تخطيطي لتخليق المشتقات (TH10-TH15).

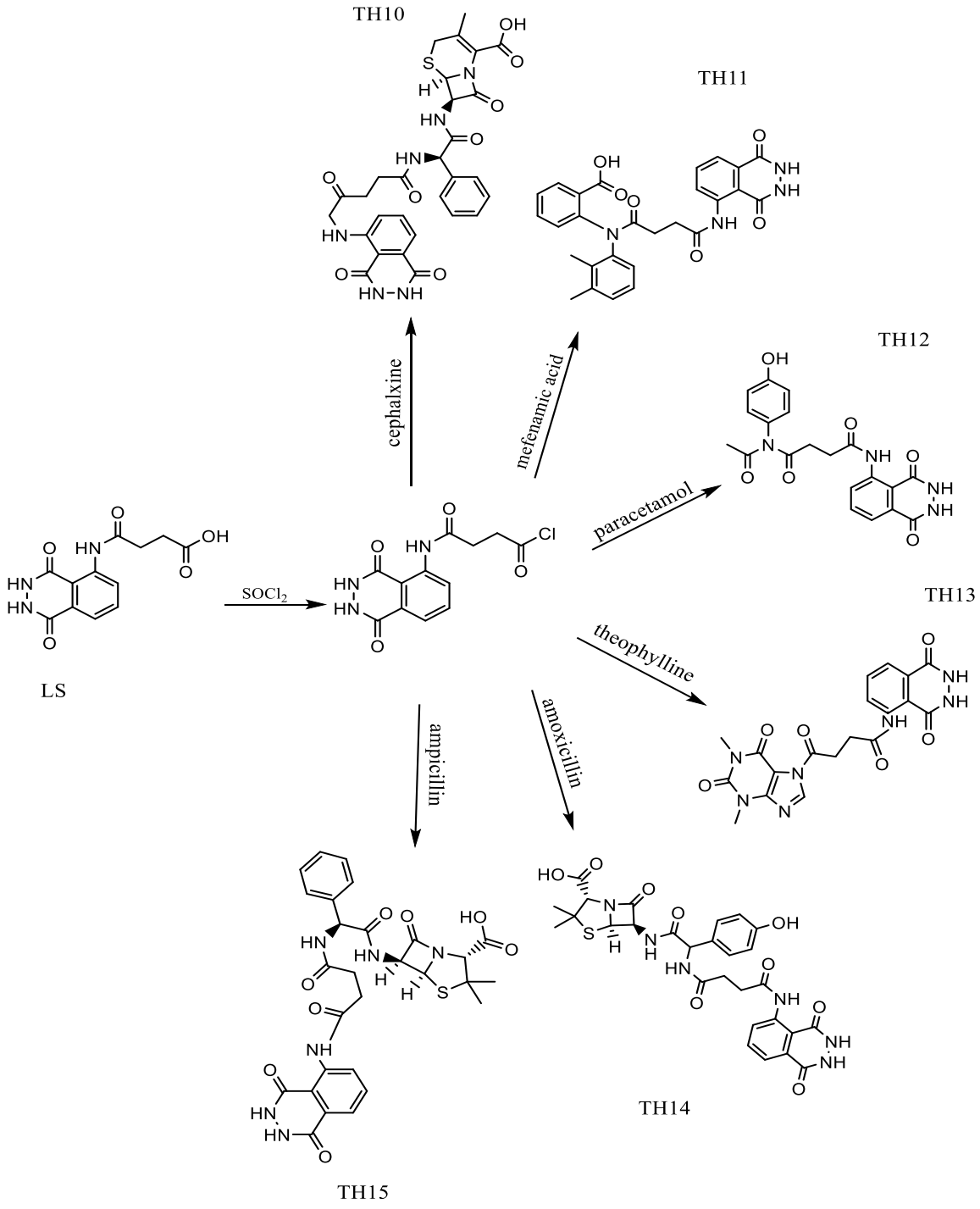

مخطط (4): وصف تخطيطي لتخليق المشتقات (TH10-TH15).

تم تشخيص هذه المواد باستخدام تقنيات تحليل العناصر الدقيقة FTIR و^{13}C-NMR و^{1}HNMR و CHNS. بالإضافة إلى ذلك ، تم فحص درجة انصهارها وقابليتها للذوبان. تم اختبار جميع المشتقات المحضرة على أنها كواشف مضادة للبكتيريا مقابل *Staphylococcus aureus* (موجبة الجرام) و *Escherichia coli*(سالبة الجرام) وأظهرت معظم المركبات المختبرة نشاطًا تجاه فئة واحدة أو كلا الفئتين من البكتيريا. تم اختبار بعض المشتقات المحضرة على أنها تحلل ضوئي بإضاءة فوق البنفسجية عند درجات حرارة مختلفة ، كما تم اختبار التحلل الضوئي على أكسيد الكوبالت باستخدام ظروف ومعايير تفاعل مختلفة.

جمهورية العراق

وزارة التعليم العالي والبحث العلمي

جامعة بابل

كلية العلوم

قسم الكيمياء

تخليق وتشخيص ودراسة بعض التطبيقات لمشتقات اللومينول الوظيفية الجديدة

رسالة

مقدمة الى مجلس كلية العلوم – جامعة بابل كجزء من متطلبات نيل درجة الماجستير

في العلوم \ الكيمياء

من قبل

طيبة صالح كاظم محمد

بكالوريوس علوم كيمياء \جامعة بابل (2019)

بإشراف

أ.د. مهند موسى كريم

أ.د. عباس جاسم عطية

1444هـ **2022 م**